

Recidivism and Peer Influence with LLM Text Embeddings in Low Security Correctional Facilities

Shanjukta Nath⁽¹⁾, Jiwon Hong⁽²⁾, Jae Ho Chang⁽²⁾,
Keith Warren⁽³⁾, and Subhadeep Paul⁽²⁾

⁽¹⁾*Department of Agricultural and Applied Economics, University of Georgia*,
⁽²⁾*Department of Statistics, The Ohio State University*
⁽³⁾*College of Social Work, The Ohio State University*

September 26, 2025

Abstract

We find AI embeddings obtained using a pre-trained transformer-based Large Language Model (LLM) of 80,000-120,000 written affirmations and correction exchanges among residents in low-security correctional facilities to be highly predictive of recidivism. The prediction accuracy is 30% higher with embedding vectors than with only pre-entry covariates. However, since the text embedding vectors are high-dimensional, we perform Zero-Shot classification of these texts to a low-dimensional vector of user-defined classes to aid interpretation while retaining the predictive power. To shed light on the social dynamics inside the correctional facilities, we estimate peer effects in these LLM-generated numerical representations of language with a multivariate peer effect model, adjusting for network endogeneity. We develop new methodology and theory for peer effect estimation that accommodate sparse networks, multivariate latent variables, and correlated multivariate outcomes. With these new methods, we find significant peer effects in language usage for interaction and feedback.

1 Introduction

Policymakers are particularly interested in predicting and assessing the risk of recidivism (repeat offending) to provide additional remedial measures for prevention, such as psychological interventions [Beaudry et al., 2021]. The reconviction rates worldwide are estimated to be high, between 18%-55% across 33 countries [Yukhnenko et al., 2023]. Given a worldwide prison population estimate of around 11 million people, the human costs to society of recidivism, therefore, are substantial. In terms of economic costs, a study in 2016 estimated the total costs of incarceration in the US at over one trillion

dollars or 6% of GDP, assigning monetary value to different types of costs to individuals [Pettus-Davis et al., 2016].

Psychosocial interventions, including cognitive behavioral therapy (CBT), therapeutic communities (TCs), halfway homes, and psychoeducation, are widely employed in various correctional settings to reduce the risk of recidivism [Beaudry et al., 2021, Doleac, 2023, Lee, 2023]. In this paper, we focus on TCs, which are low-security correctional facilities for criminal behavior and substance use disorder [De Leon, 2000]. TCs are mutual aid based programs in which residents work together, interact in group therapy as well as informal settings, and are expected to give feedback to peers in the form of affirmations for prosocial behavior and corrections for behavior that contravenes TC norms [De Leon, 2000, Perfas, 2014]. Affirmations and corrections can either be informal comments or can be written down on “slips”, brief forms that typically include the sender, the receiver, and the date and content of the affirmation/correction. Notably, Randomized controlled trials have shown TCs to reduce criminal activity and drug use [Bahr et al., 2012, Sacks et al., 2012].

However, assessing the risk of recidivism is challenging [Campbell et al., 2019, Dreszel and Farid, 2018, Lin et al., 2020, Warren et al., 2020]. Risk is often evaluated using individual-level characteristics in a supervised machine learning (ML) algorithm. Dreszel and Farid [2018] shows that the widely used COMPAS algorithm, even with high-dimensional features (137 variables) and a proprietary ML algorithm, can achieve only similar levels of prediction accuracy as non-expert human prediction without any criminal justice knowledge. Beyond prediction, a related strand of research explores the factors that reduce the risk of recidivism, including higher employment opportunities Galbiati et al. [2021], Schnepel [2018], welfare programs Tuttle [2019], Yang [2017], and neighborhood institutions Barrios-Fernández and García-Hombrados [2025].

We find a similar situation in terms of predicting recidivism in our data in this paper as well. Our data comes from 3 TCs in a midwestern state in the United States. The TCs maintained administrative records of each resident’s precise entry and exit dates, pre-entry covariates, time-stamp, sender ID, receiver ID, and the actual text of all the corrections and affirmations that residents exchanged during their time in TC. The midwestern state’s department of rehabilitation and corrections provided the data on 3-year recidivism. Using all pre-entry covariates in our setup, we can only predict 3-year recidivism up to an out-of-sample AUC value slightly above 0.5, i.e., marginally better than random guessing. However, TCs are unique in their structure of peer affirmations and corrections, along with the practice of recording them. This unique feature allows for analyzing interpersonal language exchanges within the program as predictors of critical downstream outcomes, particularly criminal recidivism.

Although the language exchange of residents holds necessary signals for downstream outcomes, we cannot directly use this unstructured data corpus for the prediction exercise. As a first step, we use transformer-based Large Language Models to represent this

language as numerical embedding vectors that can be used as input for prediction. We find that we can significantly improve recidivism prediction with an (out-of-sample) AUC of 0.70 using the transformer-based Large Language Models (LLM) embeddings [Devlin et al., 2019, Vaswani et al., 2017] of the repository of 80,000 to 120,000 written affirmations and corrections that the residents exchange as part of the mutual aid-based therapy in TCs. This is a $\approx 30\%$ improvement in predicting recidivism over using pre-entry characteristics of residents and comparable to state-of-the-art commercial softwares such as COMPASS that uses orders of hundreds of individual characteristics. This supports recent work in TC that has focused on community building, peer interactions, and peer encouragement as possible mechanisms behind the success of TCs [Campbell et al., 2019, Nath et al., 2025].

After establishing the importance of interactions on recidivism, we explore the role of peers in shaping individuals' engagement and behavior profiles while they are in the TCs. We obtain estimates of peer effects on their language embeddings to do so. But embeddings are high-dimensional and not interpretable directly. We perform Zero-Shot classification [Yin et al., 2019] to classify the embeddings into interpretable user-defined classes. Here, the classifier generates probabilities for each class supplied by the user that add up to 1. However, there are several challenges to estimating peer effects in this context, including multivariate outcomes, sparse networks, and endogeneity in network formation due to multivariate latent homophily, which the existing methods for peer effect estimation do not accommodate. To overcome these challenges, we develop new econometric methods based on instrumental variables (IV) that accommodate correlated multivariate outcomes, multidimensional latent variables, do not require dense networks, and use flexible nonparametric modeling of the effects of latent homophily. We show our estimator is \sqrt{N} consistent and asymptotically normal.

We contribute to the growing literature on text analysis to address various economic questions. The works of Brehm and Saavedra [2025], Jelveh et al. [2024], Kalamara et al. [2022], Lippmann [2022] use some of the earlier approaches to text analysis, such as sentiment analysis, word frequency counts, bag of words, topic modeling, and the dictionary methods. More recently, Ash et al. [2022], Gennaro and Ash [2022] use the early models of word embedding, such as Word2Vec [Mikolov et al., 2013], as methods for text analysis.

Unlike these papers, we use the embeddings from transformer-based foundation AI models that use the attention mechanism in Vaswani et al. [2017]. The excellent expressive ability of the embeddings of transformer-based models, such as GPT, is evident by their exceptional generative and predictive abilities, in the current generative AI revolution [Rathje et al., 2024]. This is due to the attention mechanism and bidirectional processing, whereby other words in the sentence dynamically influence the embeddings of words, defining a context for the word. In this aspect, our approach is related to Bajari et al. [2025], who used embeddings to create hedonic price indices using data from

Amazon. Further, unlike the aforementioned papers using text data, we move beyond the representation using embeddings and implement Zero-Shot classification to assign the text to interpretable user-defined classes. The Zero-Shot method turns the classification problem into an inference problem by fine-tuning deep representations from the transformer on a specialized language inference task and provides a proximity (entailment) of a given text to an arbitrary user-defined phrase. This entailment inference does not need any new training data, making it well-suited for applications like ours that do not have a large corpus of training data. Our prediction performance on recidivism using the probabilities generated for the user-defined classes (Zero-Shot) retains the predictive power of the results obtained using the high-dimensional text embeddings.

The linear-in-means peer effect model has been widely employed in econometrics for estimating peer effects [Bramoullé et al., 2009, 2020, Hayes and Levin, 2024, Johnsson and Moon, 2021, Manski, 1993]. In a seminal paper, Bramoullé et al. [2009] showed conditions under which the peer effect parameter is identifiable, enabling a Two Stage Least Squares (2SLS) solution when the network is not correlated with error conditional on covariates. However, typically in observational data, the network is endogenous, due to common latent variables explaining both network formation and outcomes. Several authors have proposed solutions to account for this unobserved heterogeneity by modeling the network generation process with a latent variable model and estimating the latent variables from observed network data [Chang and Paul, 2024, Goldsmith-Pinkham and Imbens, 2013, Johnsson and Moon, 2021, Nath et al., 2025].

The methodology developed in this paper applies to more general settings of peer effects, as our methods allow for multivariate latent traits to model the network formation relative to a univariate latent homophily variable in Goldsmith-Pinkham and Imbens [2013], Johnsson and Moon [2021], sparse networks, unlike the dense networks required in Auerbach [2022], Graham [2017], Johnsson and Moon [2021], and for multivariate outcomes. Two other papers that develop methods for peer effects in multivariate outcomes are Cohen-Cole et al. [2018], Zhu et al. [2020], but they do not account for endogeneity in network formation. Therefore, our proposed methodology expands the scope of peer effect estimation. Before implementing the new methods on real data, we assess the performance of the new estimator in numerical simulations. This analysis shows that the error rate in recovering all direct and indirect peer effect parameters declines steadily as we increase the sample size.

One key contribution of this paper’s new methodology is the estimation of network formation using the multivariate latent variables and nonparametric modeling of the effect of latent variables on the outcome, regressors, and instruments. As a precursor to the peer effects estimation, we compare the performance of four network models (tetra logit and joint fixed effect MLE from Graham [2017], RDPG model from Athreya et al. [2017], latent space without covariates in Hoff et al. [2002] and finally latent space with latent multiplicative, additive factors and observed covariates in Ma et al. [2020] in explain-

ing three critical network properties: modularity, standard deviation of row means, and transitivity of the clustering coefficient on our real data application. For both the male and female units, we find that the latent space model allowing for additive, multiplicative latent variables and observed covariates performs best in replicating the above-listed network properties.

With this new methodology, we estimate the multivariate peer effects model controlling for network endogeneity in language exchanges within the TC. We find evidence of network peer effects when aggregated by sender or receiver profiles. However, the magnitude of the direct peer influence is much larger than the indirect spillover across both male and female units. Figure B1 (Appendix) summarizes our pipeline from data to the findings and contributions.

2 Empirical Setup

This paper uses datasets from two male units and one female unit of Therapeutic Communities (TCs) located in a midwestern state in the United States. These TCs were free-standing, minimum security, community-based correctional facilities. Thus, while they were locked facilities, they were not units in a prison. These TCs drew from a mixed urban/suburban/rural catchment area; each unit had 80 beds. Since data was collected over time, the female unit had 982 residents, and the male units had 1649 residents. The two male units are located on two floors of the same TC, and henceforth they will be collectively referred to as the male unit. We observe the entry and exit dates of these residents. The residents may stay in these units for up to 180 days. They may either successfully graduate from the program at the end of their stay or leave it unsuccessfully. We find, on average, the residents stayed for about 120 days. Table B1 (in the Appendix) details the residents used in the analysis. There is a very high graduation rate from these units, with 87% of residents successfully graduating from the female unit, and the corresponding percentage of graduates for the male unit is 89%.

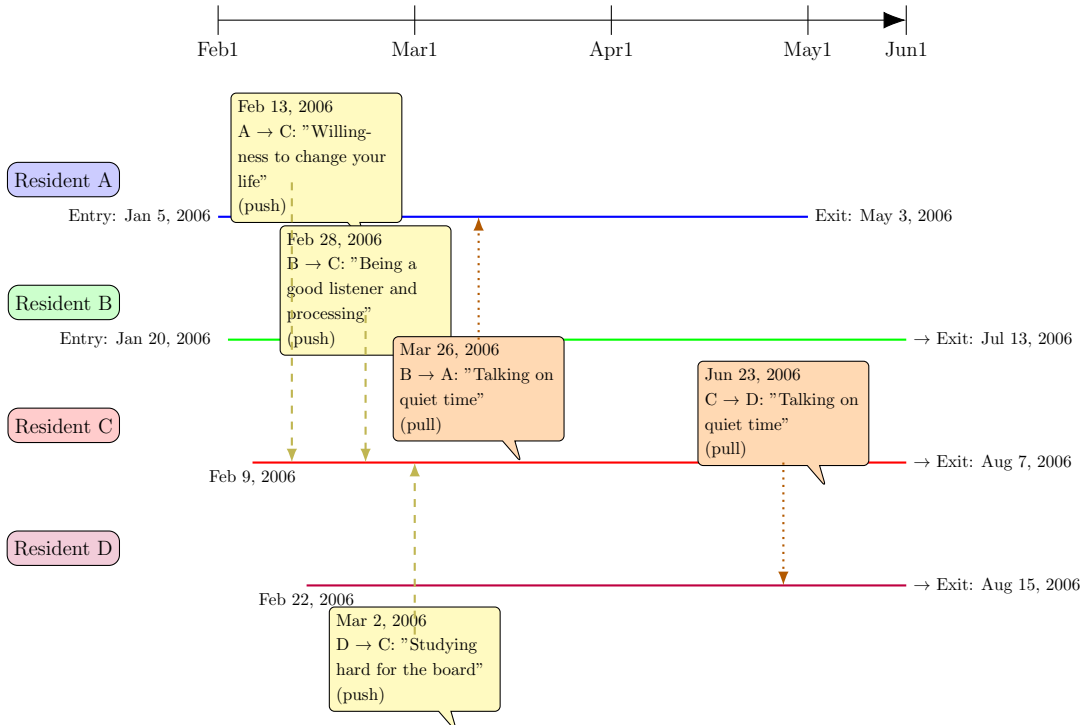
Given that we observe the time stamps of entry and exit, we observe a substantial variation in these dates and the residents' length of stay in these units. Figure B2 (a,b) shows the variation in these entry and exit dates, and panel (c) shows substantial differences in the length of the stay. The resident information from TCs is mapped with the administrative dataset maintained by the State's Department of Rehabilitation and Corrections. This administrative dataset provides the date of reincarceration of TC graduates, tracked up to 3 years. Reincarceration is one of several possible measures of recidivism, but it is the most commonly used in the criminology literature [Bouchard and Wong, 2024] and has been used in previous studies of TC outcomes [Doogan and Warren, 2016, Warren et al., 2007, 2020]. Table B1 shows that 22% of the residents had recidivism in the female unit and 25% in the male unit (among all residents, irrespective of graduation/success from TC treatment status). These numbers align with global figures obtained by Yukhnenko

et al. [2023] across 33 countries and various types of crimes.

During their stay in TCs, the residents were encouraged to exchange written affirmations and corrections with each other as part of their therapy. We observe the timestamps, text, sender, and receiver IDs for each of these exchanges in these TCs. The digitized records of these texts consist of 123,000 such exchanges between the residents in the female unit and about 83,000 exchanges between the residents in the male unit. Figure B3 (Appendix) shows the distribution of the count of affirmations (push) and corrections (pull) aggregated by sender ID in panels (a,b) and by receiver ID in panels (c,d), respectively. The female unit shows differences in the distribution of affirmations and corrections, with affirmations being less skewed. However, we see an almost overlapping distribution of corrections and affirmations in the male units.

These corrections and affirmations are short messages exchanged between the residents. Figure 1 provides a few examples of these messages and the data structure. In this figure, we create a sample of four residents who entered the facility around a similar time and exchanged messages. Note that this figure shows examples of only a few messages exchanged due to space constraints.

Figure 1: Timeline of resident stays and exchanges (2006)



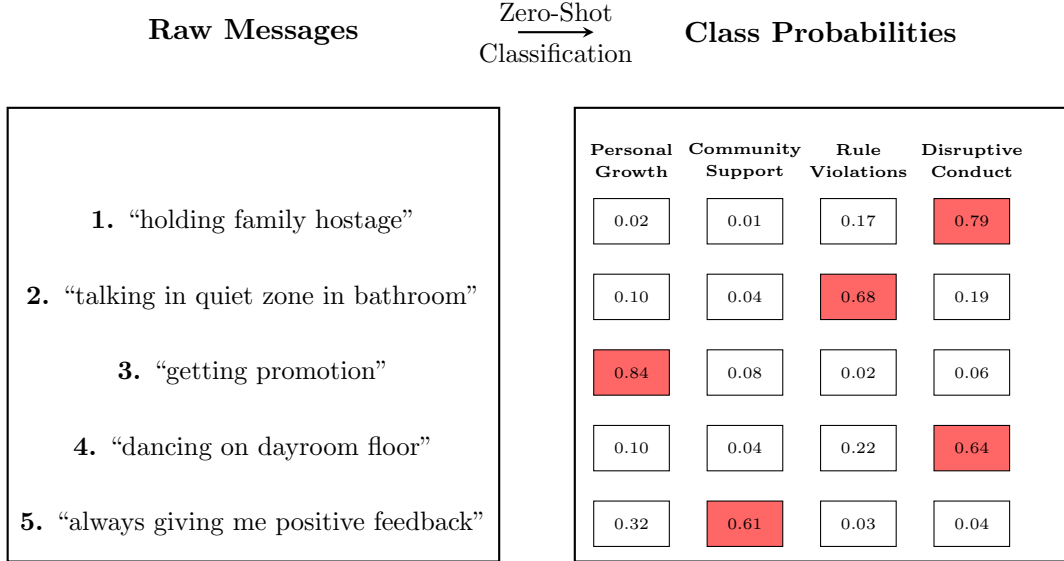
Notes: The dates of the entry, exit, and exchange of messages have been altered slightly for the construction of this figure to maintain the anonymity of residents.

We deploy transformer-based LLMs to create text embeddings separately for the 123,000 and 83,000 written exchanges in the female and male units. Precisely, we use the BERT (*bert-base-uncased*) language model from Devlin et al. [2019]. The implementation is done using the `text` package in R [Kjell et al., 2023] that allows users to access

these LLMs easily from huggingface.co. We use these embeddings to create sender and receiver profile vectors for the residents based on the language they use to interact with their peers. These embeddings represent how the behavior and engagement of individuals vary within the TC. The sender profiles indicate how individuals interact with their peers, for example, being supportive or dismissive of others. The receiver profiles, on the other hand, are related to the behavior of the individuals as perceived by their peers. This is because the messages individuals receive reflect their conduct during their stay in the TC (for example, being called out for disruptive conduct). We use these embeddings to assess two key questions- one related to predictive ability for recidivism and the other related to the mechanism of peer influence. We describe in Section 5 that these word embeddings have substantial predictive ability for recidivism.

However, it is hard to interpret these 768 dimensions meaningfully. Therefore, our second method uses a LLM-based Zero-Shot text classifier [Meshkin et al. \[2024\]](#), [Wang et al. \[2023\]](#), [Yin et al. \[2019\]](#) using the *BART* model of [Lewis et al. \[2019\]](#). In this method, the user provides a fixed class of words to the LLM along with the text messages, and the method generates predictions for the user-supplied classes for each message. Note that the classification is performed without seeing any labeled training data (and hence “Zero-Shot”), and with only the knowledge of natural language that the LLM has acquired. The classification mapping is explained in Figure 2. The figure provides examples of 5

Figure 2: Raw messages and their predicted class probabilities using transformer-based Zero-Shot classifier

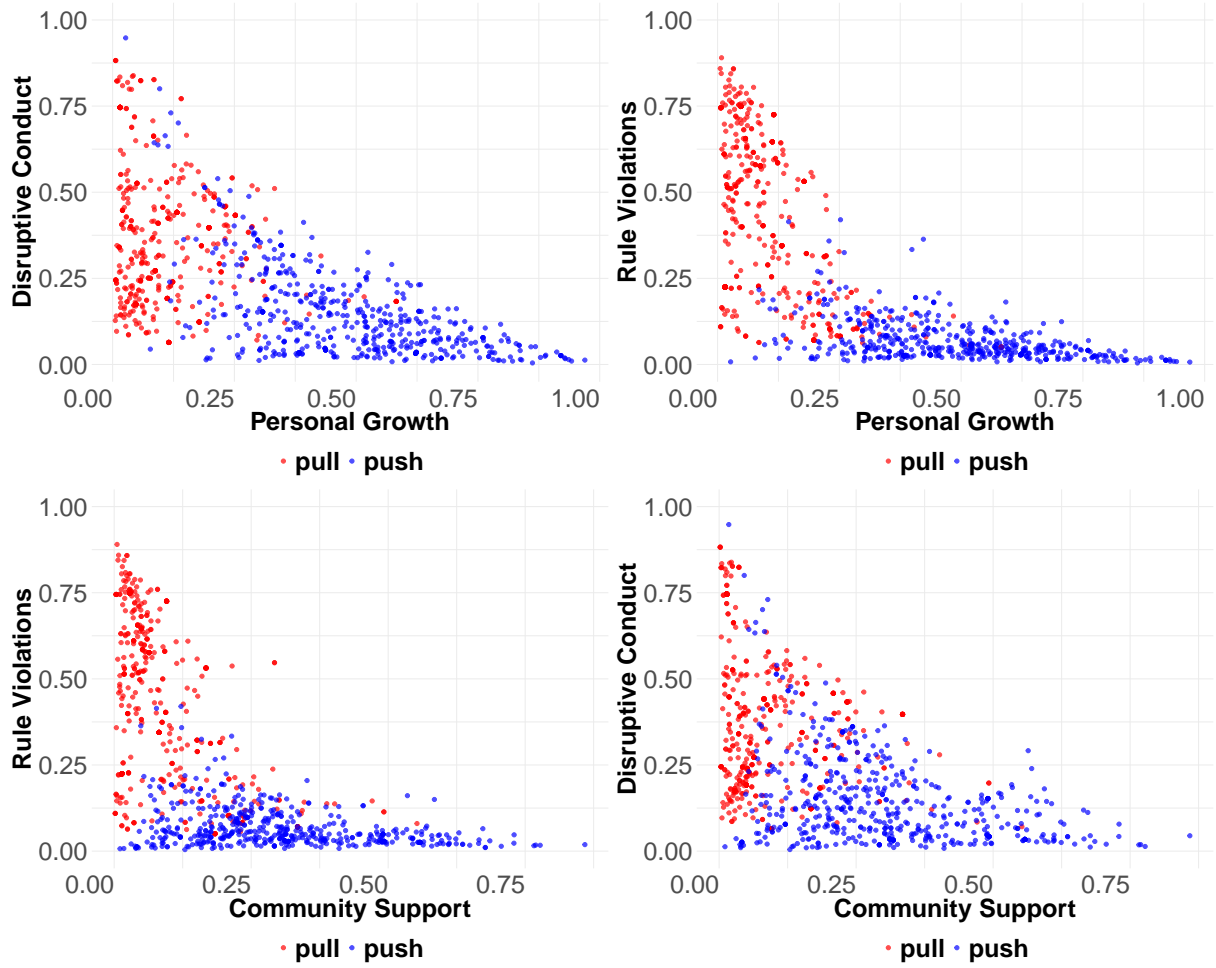


text messages from TCs and their associated LLM-based Zero-Shot classifier probabilities. This method is implemented using the `transforEmotion` package in R [[Christensen et al., 2024](#)]. Similar to the `text` package, any LLM-based Zero-Shot classifier with a pipeline on Huggingface can be implemented on the local machine without sending any data to an external server. The four user-supplied classes are chosen using the prompts to the

latest AI models, where we provide a random sample of 1000 written texts and query to provide four short phrases that best describe these messages for Zero-Shot classification. The LLM-based Zero-Shot classification method has been shown to achieve performance comparable with deep neural networks with access to labeled training data in biomedical applications [Meshkin et al., 2024].

We display the scatter plot for class probabilities by message type. The classification appears to work well as the probabilities for “rule violations” and “disruptive conduct” are much higher for corrections, and we see the opposite for affirmations (Figure 3 for females and Figure B4 for males, respectively). We review the methodology behind transformers, LLMs, and Zero-Shot classification in Section 3.

Figure 3: Class Probabilities and Message Type in Female Unit



Notes: Random sample of 1000 text messages was drawn from the female unit for this graph, with 50% sampling by message type.

Our final step is to study the underlying behavioral mechanism for these exchanges. Using the low-dimensional interpretable class probabilities, we set up a multivariate outcome model of peer effects that allows for contextual and endogenous peer effects and endogeneity in the network formation. The network links are generated using the information on entry and exit date stamps, along with the dates and frequency of the message

exchanges. We describe our peer effect estimation methodology in more detail in section 3.

3 Methodology and Theory

We describe our methodology that includes five components (described over seven subsections): (1) obtaining embedding vectors of the text exchanges from a pre-trained language model, (2) classifying the messages into user-defined categories through Zero-Shot classification, (3) using the embedding vectors into a high dimensional penalized regression model for predicting recidivism, (4) peer effect estimation using multivariate outcomes and endogenous networks, (5) modeling the network with a sparse multi-dimensional latent variable model.

3.1 LLM embedding of text and Zero-Shot classification

We deploy Pre-trained LLMs on the corpus of written messages to derive two representations: (1) context-sensitive embedding vectors and (2) probability vectors for meaningful psychological categories using Zero-Shot classification. We use the *bert-base-uncased* model [Devlin et al., 2019] for (1), and the *bart-large* model [Lewis et al., 2019] for (2). Before detailing the model structure, we briefly review the development of text embedding methods and discuss our rationale for adopting transformer-based AI models, such as BERT and BART.

A text embedding is a high-dimensional numerical vector representation of text. If two words convey similar meanings, they are represented closely in the vector space. However, earlier word embedding models, such as Word2Vec [Mikolov et al., 2013], did not consider the context for words, limiting their ability to handle words with multiple context-specific meanings. Transformer-based models, like BERT and BART, overcome these limitations using self-attention mechanisms [Vaswani et al., 2017], where the embedding for each word is dynamically influenced by the embedding of the entire input sequence, providing potentially different embeddings for each word based on context. The generative pre-training (GPT) framework Radford et al. [2018] uses semi-supervised learning in the transformer architecture. The model is pre-trained unsupervised on a large data corpus to learn embeddings or representations, followed by supervised fine-tuning for specific tasks. The language representation model BERT in Devlin et al. [2019] further improved the capabilities of pre-trained language models by introducing a bi-directional transformer, which can use both left and right context for a word as opposed to unidirectional processing (typically from left to right) in OpenAI GPT-1 of Radford et al. [2018].

The first step to processing text is tokenizing it into words or sub-words z_k for $k = 1, \dots, K$, forming a sequence $\mathbf{z} = (z_1, \dots, z_K)$ of tokens where K is the total number of tokens for each written text. For each token position k , both BART and BERT construct

an input embedding as a sum of token embedding $\mathbf{e}_k^{\text{token}}$ and a positional embedding $\mathbf{e}_k^{\text{pos}}$ as $\mathbf{e}_k = \mathbf{e}_k^{\text{token}} + \mathbf{e}_k^{\text{pos}}$. In BERT, an additional segment embedding $\mathbf{e}_k^{\text{seg}}$ is included if input text consists of a sentence pair: $\mathbf{e}_k = \mathbf{e}_k^{\text{token}} + \mathbf{e}_k^{\text{pos}} + \mathbf{e}_k^{\text{seg}}$. These vectors then form an input embedding matrix $\mathbf{E} = [\mathbf{e}_1, \dots, \mathbf{e}_K]^{\top} \in \mathbb{R}^{K \times H}$. Here H denotes the dimension of each embedding vector. Precisely, $H = 768$ for *bert-base-uncased* and $H = 1024$ for *bart-large*.

A sequence of transformer blocks processes \mathbf{E} , where the output of each block is fed as an input into the next block. Let the output of the l -th block be $\mathbf{E}^{(l)} \in \mathbb{R}^{K \times H}$, with the initial input being $\mathbf{E}^{(0)} = \mathbf{E}$. We next describe the processes involved in each of these transformer blocks and the multi-head self-attention mechanism.

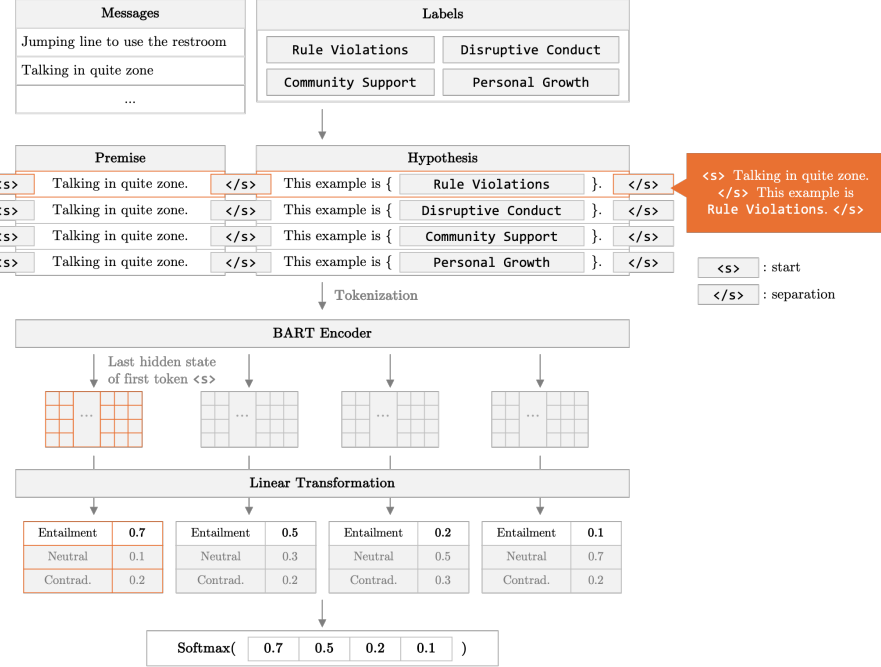
Multi-Head Self-Attention and transformer blocks To compute attention within each encoder block $l = 1, \dots, L$, the model first generates query ($\mathbf{Q}^{(l,a)}$), key ($\mathbf{K}^{(l,a)}$), and value matrices ($\mathbf{V}^{(l,a)}$) for each attention head $a = 1, \dots, A$. These matrices are obtained by multiplying the previous layer’s output $\mathbf{E}^{(l-1)}$ using head-specific learnable weight matrices $\mathbf{W}_B^{(l,a)}$ as follows, $\mathbf{B}^{(l,a)} = \mathbf{E}^{(l-1)} \mathbf{W}_B^{(l,a)} \in \mathbb{R}^{K \times d}$ for $\mathbf{B} \in \{\mathbf{Q}, \mathbf{K}, \mathbf{V}\}$, $\mathbf{W}_B^{(l,a)} \in \mathbb{R}^{H \times d}$ and $d = H/A$. For reference, *bert-base-uncased* uses $L = 12$ encoder layers with $A = 12$ attention heads, while *bart-large* uses $L = 12$ encoder layers with $A = 16$ attention heads (and hence $d = 64$ in both models). The k -th row of the matrix $\mathbf{Q}^{(l,a)}$ is denoted $\mathbf{q}_k^{(l,a)} \in \mathbb{R}^d$, with equivalent notation $\mathbf{k}_k^{(l,a)}$ and $\mathbf{v}_k^{(l,a)}$ for $\mathbf{K}^{(l,a)}$ and $\mathbf{V}^{(l,a)}$ respectively.

The query vector represents what the k -th token seeks, and the key vector indicates what each token offers others. The attention score between the k -th query and all K keys is given by $\mathbf{s}_k^{(l,a)} = [s_{k1}^{(l,a)}, s_{k2}^{(l,a)}, \dots, s_{kK}^{(l,a)}]^{\top} \in \mathbb{R}^K$. Each element in this vector is the scaled dot-product between the corresponding query and key vectors, $s_{kj}^{(l,a)} = \frac{\mathbf{q}_k^{(l,a)\top} \mathbf{k}_j^{(l,a)}}{\sqrt{d}}$. The attention weights are then obtained by normalizing $s_{kj}^{(l,a)}$ using the softmax function as $m_{kj}^{(l,a)} = \frac{\exp(s_{kj}^{(l,a)})}{\sum_{q=1}^K \exp(s_{kq}^{(l,a)})}$. Let $\mathbf{M}^{(l,a)} \in \mathbb{R}^{K \times K}$ be the attention weights matrix for all tokens in \mathbf{z} . The output matrix is given by $\mathbf{H}^{(l,a)} = \mathbf{M}^{(l,a)} \mathbf{V}^{(l,a)} \in \mathbb{R}^{K \times d}$. Next, the outputs from A heads are combined as: $\mathbf{H}^{(l)} = [\mathbf{H}^{(l,1)}, \mathbf{H}^{(l,2)}, \dots, \mathbf{H}^{(l,A)}] \in \mathbb{R}^{K \times H}$. The column-concatenated matrix $\mathbf{H}^{(l)}$ is then processed within the encoder block to generate the block’s final output $\mathbf{E}^{(l)}$ (Figure B5 in Appendix).

Text Embedding using BERT To numerically encode the semantic content of each message, we use the output from the 11th encoder block (i.e., the penultimate block) of *bert-base-uncased* model to construct an “embedding profile” for each participant — a high-dimensional vector summarizing their language use across multiple messages during their stay in TC. We choose the penultimate layer as that layer is widely thought to contain the unsupervised representation of data in the representation learning framework [Bengio et al., 2013], while the last layer is trained or fine-tuned to be task-specific. One can, in principle, also choose an embedding representation from an earlier layer, but not

the last layer. Let $\mathbf{f}_{c,k}^{\text{token}} \in \mathbb{R}^H$ denote the embedding of the k -th token in the c -th message, extracted from the 11th encoder. We obtain the message-level embedding by taking the average of these vectors over all tokens in the message as $\mathbf{f}_c^{\text{msg}} = \frac{1}{N_c} \sum_{k=1}^{N_c} \mathbf{f}_{c,k}^{\text{token}}$, where N_c is the number of tokens in message c . We then compute the “sender embedding profile” for a sender s by taking an average of the the message-level embeddings, $\mathbf{f}_s^{\text{sender}} = \frac{1}{N_s} \sum_{c \in \mathcal{C}_s} \mathbf{f}_c^{\text{msg}}$, where \mathcal{C}_s denotes the set of messages sent by sender s , and $N_s = |\mathcal{C}_s|$ is the number of such messages. The embedding profile for each receiver can be obtained analogously.

Figure 4: Process of Zero-Shot classification



3.2 Zero-Shot Classification

To interpret the embeddings, we relate them to interpretable psychological constructs, using the “Zero-Shot” classification framework [Yin et al., 2019]. In Zero-Shot classification, a user provides an arbitrary number of labels, and the LLM assigns given texts to the most appropriate label. This enables us to assign written affirmations and corrections to psychologically relevant categories without requiring additional training.

In Zero-shot learning, the classification problem is turned into a language inference problem. We use *bart-large* model fine-tuned on the MNLI (Multi-Genre Natural Language Inference) task dataset, a dataset designed for language inference task. In MNLI, each input consists of a premise and a hypothesis, and the pre-trained BART model is trained to classify the semantic relationship between them as one of three predefined MNLI classes: entailment, neutral, or contradiction. A premise-hypothesis combination is concatenated into a single input sequence using special tokens following the format: `<s> premise </s> hypothesis </s>`, which allows the model to process both segments

jointly while preserving their roles.

The encoder uses a self-attention mechanism that allows the model to capture contextual dependencies between tokens across both segments. This enables the model to assess how strongly the premise supports, contradicts, or is unrelated to the hypothesis. During training, the embedding of the first token $\langle s \rangle$ from the final encoder layer is passed to a classification head, which outputs a logit vector over the three MNLI classes.

Figure 4 illustrates how a TC text message is classified into user-defined categories using this framework. In our application, each peer message is treated as a premise, and we define four psychologically meaningful word strings: “Rule Violations”, “Disruptive Conduct”, “Community Support”, and “Personal Growth”. Each of the four strings is converted into a hypothesis using a fixed template: “This example is {}.”

For each message c , the model generates four premise-hypothesis pairs by combining the message with each label-based-hypothesis indexed by $\ell = 1, \dots, 4$. For each pair, the model obtains a probability vector for entailment $\mathbf{s}_c = (p_{c,\ell}^{\text{entail}})_{\ell=1}^4 \in \mathbb{R}^4$, which reflect how strongly the input message supports each of the user-defined categories. These four entailment scores are then passed through a softmax function to obtain a probability vector over the labels: $\boldsymbol{\pi}_c = \text{softmax}(\mathbf{s}_c)$. Finally, we aggregate these scores at the level of individuals to create personal class profiles, analogous to the embedding-based profiles described earlier, but in a more tractable lower-dimensional space.

3.3 Prediction models

We fit a penalized regression lasso method [Tibshirani, 1996] to predict recidivism using the resident-level covariates along with the individual embedding profiles. Suppose Y_i denotes the recidivism status for individual i , which takes the value 1 if the individual recidivates and 0 if the person does not recidivate. Therefore, we can model Y_i with a Bernoulli distribution with probability of success being p_i and then further model p_i using the covariates and embedding profiles. However, since the embedding profiles are high-dimensional, we use a penalized logistic regression method (logistic-lasso). Suppose \mathbf{X} is the $N \times p$ matrix of observed covariates and \mathbf{T} is the $N \times H$ matrix containing the dimensions of text embeddings obtained from the LLM model as columns. Then the logistic regression model is $\log\left(\frac{p_i}{1-p_i}\right) = \beta_0 + \mathbf{X}_i\beta_1 + \mathbf{T}_i\beta_2$, where β_1 and β_2 are p and H dimensional parameter vectors respectively. We optimize for β_1, β_2 by maximizing the penalized likelihood function with ℓ_1 penalty as follows,

$$(\hat{\beta}_1, \hat{\beta}_2) = \text{argmin}\{-\ell(\beta_1, \beta_2, \mathbf{X}, \mathbf{T}) + \lambda_1\|\beta_1\|_1 + \lambda_2\|\beta_2\|_1\}.$$

The parameters λ_1, λ_2 denote the penalty parameters which maybe different for the observed covariates and the embedding vectors. We assess the model’s predictive accuracy with out-of-sample AUC values through a five-fold cross-fitting.

Beyond predicting recidivism, we also want to interpret the link between individual behavioral and emotional profiles as manifested by the messages with recidivism. In order

to do so we perform a Zero-Shot classification as described before to classify the messages into the four groups. Let \mathbf{Q} denote the $N \times 4$ matrix containing the average of probabilities assigned to the messages sent (respectively received) by each individual. Since the predictors are now low-dimensional (just four dimensions in addition to the covariates), we will not need to penalize the coefficients. However, we note that some of the covariates are now ‘‘compositional’’, since $\sum_j Q_{ij} = 1$ for each resident i . Therefore, following standard techniques of dealing with compositional predictors, we designate one covariate as baseline and take log ratios (ALR) of other covariates with respect to the baseline covariate [Aitchison, 1982]. This is important for interpreting the model coefficients, but not for prediction accuracy. We note that we could just continue with the original predictors and drop the intercept, and have a model with comparable prediction accuracy.

3.4 Multivariate Peer Effects Model with Endogenous Network Formation

We consider the multivariate peer effect model, which captures dependencies among multiple outcomes observed across spatially or network-connected entities. Suppose we have N entities and we observe m outcome variables, and p covariates for each entity. Further, we observe a network among the entities whose adjacency matrix is \mathbf{A} , where the elements a_{ij} represent the relationship between entities i and j . Then we define the multivariate peer effect model as:

$$\mathbf{Y} = \mathbf{G}\mathbf{Y}\mathbf{D} + \mathbf{X}\mathbf{B}_1 + \mathbf{G}\mathbf{X}\mathbf{B}_2 + \mathbf{E}, \quad (1)$$

where $\mathbf{Y} \in \mathbb{R}^{N \times m}$ is the matrix of outcome variables, $\mathbf{G} = (g_{ij}) \in \mathbb{R}^{N \times N}$ where $g_{ij} := \frac{a_{ij}}{\sum_{j \neq i} a_{ij}}$, is the row-normalized counterpart of the network adjacency matrix \mathbf{A} , and $\mathbf{X} \in \mathbb{R}^{N \times p}$ is the matrix of observed covariates. We write $\mathbf{Y}_i \in \mathbb{R}^m$ and $\mathbf{Y}_{\cdot j} \in \mathbb{R}^N$ to denote the i -th row and j -column vectors of an $N \times m$ matrix \mathbf{Y} , respectively. The parameters have the following interpretation. The matrix $\mathbf{D} \in \mathbb{R}^{m \times m}$ is the peer effect parameter matrix. The diagonal of \mathbf{D} are the direct peer spillover effects on the same dimensions of \mathbf{Y} , and the off-diagonal elements are the indirect peer spillover effects of a dimension on another dimension. The matrices $\mathbf{B}_1, \mathbf{B}_2 \in \mathbb{R}^{p \times m}$ are coefficient matrices for \mathbf{X} and $\mathbf{G}\mathbf{X}$, respectively. However, since the network is endogenous, we cannot identify and consistently estimate \mathbf{D} from this model using Bramoullé et al. [2009]’s IV 2LSLS framework. For concreteness, we assume for each individual there is a vector \mathbf{U}_i of latent homophily variables that is correlated with both the network adjacency matrix \mathbf{A} and the error matrix \mathbf{E} . We assume the error matrix $\mathbf{E} \in \mathbb{R}^{N \times m}$ is such that for each row $\mathbb{E}[\mathbf{E}_i | \mathbf{U}_i] = \mathbf{h}^E(\mathbf{U}_i)$ for some unknown function \mathbf{h}^E , and $\mathbb{V}[\mathbf{E}_i | \mathbf{U}_i] = \mathbf{V}$. The matrix \mathbf{V} allows dependence across outcome dimensions. The vectors $\mathbf{E}_i, \mathbf{X}_i, \mathbf{U}_i$ are assumed to be i.i.d. across individuals i . We let $A_{ij} = f(\mathbf{U}_i, \mathbf{U}_j, \xi_{ij})$, where ξ_{ij} s over all (i, j) are assumed to be i.i.d and independent of $\mathbf{X}, \mathbf{E}, \mathbf{U}$. We postpone the discussion on models for network formation until the next section. We further assume that $\mathbb{E}[\mathbf{E}_i | \mathbf{X}_i, \mathbf{U}_i] = \mathbb{E}[\mathbf{E}_i | \mathbf{U}_i]$, i.e.,

conditional on \mathbf{U}_i , the covariates \mathbf{X}_i and error term \mathbf{E}_i are uncorrelated.

This model is similar to the multivariate extension of the spatial autoregressive (MSAR) model proposed in [Zhu et al., 2020]. However, the model in Zhu et al. [2020] can be used for peer effect estimation only under the assumption of exogenous network formation, i.e., \mathbf{G} is uncorrelated with \mathbf{E} . Further, model (1) can also be thought of as a multivariate extension of the endogenous and simultaneous peer effect model in Johnsson and Moon [2021], both in terms of multidimensional outcome variables (\mathbf{Y}) and latent variables (\mathbf{U}).

To identify the parameter matrices, we take an instrumental variable approach similar to Johnsson and Moon [2021], but extend the methodology in several directions as we detail below. We define the combined regressor and instrument matrices as:

$$\mathbf{Z} = [\mathbf{GY}, \mathbf{X}, \mathbf{GX}] \in \mathbb{R}^{N \times (m+2p)}, \quad \mathbf{K} = [\mathbf{X}, \mathbf{GX}, \mathbf{G}^2\mathbf{X}] \in \mathbb{R}^{N \times 3p}.$$

The stacked parameter matrix is:

$$\boldsymbol{\beta} = [\mathbf{D}, \mathbf{B}_1, \mathbf{B}_2]^T \in \mathbb{R}^{(m+2p) \times m}.$$

Using this notation, equation (1) can be written compactly as $\mathbf{Y} = \mathbf{Z}\boldsymbol{\beta} + \mathbf{E}$. A natural estimator for $\boldsymbol{\beta}$ is the two-stage least squares (2SLS) estimator:

$$\hat{\boldsymbol{\beta}}_{\text{IV}} = (\mathbf{Z}^\top \mathbf{K}(\mathbf{K}^\top \mathbf{K})^{-1} \mathbf{K}^\top \mathbf{Z})^{-1} \mathbf{Z}^\top \mathbf{K}(\mathbf{K}^\top \mathbf{K})^{-1} \mathbf{K}^\top \mathbf{Y}. \quad (2)$$

This estimator is a multivariate extension of the estimator proposed in Bramoullé et al. [2009], Kelejian and Prucha [1998] and is a consistent estimator provided the network is exogenous, which is not the case in our setup. Taking expectations on both sides of Equation 1 conditioning on \mathbf{U} and subtracting this from equation 1, we obtain

$$\mathbf{Y} - \mathbb{E}[\mathbf{Y}|\mathbf{U}] = (\mathbf{Z} - \mathbb{E}[\mathbf{Z}|\mathbf{U}])\boldsymbol{\beta} + (\mathbf{E} - \mathbb{E}[\mathbf{E}|\mathbf{U}]). \quad (3)$$

If we redefine, $\tilde{\mathbf{Y}} = \mathbf{Y} - \mathbb{E}[\mathbf{Y}|\mathbf{U}]$, $\tilde{\mathbf{Z}} = \mathbf{Z} - \mathbb{E}[\mathbf{Z}|\mathbf{U}]$, and $\tilde{\mathbf{K}} = \mathbf{K} - \mathbb{E}[\mathbf{K}|\mathbf{U}]$. Then we can write the above equation as, $\tilde{\mathbf{Y}} = \tilde{\mathbf{Z}}\boldsymbol{\beta} + \tilde{\mathbf{E}}$, where $\tilde{\mathbf{E}} = \mathbf{E} - \mathbb{E}[\mathbf{E}|\mathbf{U}]$. For this redefined linear model we can solve for $\boldsymbol{\beta}$ using IV-2SLS with the redefined instrument matrix $\tilde{\mathbf{K}}$. The moment equation for this is given by

$$\mathbb{E}[(\mathbf{K}_i - \mathbb{E}[\mathbf{K}_i|\mathbf{U}_i])^T (\mathbf{Y}_i - \mathbb{E}[\mathbf{Y}_i|\mathbf{U}_i] - (\mathbf{Z}_i - \mathbb{E}[\mathbf{Z}_i|\mathbf{U}_i])\boldsymbol{\beta})] = 0 \quad (4)$$

The following lemma provides sufficient conditions for the identification of the true parameter matrix $\boldsymbol{\beta}_0$.

Lemma 1. *Under assumptions that the $3p \times (m+2p)$ matrix $\mathbb{E}[(\mathbf{K}_i - \mathbb{E}[\mathbf{K}_i|\mathbf{U}_i])^T ((\mathbf{Z}_i - \mathbb{E}[\mathbf{Z}_i|\mathbf{U}_i])]$ has full column rank, the true parameter $\boldsymbol{\beta}_0$ can be obtained by solving the $3p \times m$ moment matrix condition in Equation 4.*

Therefore, given access to the latent positions \mathbf{U} and the three conditional mean functions, the parameter $\boldsymbol{\beta}_0$ can be estimated using 2SLS. Note that the rank condition in Lemma 1 can generally be satisfied with $p > m$, i.e., if we have more covariates than dimensions. However, the moment equation cannot be estimated as we do not observe \mathbf{U} and do not know the conditional expectations of $\mathbf{Y}, \mathbf{Z}, \mathbf{K}$ given \mathbf{U} . We next address how to estimate both of these.

3.5 Latent positions and Non-Parametric estimation with Sieves

As mentioned earlier, we model the network data using a latent variable model $A_{ij} = f(\mathbf{U}_i, \mathbf{U}_j, \xi_{ij})$ and posit that the node level latent variables \mathbf{U}_i are involved in both the network formation model and are correlated with the error term of the outcome model. These latent variables represent unobserved characteristics of individuals, which may be responsible for tie formation (latent homophily), and an unknown function of these latent variables is part of the error term in the outcome model. Therefore, these latent variables can be estimated from the observed network. This is a core assumption made in recent methodological advances in peer effect estimation [Goldsmith-Pinkham and Imbens, 2013, Johnsson and Moon, 2021, McFowland III and Shalizi, 2023, Nath et al., 2025]. However, while McFowland III and Shalizi [2023], Nath et al. [2025] focused on the longitudinal peer effect model, we consider the simultaneous peer effect model. Further, McFowland III and Shalizi [2023], Nath et al. [2025] assumed the latent variables enter the model for \mathbf{Y} linearly as $\mathbf{U}\beta$. In contrast, we assume the conditional expectations of $\mathbf{Y}, \mathbf{Z}, \mathbf{K}$ to be unknown functions $\mathbf{h}(\mathbf{U})$ of the latent variables. In this aspect, our approach resembles Johnsson and Moon [2021], however, we consider more general latent variable models for network data with multi-dimensional latent variables which are more realistic for modeling individual characteristics. Further, the theoretical results in Johnsson and Moon [2021] requires the network to be “dense” in the sense that every individual is expected to be connected to $O(N)$ individuals and consequently, total number of edges in the network is expected to be $O(N^2)$. This is quite unrealistic as real-world networks tend to be sparse with individuals connected to only a few other people, even when the network size is huge (e.g., in online social networks, even if there are millions of people present in the network, an individual member only has a few hundred or thousands of connections). In contrast, our results here hold for sparse networks.

We define the stacked data matrix $\mathbf{W} := [\mathbf{Y}, \mathbf{Z}, \mathbf{K}] \in \mathbb{R}^{N \times (2m+5p)}$. The conditional mean functions are defined as $\mathbf{h}^Y(\mathbf{U}) := \mathbb{E}[\mathbf{Y} | \mathbf{U}]$, $\mathbf{h}^Z(\mathbf{U}) := \mathbb{E}[\mathbf{Z} | \mathbf{U}]$, and $\mathbf{h}^K(\mathbf{U}) := \mathbb{E}[\mathbf{K} | \mathbf{U}]$. These are collected into the full conditional mean matrix $\mathbf{h}(\mathbf{U}) := [\mathbf{h}^Y(\mathbf{U}), \mathbf{h}^Z(\mathbf{U}), \mathbf{h}^K(\mathbf{U})] \in \mathbb{R}^{N \times (2m+5p)}$. The function $\mathbf{h} : \mathbb{R}^d \rightarrow \mathbb{R}^{2m+3p}$ is an unknown non-linear function of \mathbf{U}_i . Let $h_j(\cdot) : \mathbb{R}^N \rightarrow \mathbb{R}$ denote the j th component of $\mathbf{h}(\cdot)$, for $j = 1, \dots, (2m + 5p)$. Then, for each \mathbf{U}_i , $h_j(\mathbf{U}_i) \in \mathbb{R}$ is the scalar value of the j th conditional mean component. In what follows, to keep the notation simple, let \mathbf{u} denote a generic row \mathbf{U}_i .

To estimate each component function $h_j(\mathbf{u})$, we use tensor-product basis functions Zhang and Simon [2023] given by $\phi_k(\mathbf{u}) = \prod_{\ell=1}^d \psi_{k_\ell}^{(\ell)}(u_\ell)$, where each $\psi_{k_\ell}^{(\ell)}$ is a univariate basis function (polynomial or cosine) on the ℓ -th coordinate of \mathbf{u} . With these basis functions, we approximate each component function $h_j(\mathbf{u})$, by a linear combination of basis functions:

$$h_j(\mathbf{u}) \approx \sum_{k=1}^{L_N} \phi_k(\mathbf{u}) \alpha_k^j = \sum_{k=1}^{L_N} \prod_{\ell=1}^d \psi_{k_\ell}^{(\ell)}(u_\ell) \alpha_k^j,$$

where $\boldsymbol{\alpha}^j = (\alpha_1^j, \dots, \alpha_{L_N}^j)^\top \in \mathbb{R}^{L_N}$ is the coefficient vector, and the number of basis

functions to use L_N is possibly a function of N . Note this formulation allows for different univariate basis functions indexed by ψ_{k_ℓ} for each component basis ϕ_k and each dimension of u_ℓ . It also allows for interactions among the predictors.

For the generic vector \mathbf{u} , let $\boldsymbol{\phi}^{L_N}(\mathbf{u}) := (\phi_1(\mathbf{u}), \dots, \phi_{L_N}(\mathbf{u}))^\top \in \mathbb{R}^{L_N}$. Then we construct the design matrix for all N observations as: $\boldsymbol{\Phi}_N := [\boldsymbol{\phi}^{L_N}(\mathbf{u}_1), \dots, \boldsymbol{\phi}^{L_N}(\mathbf{u}_N)]^\top \in \mathbb{R}^{N \times L_N}$. The coefficient vector $\boldsymbol{\alpha}^j$ is obtained by regressing the observed vector $\mathbf{w}_{\cdot j}$ on the basis matrix $\boldsymbol{\Phi}_N$ via ordinary least squares, as $\hat{\boldsymbol{\alpha}}^j = (\boldsymbol{\Phi}_N^\top \boldsymbol{\Phi}_N)^{-1} \boldsymbol{\Phi}_N^\top \mathbf{w}_{\cdot j}$. The fitted values for the j th component function at all sample points are then given by: $\hat{h}_j(\mathbf{U}) := \boldsymbol{\Phi}_N \hat{\boldsymbol{\alpha}}^j = \mathbf{P}_{\boldsymbol{\Phi}_N} \mathbf{w}_{\cdot j}$, where $\mathbf{P}_{\boldsymbol{\Phi}_N} := \boldsymbol{\Phi}_N (\boldsymbol{\Phi}_N^\top \boldsymbol{\Phi}_N)^{-1} \boldsymbol{\Phi}_N^\top$ is the projection matrix associated with the basis space, and A^- denotes any symmetric generalized inverse of A .

Since latent positions \mathbf{U} are unknown, we use a two-step procedure. For estimating \mathbf{U} , we model the network using latent variable models such as the RDPG model [Athreya et al., 2017, Rubin-Delanchy et al., 2022, Xie and Xu, 2023] and the additive and multiplicative effects latent space model [Hoff, 2021, Hoff et al., 2002, Li et al., 2023, Ma et al., 2020]. Then our two-stage procedure is as follows. (i) we first construct an estimator $\hat{\mathbf{U}} := (\hat{\mathbf{u}}_1, \dots, \hat{\mathbf{u}}_N)^\top$ for the latent traits using spectral embedding for RDPG models or maximum likelihood estimation for additive and multiplicative effects latent space models, and (ii) we evaluate the basis functions at $\hat{\mathbf{U}}$ and apply the same projection strategy. With these estimated latent vectors, we define the estimated design matrix as $\hat{\boldsymbol{\Phi}}_N := \boldsymbol{\Phi}_N(\hat{\mathbf{U}}) = [\boldsymbol{\phi}^{L_N}(\hat{\mathbf{u}}_1), \dots, \boldsymbol{\phi}^{L_N}(\hat{\mathbf{u}}_N)] \in \mathbb{R}^{N \times L_N}$. The final estimated conditional mean functions are $\hat{\mathbf{h}}^W(\hat{\mathbf{U}}) := \mathbf{P}_{\hat{\boldsymbol{\Phi}}_N} \mathbf{W}$ where $\mathbf{P}_{\hat{\boldsymbol{\Phi}}_N} := \hat{\boldsymbol{\Phi}}_N (\hat{\boldsymbol{\Phi}}_N^\top \hat{\boldsymbol{\Phi}}_N)^{-1} \hat{\boldsymbol{\Phi}}_N^\top$.

Denote $\mathbf{M}_{\hat{\boldsymbol{\Phi}}_N} = \mathbf{I}_N - \mathbf{P}_{\hat{\boldsymbol{\Phi}}_N}$. Then, our Two-Stage Least Squares (2SLS) estimator is defined as:

$$\begin{aligned} \hat{\boldsymbol{\beta}}_{2SLS} &= \left(\mathbf{Z}_N^T \mathbf{M}_{\hat{\boldsymbol{\Phi}}_N} \mathbf{K}_N (\mathbf{K}_N^T \mathbf{M}_{\hat{\boldsymbol{\Phi}}_N} \mathbf{K}_N)^{-1} \mathbf{K}_N^T \mathbf{M}_{\hat{\boldsymbol{\Phi}}_N} \mathbf{Z}_N \right)^{-1} \\ &\quad \times \mathbf{Z}_N^T \mathbf{M}_{\hat{\boldsymbol{\Phi}}_N} \mathbf{K}_N (\mathbf{K}_N^T \mathbf{M}_{\hat{\boldsymbol{\Phi}}_N} \mathbf{K}_N)^{-1} \mathbf{K}_N^T \mathbf{M}_{\hat{\boldsymbol{\Phi}}_N} \mathbf{Y}_N. \end{aligned} \quad (5)$$

3.6 Network models

In terms of latent variable network models, we first consider the Latent Space Model (LSM), which is a general random graph model that includes both additive and multiplicative latent variables and can also accommodate covariates [Hoff, 2021, Hoff et al., 2002, Li et al., 2023, Ma et al., 2020]. The model is parameterized by d -dimensional unknown vectors \mathbf{q}_i and unknown scalars v_i for all nodes $i = 1, \dots, n$.

We also assume that we have edge level covariates $\mathbf{X} = (x_{ij})$ available to us. A network adjacency matrix $\mathbf{A} = (a_{ij})$ from this model is generated as follows [Chang and Paul, 2024, Li et al., 2023, Ma et al., 2020]:

$$a_{ij} \stackrel{ind.}{\sim} f_{ij} := f(a; \theta_{ij}), \quad \theta_{ij} := \sigma(\mathbf{q}_i' \mathbf{q}_j + v_i + v_j + x_{ij} \beta), \quad 1 \leq i < j \leq n$$

where f is a family of distributions satisfying certain smoothness conditions, and $\sigma : \mathbb{R} \rightarrow \mathbb{R}$ is a known link function. In this paper, we consider a particular sparse version

of the model due to [Li et al. \[2023\]](#) that assumes f to be a Bernoulli distribution, link function σ to be the logistic function, and there exists a sparsity parameter ρ_N such that $\theta_{ij} = \text{logistic}(\mathbf{q}_i' \mathbf{q}_j + v_i + v_j + x_{ij}\beta + \rho_N)$. Defining $\omega_N = \exp(\rho_N)$, we assume $\omega_N \rightarrow 0$ and $\omega_N = \omega(N^{-1/2})$. Let $\mathbf{u}_i \triangleq (\mathbf{q}_i', v_i)'$ denote a parameter vector containing all latent variables associated with node i . Then, we can write the latent variable matrix collectively as

$$\mathbf{U} := [\mathbf{u}_1, \dots, \mathbf{u}_N]' = \mathbf{Q}\mathbf{Q}' + \mathbf{v}\mathbf{1}_N' + \mathbf{1}_N\mathbf{v}'.$$

A special case of this model is Random Dot Product Graph (RDPG) model, which can be expressed as follows,

$$(a_{ij} | \mathbf{u}_i, \mathbf{u}_j) \stackrel{\text{ind.}}{\sim} \text{Bernoulli}(\rho_N \mathbf{u}_i' \mathbf{u}_j),$$

where ρ_N again controls the sparsity of the model. We will assume $\rho_N = \omega(\frac{\log^4 N}{N})$. Note the expected density (i.e., probability of an edge) scales with N as ρ_N , or in other words, the expected degree scales as $N\rho_N$ in this model, making the model suitable for sparse networks. This model does not account for the additive latent variables v_i 's but contains d -dimensional multiplicative latent variables, and the link function $\sigma(\cdot)$ is specified as identity. Clearly, both these models allow for multidimensional latent variables in the network formation model and is more general than the single latent variable model considered in [Johnsson and Moon \[2021\]](#). Both models are also capable of modeling sparse networks, which the models in [Auerbach \[2022\]](#), [Graham \[2017\]](#), [Johnsson and Moon \[2021\]](#) are not capable of. We compare the model fit from these network models with the network model considered in [Graham \[2017\]](#), [Johnsson and Moon \[2021\]](#) for the network data in our application in real data analysis (see section 5.2).

We employ the maximum likelihood estimator with Lagrange adjustment in [Li et al. \[2023\]](#) for the estimation of the LSM model. Let $\hat{\mathbf{U}}$ denote the maximum likelihood estimator over the constrained parameter space

$$\Xi_d := \{\mathbf{U} \in \mathbb{R}^{N \times (d+1)}; \mathbf{Q}'\mathbf{1}_N = \mathbf{0}_d, \mathbf{Q}'\mathbf{Q} \text{ is diagonal}, \|\mathbf{U}\|_{2,\infty} = O(1) \text{ as } N \rightarrow \infty\}.$$

Under the set of assumptions laid out in [Li et al. \[2023\]](#), an upper bound on the error rate of estimating the latent positions in Frobenius norm [[Li et al., 2023](#)] is $\frac{1}{N}\|\hat{\mathbf{U}} - \mathbf{U}\|_F^2 = O_p(\frac{1}{N\omega_N})$.

Although the LSM described above contains the RDPG model as its special case, there exists a rich amount of results with better convergence rates of the estimate of \mathbf{U} when one uses spectral embedding to approximate \mathbf{U} in the case of RDPG [[Athreya et al., 2017](#), [Cape et al., 2019](#), [Xie and Xu, 2023](#)]. Specifically, the spectral embedding of the adjacency matrix A can be written as $\hat{\mathbf{U}} = \mathbf{U}_A |\mathbf{S}_A|^{1/2}$, where \mathbf{U}_A denotes the matrix containing the leading d eigenvectors of \mathbf{A} , which are assumed, without loss of generality, to be ordered by decreasing absolute eigenvalue magnitude. The matrix $|\mathbf{S}_A|$ is a diagonal matrix containing the absolute values of the corresponding eigenvalues. Then, a faster

convergence rate than LSM can be obtained in terms of the $2 \rightarrow \infty$ norm as [Rubin-Delanchy et al., 2022] $\|\hat{\mathbf{U}} - \mathbf{U}\mathbf{H}\|_{2,\infty} = O_{hp}\left(\frac{\log^c N}{N^{1/2}}\right)$. Here we mean $X_n = O_{hp}(1)$ by: for every $c > 0$ there exist constants $M(c), n_0(c) > 0$ such that $\Pr(|X_n| > M) < n^{-c}$ for all $n > n_0$.

Our method, combining all the above components, is described in Algorithm 1. Note that the step estimating $\hat{\mathbf{U}}$ with spectral embedding in the algorithm will be replaced with MLE when the latent space model is used for the underlying network.

3.7 Theoretical results

For a matrix A we denote its spectral norm as $\|A\| = \max_{\|x\|=1} |Ax|$, Frobenius norm as $\|A\|_F = \sqrt{\sum_{ij} a_{ij}^2}$ and the $2 \rightarrow \infty$ norm as $\|A\|_{2,\infty} = \max_i \sqrt{\sum_j a_{ij}^2}$. We use the stochastic order notation $o_p(1)$ to mean that if $x_N = o_p(1)$, then $x_N \xrightarrow{p} 0$. We start with a list of assumptions. The first assumption is a collection of conditions described above in the description of the model, making the model well-behaved and identification possible, similar to those in [Johnsson and Moon, 2021].

Assumption 1. *The vectors $(\mathbf{X}_i, \mathbf{U}_i, \mathbf{E}_i)$ are i.i.d. across individuals $i = 1, \dots, N$, $A_{ij} = f(\mathbf{U}_i, \mathbf{U}_j, \xi_{ij})$, where ξ_{ij} s over all (i, j) are i.i.d and independent of $\mathbf{X}, \mathbf{E}, \mathbf{U}$, and $\mathbb{E}(\mathbf{E}_i | \mathbf{X}_i, \mathbf{U}_i) = \mathbb{E}(\mathbf{E}_i | \mathbf{U}_i)$. In addition, let $\mathbb{E}(\mathbf{X}_1) = \mathbf{0}_p$, and we have a universal constant $M > 0$ such that $\Pr(\|\mathbf{e}_1\|_\infty \leq M) = \Pr(\|\mathbf{x}_1\|_\infty \leq M) = 1$.*

We note again that the network \mathbf{A} is endogenous by the dependence between \mathbf{U}_i and \mathbf{E}_i . In addition, this implies that

$$\mathbb{E}(\mathbf{E}_i | \mathbf{X}_i, \mathbf{A}, \mathbf{U}_i) = \mathbb{E}(\mathbf{E}_i | \mathbf{X}_i, \mathbf{A}(\mathbf{U}_i, \mathbf{U}_{-i}, \xi_{ij}), \mathbf{U}_i) = \mathbb{E}(\mathbf{E}_i | \mathbf{X}_i, \mathbf{U}_i) = \mathbb{E}(\mathbf{E}_i | \mathbf{U}_i),$$

i.e., covariates and observed network are uncorrelated with the model error conditional on the latent variables \mathbf{U}_i .

Assumption 2. *Assume the following on the Sieve estimation.*

(i) $L_N = o(N)$.

(ii) *We have*

$$\lim_{N \rightarrow \infty} \mathbf{v}' \mathbb{E}[\phi^{L_N}(\mathbf{u}_1) \phi^{L_N}(\mathbf{u}_1)'] \mathbf{v} = \lim_{N \rightarrow \infty} \sum_{1 \leq i, j \leq L_N} v_i v_j \mathbb{E} \left[\prod_{1 \leq k, l \leq d} \psi_{i_k}^{(k)}(u_{1k}) \psi_{j_l}^{(l)}(u_{1l}) \right] > 0$$

for any $\mathbf{v} = (v_1, \dots, v_{L_N}) \in S^{L_N-1}$.

(iii) *Almost surely, there exists $\zeta_0(L_N)$ such that*

$$\sup_{\mathbf{u} \in \mathcal{U}} \|\phi^{L_N}(\mathbf{u})\|^2 = \sup_{\mathbf{u} \in \mathcal{U}} \sum_{j \leq L_N} \left(\prod_{k \leq d} \psi_{j_k}^{(k)}(u_k) \right)^2 \leq \zeta_0(L_N)^2 \quad \& \quad \frac{\zeta_0(L_N)^2 L_N}{N} = o(1),$$

and a sequence $\boldsymbol{\alpha}_{L_N}^j$ and a number $\kappa > 0$ such that

$$\sup_{f \in \{Y, Z, K\}} \sup_{j \in \mathcal{I}(f)} \sup_{\mathbf{u} \in \mathcal{U}} \left| h_j^f(\mathbf{u}) - \boldsymbol{\phi}^{L_N}(\mathbf{u})' \boldsymbol{\alpha}_{L_N}^j \right| = O(L_N^{-\kappa})$$

and $L_N^{-\kappa} = o(1/\sqrt{N})$.

The above assumption is an extension of the assumption in [Johnsson and Moon \[2021\]](#) to multivariate basis functions which says the true component-wise functions $h_j(u)$ are well approximated by the sieve approximations for all vectors u and all components j .

Assumption 3. *There exists a positive number $\zeta_1(k)$ such that for all $k = 1, \dots, L_N$,*

$$|\phi_k(\mathbf{u}) - \phi_k(\mathbf{u}')| = \left| \prod_{l \leq d} \psi_{k_l}^{(l)}(u_l) - \prod_{l \leq d} \psi_{k_l}^{(l)}(u'_l) \right| \leq \zeta_1(k) \|\mathbf{u} - \mathbf{u}'\|$$

and

$$\{1 \vee \zeta_0(L_N)^2\} \sum_{k=1}^{L_N} \zeta_1^2(k) = \begin{cases} o\left(\frac{N}{\log^{2c} N}\right) & \text{if } \mathbf{A} \sim RDPG \\ o(N\omega_N) & \text{if } \mathbf{A} \sim LSM. \end{cases}$$

Our last assumption restricts $\{\phi_k; k \leq L_N\}$ to be a $\zeta_1(k)$ -Lipschitz where the order of $\zeta_1(1), \dots, \zeta_1(L_N)$ is determined by the random graph model and appropriate sparsity parameters we assume.

We derive the asymptotic distribution of the 2SLS estimator $\hat{\boldsymbol{\beta}}_{v,2SLS}$. Here, we write $\delta_{\max} := \max_{i \leq N} \sum_{j \neq i} a_{ij}$ and $\delta_{\min} := \min_{i \leq N} \sum_{j \neq i} a_{ij}$ to denote the maximum and minimum node degrees, respectively.

Theorem 1. *Assume the assumptions in the section 3.7. Let the graph \mathbf{A} be generated via either RDPG or LSM as described in section 3.6, respectively. Further assume that*

$$\frac{\|\mathbf{A}\|_{2,\infty}^2}{\delta_{\min}^2} = o_p(1/\sqrt{N}), \quad (6)$$

$$\max_{i_1, \dots, i_4 \leq N} \mathbb{E} \left(\frac{\|\mathbf{a}_{i_1}\|^2 \|\mathbf{a}_{i_2}\|^2 \|\mathbf{a}_{i_3}\| \|\mathbf{a}_{i_4}\| \|\mathbf{A}\|_{2,\infty}^2}{\delta_{i_1}^2 \delta_{i_2}^2 \delta_{\min}^4} \right) = o(1/N^2). \quad (7)$$

Then, as $N \rightarrow \infty$,

$$\sqrt{N} \left(\hat{\boldsymbol{\beta}}_{v,2SLS} - \boldsymbol{\beta}_v^0 \right) \Rightarrow \mathcal{N} \left[0_{m(m+2p)}, \Sigma_{\tilde{E}} \otimes \left\{ (\Sigma_{\tilde{Z}\tilde{K}} \Sigma_{\tilde{K}}^{-1} \Sigma_{\tilde{K}\tilde{Z}})^{-1} \right\} \right]$$

where $\Sigma_{\tilde{E}} := \mathbb{E}(\tilde{\mathbf{e}}_1 \tilde{\mathbf{e}}_1')$ = V and $\Sigma_{\tilde{Z}\tilde{K}}, \Sigma_{\tilde{K}}, \Sigma_{\tilde{K}\tilde{Z}}$ are defined in [Lemma 5](#) in the Appendix.

The proofs of all results are in the [Appendix A](#). Several additional technical lemmas are needed, which are all stated and proved in the [Appendix A](#).

Note that the conditions on the graph density indicate that consistent and asymptotically normal estimation is possible even for *sparse graphs*. Under a binary graph (a_{ij} s are

Algorithm 1 Vectorized 2SLS with Network Endogeneity in MSAR

Require: $Y \in \mathbb{R}^{N \times m}$ (Outcomes), $X \in \mathbb{R}^{N \times p}$ (Covariates), $A \in \mathbb{R}^{N \times N}$ (Adjacency matrix), latent dimension d

Ensure: Vectorized coefficient matrix $\hat{\beta}_v$, Variance-Covariance matrix of coefficients $\hat{\Sigma}_\beta$.

- 1: **Step 1: Spectral Embedding (RDPG)**
- 2: $\hat{U} \leftarrow \text{SpectralEmbed}(A, d)$ {Top d eigenvectors and absolute eigenvalues}
- 3: **Step 2: Construct Peer Lag Matrices**
- 4: $GY \leftarrow GY, GX \leftarrow GX, G^2X \leftarrow G(GX)$
- 5: $Z \leftarrow [GY, X, GX], K \leftarrow [X, GX, G^2X]$
- 6: **Step 3: Latent Adjustment**
- 7: Form sieve design matrix $\hat{\Phi}_N = [\phi^{L_N}(\hat{u}_1), \dots, \phi^{L_N}(\hat{u}_N)] \in \mathbb{R}^{N \times L_N}$.
- 8: Compute sieve projection $P_{\hat{\Phi}_N} := \hat{\Phi}_N(\hat{\Phi}_N^\top \hat{\Phi}_N)^{-1} \hat{\Phi}_N^\top$
- 9: $\tilde{Y}^* \leftarrow Y - P_{\hat{\Phi}_N} Y, \tilde{Z}^* \leftarrow Z - P_{\hat{\Phi}_N} Z, \tilde{K}^* \leftarrow K - P_{\hat{\Phi}_N} K$
- 10: **Step 4: Vectorization**
- 11: $\tilde{Y}_v^* \leftarrow \text{vec}(\tilde{Y}^*) \{ \in \mathbb{R}^{Nm} \}$
- 12: $\tilde{Z}_v^* \leftarrow I_m \otimes \tilde{Z}^* \{ \in \mathbb{R}^{mN \times m(m+2p)} \}$
- 13: $\tilde{K}_v^* \leftarrow I_m \otimes \tilde{K}^* \{ \in \mathbb{R}^{mN \times 3mp} \}$
- 14: **Step 5: IV Estimation and Covariance Calculation**
- 15: $P_{\tilde{K}_v^*} \leftarrow \tilde{K}_v^* (\tilde{K}_v^{*\top} \tilde{K}_v^*)^{-1} \tilde{K}_v^{*\top} \{ \in \mathbb{R}^{mN \times mN} \}$
- 16: $\hat{\beta}_v \leftarrow (\tilde{Z}_v^{*\top} P_{\tilde{K}_v^*} \tilde{Z}_v^*)^{-1} \tilde{Z}_v^{*\top} P_{\tilde{K}_v^*} \tilde{Y}_v^* \{ \in \mathbb{R}^{m(m+2p)} \}$
- 17: $\hat{E}'_v \leftarrow \tilde{Y}_v^* - \tilde{Z}_v^* \hat{\beta}_v \{ \in \mathbb{R}^{Nm} \}$
- 18: $\hat{E}' \leftarrow \text{reshape}(\hat{E}'_v, N, m)$ {Reshape vector to an $N \times m$ matrix}
- 19: $\hat{V}' \leftarrow \frac{1}{N} \hat{E}'^\top \hat{E}'$
- 20: $\hat{\Sigma}_\beta \leftarrow (\tilde{Z}_v^{*\top} P_{\tilde{K}_v^*} \tilde{Z}_v^*)^{-1} \tilde{Z}_v^{*\top} P_{\tilde{K}_v^*} (\hat{V}' \otimes I_N) P_{\tilde{K}_v^*} \tilde{Z}_v^* (\tilde{Z}_v^{*\top} P_{\tilde{K}_v^*} \tilde{Z}_v^*)^{-1}$

either 1 or 0), for example, the first condition in (6) only requires $\delta_{\max}/\delta_{\min}^2 = o_p(1/\sqrt{N})$. A sufficient condition for the second part in (7) can be

$$\mathbb{E} \left[\frac{(\delta_{i_3} \delta_{i_4})^{1/2} \delta_{\max}}{\delta_{i_1} \delta_{i_2} \delta_{\min}^4} \right] \leq \mathbb{E} \left(\frac{\delta_{\max}^2}{\delta_{\min}^6} \right) = o(1/N^2).$$

These conditions hold under a moderate expected density of the graph. For example, if we let $\delta_{\min} \asymp \delta_{\max}$ and the average expected density of the graph grows as $O(\frac{1}{\sqrt{N}})$, then all conditions are satisfied. This is in contrast to the results in [Johnsson and Moon \[2021\]](#), which only hold if the average expected density of the graph grows as $O(1)$, making the graph unrealistically dense.

An intermediate lemma en route to proving the main theorem further clarifies the distinction between the density requirements for the RDPG and the LSM models.

Lemma 2. *Let Assumption 3 hold. Under the conditions on RDPG model in [Rubin-](#)*

Delanchy et al. [2022] and sparsity parameter $\rho_N = \omega(\frac{\log^4 N}{N})$, we have

$$\frac{1}{N} \|\hat{\Phi}_N - \Phi_N\|_F^2 = O_{hp} \left(\frac{\log^{2c} N}{N} \sum_{k \leq L_N} \zeta_1(k)^2 \right)$$

and under the conditions on the sparse LSM model with sparsity parameter $\omega_N = \omega(N^{-1/2})$ in *Li et al. [2023]*, we have

$$\frac{1}{N} \|\hat{\Phi}_N - \Phi_N\|_F^2 = O_{hp} \left(\frac{1}{N\omega_N} \sum_{k \leq L_N} \zeta_1(k)^2 \right).$$

Clearly, Lemma 2 provides a result on the concentration of the sieve design matrix when the true latent positions \mathbf{U} are replaced with their estimated counterparts $\hat{\mathbf{U}}$. Both the RDPG and the LSM models can accommodate sparse networks through the sparsity parameters ρ_N and ω_N respectively. However, our result with the RDPG model has a better concentration of the $\hat{\Phi}_N$ to Φ_N , for whenever ω_N is smaller than $\frac{1}{\log^{2c} N}$, i.e., if the network is even slightly sparse. However, we emphasize that our results for both models accommodate sparse networks with density requirement for RDPG being $\frac{\log^4 N}{N}$ and LSM being $\frac{N^{1/2}}{N}$ (in addition to what is required to satisfy conditions 6 and 7 in the main theorem).

Table 1: Monte Carlo Simulations RDPG Model

N	Y1 Equation		Y2 Equation	
	D_{11}	D_{12}	D_{21}	D_{22}
$h^Y(U) = U\Theta_Y$				
100	1.349	0.284	1.662	0.383
300	1.057	0.224	1.041	0.217
500	0.471	0.098	0.472	0.100
$h^Y(U) = [U[, 1], U[, 2], U[, 1]^2, U[, 2]^2]\Theta_Y$				
100	0.638	0.218	0.777	0.279
300	0.256	0.090	0.157	0.055
500	0.205	0.073	0.113	0.039
$h^Y(U) = [U[, 1], U[, 2], U[, 1]^2, U[, 2]^2, U[, 1] * U[, 2]]\Theta_Y$				
100	1.671	0.635	1.167	0.460
300	0.514	0.195	0.693	0.258
500	0.156	0.062	0.220	0.091

Notes: Columns (2)-(5) report the Mean Squared Error (MSE) of the Multivariate IV 2SLS estimator adjusting for network endogeneity for both the direct and the indirect spillover effects (\hat{D}).

4 Simulations

In this section, we describe a simulation study we performed to evaluate the finite-sample performance of the proposed estimation strategy in the presence of latent homophily and network endogeneity. Specifically, we consider two main scenarios for network and outcome generation: (i) a Random Dot Product Graph (RDPG) model and (ii) a latent space model with covariates. We generate network data, observed covariates, latent variables, and outcomes for each scenario according to the corresponding data-generating process. The simulated data are then used to compare several alternative adjustment strategies for latent confounding within the 2SLS estimation framework. We evaluate both nonparametric sieve-adjustment methods, which use polynomial or tensor product polynomial basis expansions, as well as linear functions of the estimated latent positions. As our primary evaluation metric, we use the mean squared error, calculated across simulation replications.

Table 1 documents the performance of the estimator when the network is generated from the RDPG model and the spectral embedding is used to estimate the latent variables. The dimension of latent variables in the outcome model is fixed at 2. There are two correlated outcomes where the data generation follows Equation 1 with endogeneity in network formation. The peer influence parameter matrix is set at $\begin{bmatrix} 0.3 & 0.2 \\ 0.25 & 0.6 \end{bmatrix}$ where the diagonal elements capture the direct peer influence spillovers and the off-diagonal elements capture the indirect spillovers in the outcome. The dimension of the coefficients on $h^Y(U)$ varies across the three scenarios. For each scenario, the data is generated 100 times, followed by estimation of β_v using the steps in algorithm 1. The table shows that the mean squared error steadily declines with the number of nodes in the network. This supports the fact that the estimator works well in recovering the true parameter of interest as the sample size increases.

Next, we change the data generation and estimation of latent variables, where latent space models that allow for both multiplicative and additive unobserved variables, along with observed covariates, are used for generating the network. A Projected Gradient Descent (PGD) algorithm with Universal Singular Value Thresholding (USVT) initialization is used to estimate the MLE \hat{U} [Ma et al., 2020]. Note that even though this solves a non-convex optimization problem, the solution has nice theoretical guarantees which we have used in the proofs above. The covariate that explains the network formation is not part of the data generation for the outcomes. The network formation consists of one additive latent factor, two multiplicative latent factors, and two observed covariates. The outcome data generation consists of $[AY, X, AX, h^Y(U)]$ where AY is $N \times 2$ matrix, X is $N \times 5$, AX is $N \times 5$ and dimension of $h^Y(U)$ varies across the 3 scenarios. The peer influence matrix D used in the data generation for the latent space model with covariates is fixed at $\begin{bmatrix} 0.8 & 0.2 \\ 0.3 & 0.6 \end{bmatrix}$. Table 2 reports the mean squared error (MSE) across 50 simulations

Table 2: Monte Carlo Simulations Latent Space Model with Covariates

N	Y1 Equation		Y2 Equation	
	D_{11}	D_{12}	D_{21}	D_{22}
$h^Y(U) = U\Theta_Y$				
100	2.434	3.711	1.489	2.241
300	0.874	1.169	0.686	1.064
500	0.413	0.644	0.666	0.833
$h^Y(U) = [U[, 1], U[, 2], U[, 1]^2, U[, 2]^2]\Theta_Y$				
100	1.362	1.700	4.380	5.600
300	0.670	0.861	3.957	5.093
500	0.263	0.338	0.987	1.268
$h^Y(U) = [U[, 1], U[, 2], U[, 1]^2, U[, 2]^2, U[, 1] * U[, 2]]\Theta_Y$				
100	1.820	2.261	3.256	4.055
300	1.120	1.423	1.933	2.478
500	0.605	0.769	0.838	1.072

Notes: Columns (2)-(5) report the Mean Squared Error (MSE) of the Multivariate IV 2SLS estimator adjusting for network endogeneity for both the direct and the indirect spillover effects (\hat{D}).

for each scenario as the sample size increases from 100 to 300 to 500. It shows that the MSE consistently declines as the sample size increases for all four parameters of the peer influence D matrix for all three scenarios.

5 Results

5.1 Predict Recidivism using Text Messages

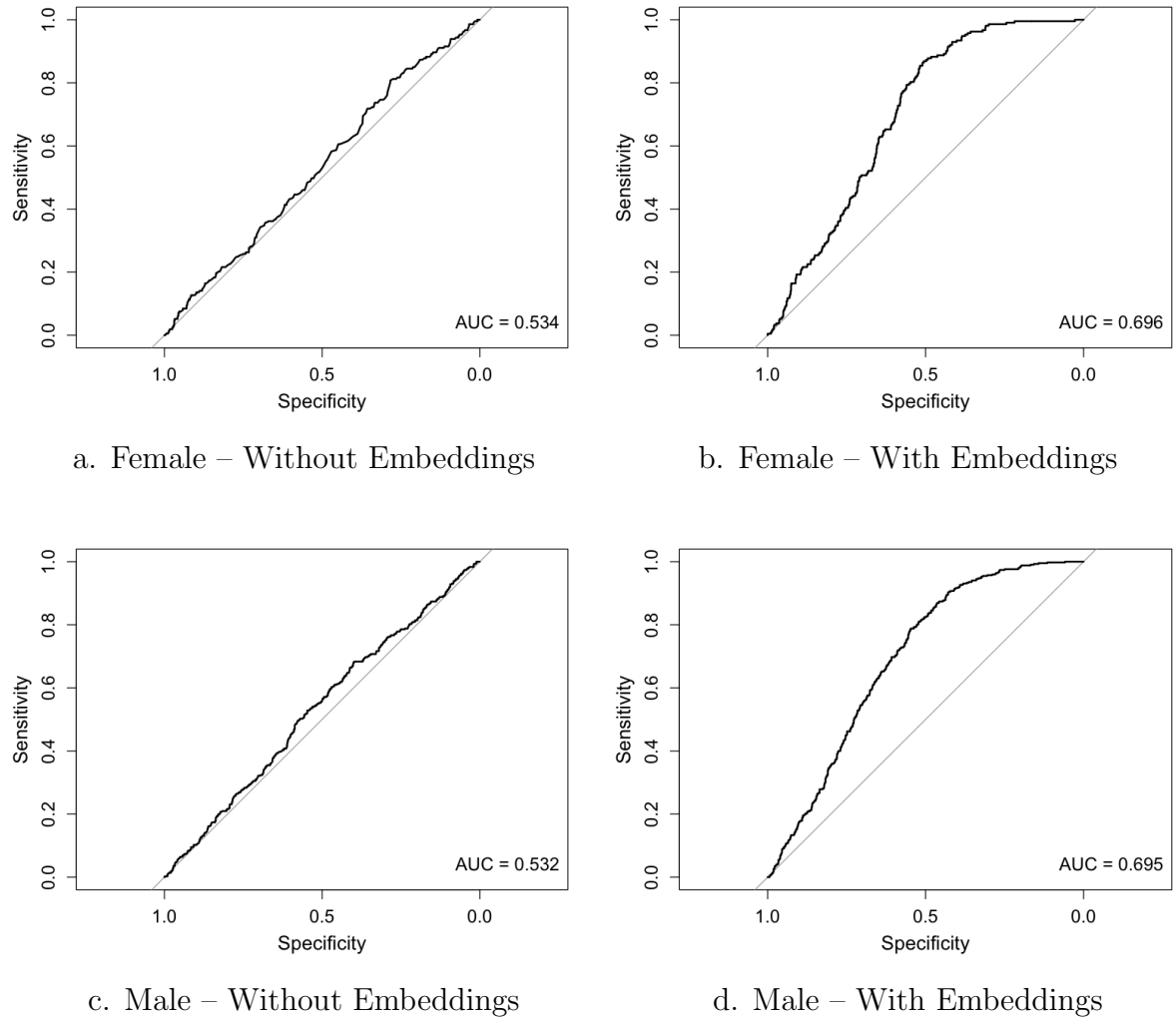
We first investigate the ability of text exchanges to predict recidivism. Recall, we estimate the LLM embeddings for the messages and use those embeddings as predictors in a high-dimensional regression LASSO prediction method. LASSO is implemented with cross-fitting to do the entire prediction exercise out-of-sample.¹ The penalty parameter is chosen using cross-validation on the entire dataset, and then it is saved and passed into the estimation and prediction for each fold in cross-fitting.

Figure 5 provides the Receiver Operator Characteristic (ROC) curves and the Area Under the Curve (AUC) for two models, one with both pre-entry covariates (X) and embeddings (T), and an alternative model without the text embeddings (only X) as pre-

¹Cross-fitting divides the sample into K-folds, and the prediction for the residents in the k^{th} fold uses the model trained on the data from the remaining $K - 1$ folds.

dictors. Panels (a) and (b) show that the prediction accuracy is 30% higher for recidivism in the female unit when we incorporate the LLM-based text embeddings relative to the model with only pre-entry covariates X . The dimension reduction is substantial for the former model, as about 26-37 predictors out of text embeddings (768) and pre-entry covariates remain across the five folds in LASSO model fit. Panels (c) and (d) compare the prediction accuracy for the male units with and without the embeddings. The prediction accuracy improvement for the males is 30.6%. Figure B6 repeats the same analysis but for the case when the text embeddings are aggregated by the ID of the receiver rather than the sender in Figure 5. We find comparable improvements (32.6% for females and 32% for males) in predictive accuracy when the text embeddings are aggregated by the receiver profiles and included as predictors in the LASSO model along with the pre-entry covariates. Recall from section 2 that the sender profile indicates how an individual interacts with their peers, while the receiver profiles indicate how others perceive an individual.

Figure 5: Predict Recidivism with and without text embeddings Aggregated by Sender



Notes: Five-fold cross-fitting is used to estimate the out-of-sample AUC for all models.

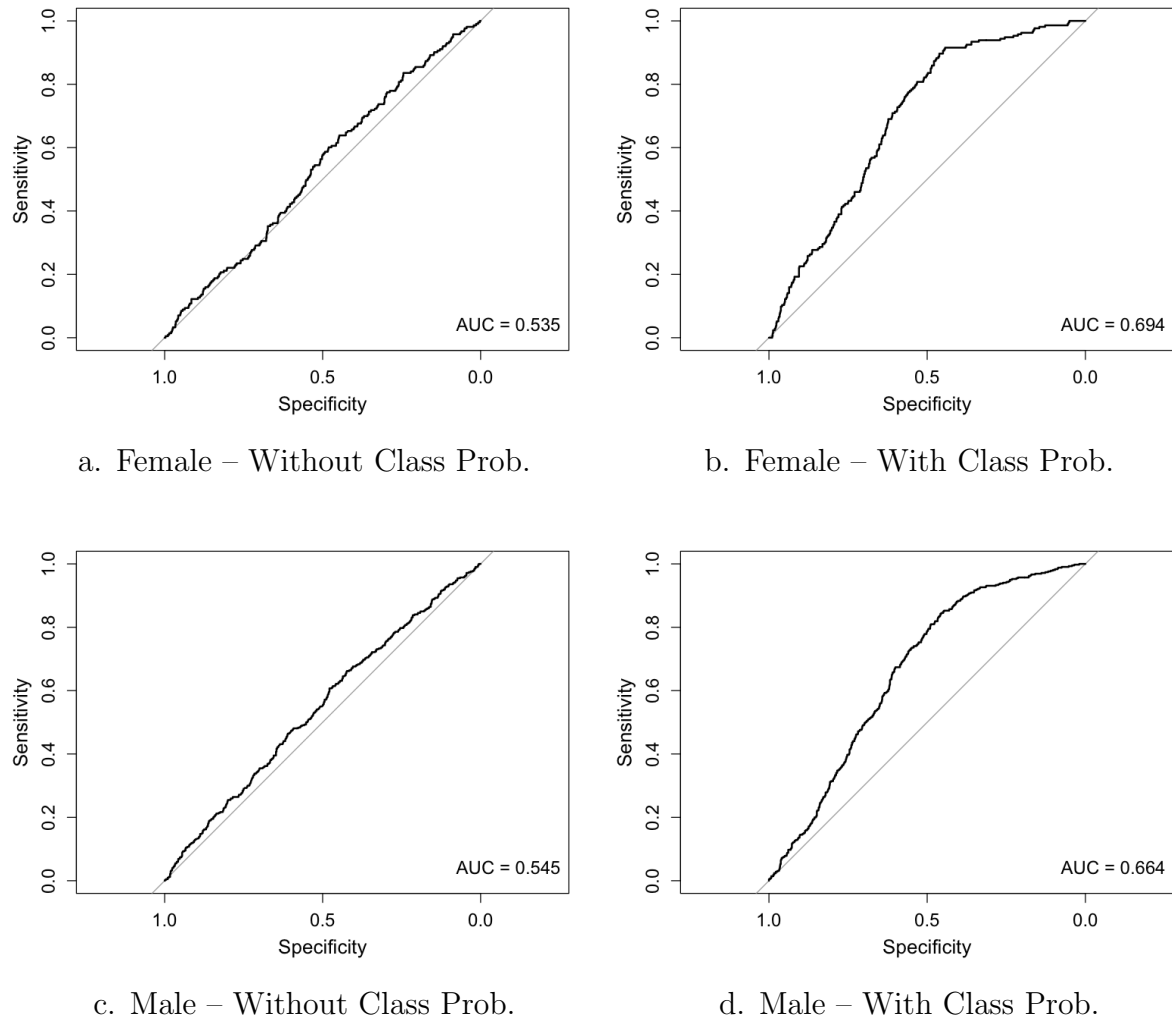
Second, prediction accuracy is assessed using the class probabilities generated by the transformer-based Zero-Shot classifier. This analysis uses the classes “Personal Growth”, “Community Support”, “Rule Violations”, and “Disruptive Conduct”. Each of these classes is chosen to be indicative of behaviors that are either meaningfully detrimental to community peace and cohesion or supportive of personal growth and community well-being. We use the class probabilities as predictors instead of the above text embeddings. Considering there are only four classes in our specification, there is no need to use LASSO. Instead, we use a logistic regression model. However, since the class probabilities are compositional data, we transform the probabilities into additive log ratios, using disruptive conduct as the reference category. We again obtain substantial improvement in out-of-sample prediction accuracy (29.7% for females and 22% for males) when including class probabilities along with the matrix of observed covariates (Figure 6).

For each of these folds, we conduct a variable importance assessment. For this, McFadden’s pseudo R^2 is computed first for the full model as $1 - \frac{\text{deviance all covariates}}{\text{deviance null model}}$. Next we iteratively drop one covariate at a time and compute McFadden’s pseudo R^2 for each model. The reduction in pseudo R^2 relative to the full model, which includes the class probabilities as predictors, is displayed in Figure 7. The interpretation of variable importance should account for the reference category (Disruptive Conduct). Here, the reduction is shown as box plots, since we use five-fold cross-validation for prediction, which provides us with a different model for each fold. In addition, panels (c) and (d) provide the marginal effects of increasing community support relative to the disruptive conduct baseline category on predicted probability of recidivism, holding everything else at their median values and fixing the white dummy at white and the education level to its lowest category. We see a sharp reduction in the likelihood of recidivism with increasing community support for both male and female residents relative to disruptive conduct (baseline category)². Note by definition, 1 unit increase in the ALR means $e \approx 2.718$ increase in the ratio of community support proportion to disruptive conduct proportion in the classification of messages sent by an individual. Since this is a non-linear model, the changes in the marginal effects for a 1 unit change in ALR vary with the value of ALR and can be represented as the marginal curves in panels (c) and (d). For example, panel (c) shows that as the ratio of community support proportion to disruptive conduct proportion increases from $\exp(-1) \approx 0.36$ to $\exp(0) = 1$, the predicted probability of recidivism reduces from around 0.22 to 0.12 for the female unit. Similarly, panel (d) shows that as the ratio of community support proportion to disruptive conduct proportion increases from $\exp(-2) \approx 0.14$ to $\exp(0) = 1$, the predicted probability of recidivism reduces from around 0.40 to 0.16 for the male unit.

Finally, we provide prediction results on recidivism aggregated by receiver profiles with and without the class probabilities (Figure B7). We find the prediction accuracy

²The estimates used for this analysis correspond to the model saved for the 5th fold of the 5-fold cross-validation exercise.

Figure 6: Predict Recidivism with and without class probabilities Aggregated by Sender



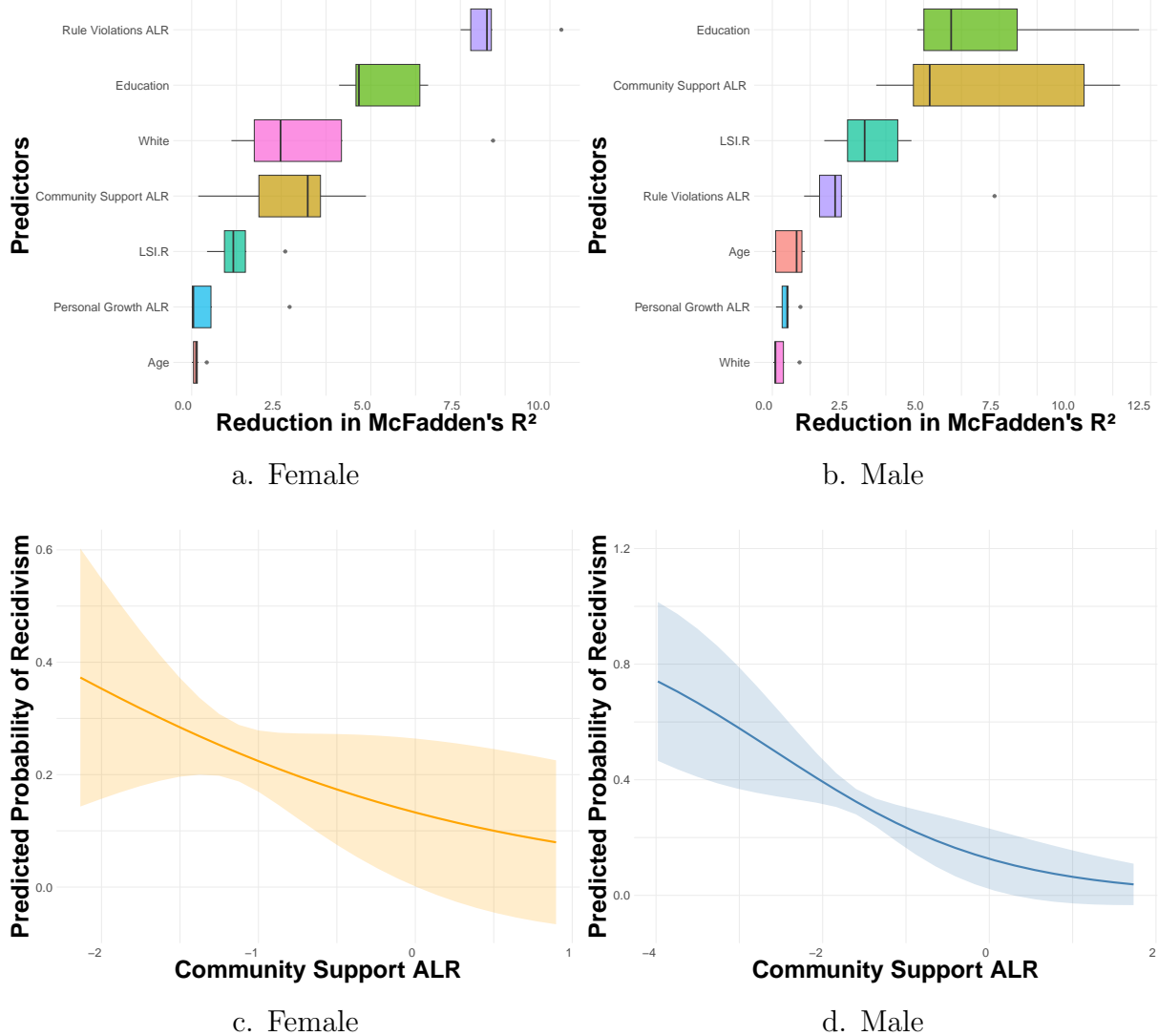
Notes: Five-fold cross-fitting is used to estimate the out-of-sample AUC for all models. The class probabilities are obtained using Zero-Shot classification, and we use the additive log ratios for this analysis, with disruptive behavior as the baseline category.

improves to the tune of 35% and 23% for the female and male units, respectively.

5.2 Endogenous Network Formation

We compare five estimators for four network models in terms of their ability to replicate observed salient features of the TC networks. These estimators/models are (1) tetra logit estimator (tet.logit) and the (2) joint fixed effect maximum likelihood estimator (jfe) in [Graham \[2017\]](#) that allow for single latent variable (additive) and covariates, 3) Spectral embedding in RDPG model [\[Athreya et al., 2017\]](#) which allows for multivariate latent factors but no covariates (rdpg), 4) MLE in latent space model that allows for both multiplicative and additive latent factors but no observed covariates [Hoff et al. \[2002\]](#) (lsm) and finally 5) MLE in latent space model from [Ma et al. \[2020\]](#) that allows for both

Figure 7: Variable Importance and Marginal Effects

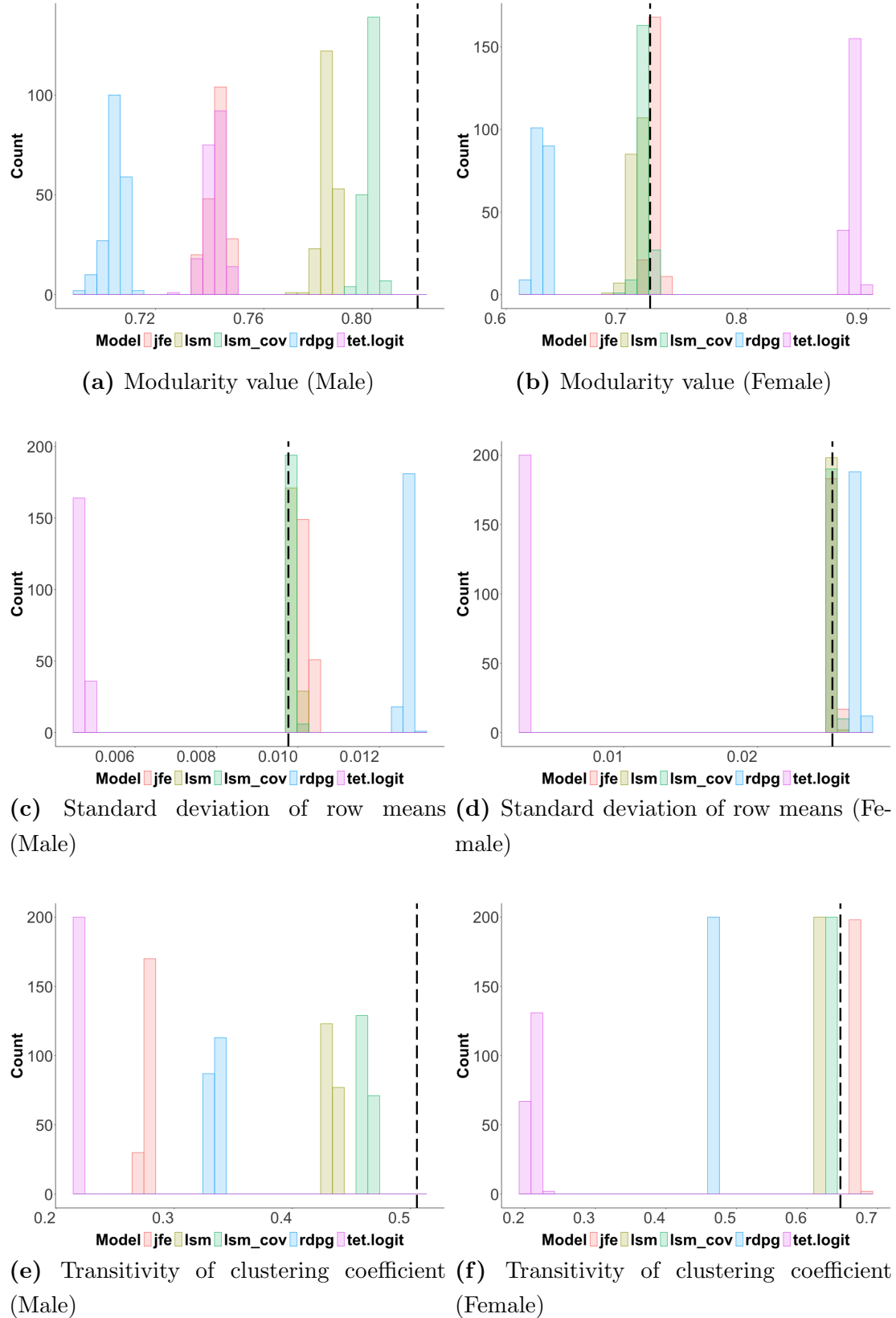


Notes: Panel (a) and (b) display the reduction in McFadden's pseudo R^2 as one covariate is omitted at a time from the full model that includes the covariates and the class probabilities. Panels (c) and (d) display community support ALR's marginal effect on the predicted recidivism probability for female and male units, respectively.

multiplicative and additive latent factors and observed covariates (lsm-cov).

Among the above-listed estimators that allow for observed covariates for network formation, we use the time difference (in days) between the residents' entry dates as a node-pair level covariate. The entry dates of residents can be assumed to be random and not explained by their observed or unobserved characteristics, since a complex function of court decisions and availability of beds in TCs determines them. However, the proximity of entry dates is an important determinant of whether residents will exchange messages since overlap in their time in the TC is a necessary condition to exchange messages. We

Figure 8: Comparison of Structural Properties of Networks



Notes: The dotted black vertical line displays the true network, and the distribution is obtained using 200 networks simulated from the fitted model, which varies for each of the estimators.

do not use the proximity in exit dates or time in TC as a predictor of network formation, as the unobserved heterogeneity of residents likely impacts these variables, and they are not pre-determined to network formation.

We compare the estimators in terms of their ability to replicate three widely observed structural network properties: modularity [Girvan and Newman, 2002], standard deviation of row means, and transitivity or the clustering coefficient [Newman, 2018]. The steps deployed for comparison are as follows. Let us consider the network data for the male unit. We implement each estimator on the observed male unit network to estimate the respective fitted models. Next, we simulate 200 networks using these fitted models (200 for each estimator listed above). The structural properties over these simulated networks are then compared with the true network to assess how well the simulated data can replicate the truth. Figure 8 displays the performance. We observe that the latent space model that allows for both multiplicative and additive latent factors, along with covariates (proximity in entry dates), outperforms all other models for every property in the male unit. For the female unit, it performs the best for the standard deviation of row means and transitivity of the clustering coefficient, and at least as good as the other estimators for modularity.

5.3 Peer Effects in Text

This section provides our results on the peer effects model, where the outcome variables are the class probabilities generated by Zero-Shot classification. Our preferred specification involves estimating the network formation model using a latent space model, which allows for both multiplicative and additive latent variables and observed covariates (lsm-cov). This selection is based on the results obtained in the previous section, which show that the latent space model with covariates performs the best in replicating key structural properties of the true male and female unit networks.

Tables 3 and 4 provide the results for IV 2SLS in text class probabilities after adjusting for the unobserved heterogeneity in the outcome model (Algorithm 1) for females and males, respectively. The dimension of the multiplicative factor is chosen using data-driven cross-validation methods for networks in Li et al. [2020]. The choice of data-driven dimensions for the multiplicative factors is 14 for the female and 19 for the male units, respectively. In addition, the model for network formation contains one additive nodal latent variable and an observed edge-level covariate that captures the difference in the residents' entry dates.

First, we discuss the diagonal elements in Table 3, which inform us about the spillovers of peer probabilities on female residents for the same class. There is evidence of a peer effect in all three classes relative to disruptive conduct at the 5% significance level. Moreover, there is also evidence of peer spillovers from personal growth and community support categories on rule violations category. We can interpret these results as follows, for example. An individual is more likely to send messages of peer community support if their

Table 3: Peer Effects in Class Probabilities (Female)

	Personal Growth ALR	Community Support ALR	Rule Violations ALR
a. Sender Profiles			
Peer Personal Growth ALR	0.882 (0.429)	-0.629 (0.433)	0.606 (0.306)
Peer Community Support ALR	0.194 (0.529)	1.955 (0.533)	-0.665 (0.377)
Peer Rule Violations ALR	-0.130 (0.490)	-0.021 (0.494)	1.612 (0.349)
b. Receiver Profiles			
Peer Personal Growth ALR	2.321 (0.413)	1.381 (0.436)	0.448 (0.276)
Peer Community Support ALR	-1.252 (0.487)	-0.475 (0.515)	-0.476 (0.326)
Peer Rule Violations ALR	0.536 (0.350)	-0.003 (0.370)	1.526 (0.234)

Notes: The outcome variables are mean class probabilities for each resident's text exchanges aggregated by sender profiles in panel (a) and by receiver profiles in panel (b). The adjustment is done using a latent space model that allows for the inclusion of covariates (proximity in entry dates).

peers are also sending messages of community support. Table B2 presents the results when unobserved heterogeneity in the outcome model and network formation are not accounted for, for comparison.

Next, the same analysis is repeated for the female unit, but the aggregation is done by the receiver profiles (panel b in Table 3). When aggregated by the receiver profiles, we find evidence of direct spillover effects only in personal growth ALR and rule violations ALR at the 95% confidence interval. As for the indirect spillovers, we see a positive indirect spillover of peer personal growth on community support. On the contrary, peer community support negatively impacts personal growth. This negative coefficient might emanate from highly positive correlations between peer personal growth and community support ALR relative to disruptive conduct.

The peer effects estimation is next done for the residents in the male units (Table 4). The estimates, when aggregated by sender profiles, suggest that there are statistically significant positive direct spillovers of community support and rule violations ALR at the 95% confidence level. For all of the indirect spillovers, the 95% confidence interval includes 0. In panel (b) of Table 4 estimates are provided for receiver profile aggregation.

Table 4: Peer Effects in Class Probabilities (Male)

	Personal Growth ALR	Community Support ALR	Rule Violations ALR
a. Sender Profiles			
Peer Personal Growth ALR	0.305 (0.464)	-0.839 (0.468)	0.046 (0.302)
Peer Community Support ALR	0.699 (0.471)	1.741 (0.475)	-0.009 (0.306)
Peer Rule Violations ALR	-0.559 (0.371)	-0.305 (0.375)	0.879 (0.241)
b. Receiver Profiles			
Peer Personal Growth ALR	1.615 (0.409)	0.644 (0.439)	-0.034 (0.270)
Peer Community Support ALR	-0.461 (0.393)	0.434 (0.422)	-0.025 (0.259)
Peer Rule Violations ALR	-0.134 (0.289)	-0.088 (0.310)	1.126 (0.191)

Notes: The outcome variables are mean class probabilities for each resident's text exchanges aggregated by sender profiles in panel (a) and by receiver profiles in panel (b). The adjustment is done using a latent space model that allows for the inclusion of covariates (proximity in entry dates).

The direct spillovers are all positive, but the ones for personal growth and rule violations are statistically significant at the 5% level. The indirect spillovers are again small relative to the standard errors. For comparison Table B3 provides the estimates without adjusting for unobserved heterogeneity.

Overall, we find evidence of peer influence in the ALR of text class probabilities both when aggregated by the sender profiles and when aggregated by the receiver profiles. However, the magnitude and standard errors change considerably once we account for unobserved heterogeneity in outcome and network formation. Direct peer influence spillovers have a larger impact than indirect spillovers for both male and female units.

6 Conclusion

This paper deploys large language models to construct text embeddings from a large corpus of written exchanges between residents in low-security correctional facilities called Therapeutic Communities. These exchanges have substantial explanatory power in pre-

dicting recidivism up to three years after exiting the facility. The out-of-sample predictive accuracy is 30% higher with these text embeddings relative to using only pre-entry covariates in the prediction exercise. The paper further uses Zero-Shot classification to interpret these embeddings and learn about peer influences in sender and receiver profiles of these messages. To study peer effects on correlated multivariate LLM representations of language, we provide new methodological and theoretical results on an instrumental variable approach that allows for multiple dimensions of latent homophily, sparse network settings, and multivariate outcomes.

Acknowledgement and IRB

The Therapeutic Community data used for this paper were exempted from IRB review based on IRB Protocol 2007B0162 by The Ohio State University. SP's research was partially funded by a grant from NSF DMS (2529302). We thank the Ohio Supercomputer Center (OSC) for providing us with computing resources through an academic account.

References

John Aitchison. The statistical analysis of compositional data. *Journal of the Royal Statistical Society: Series B (Methodological)*, 44(2):139–160, 1982.

Elliott Ash, Daniel L Chen, and Suresh Naidu. Ideas have consequences: The impact of law and economics on american justice. Technical report, National Bureau of Economic Research, 2022.

Avanti Athreya, Donniell E Fishkind, Minh Tang, Carey E Priebe, Youngser Park, Joshua T Vogelstein, Keith Levin, Vince Lyzinski, and Yichen Qin. Statistical inference on random dot product graphs: a survey. *The Journal of Machine Learning Research*, 18(1):8393–8484, 2017.

Eric Auerbach. Identification and estimation of a partially linear regression model using network data. *Econometrica*, 90(1):347–365, 2022.

Stephen J Bahr, Amber L Masters, and Bryan M Taylor. What works in substance abuse treatment programs for offenders? *The Prison Journal*, 92(2):155–174, 2012.

Patrick Bajari, Zhihao Cen, Victor Chernozhukov, Manoj Manukonda, Suhas Vijaykumar, Jin Wang, Ramon Huerta, Junbo Li, Ling Leng, George Monokroussos, et al. Hedonic prices and quality adjusted price indices powered by ai. *Journal of Econometrics*, 2025.

Andrés Barrios-Fernández and Jorge García-Hombrados. Recidivism and neighborhood institutions: evidence from the rise of the evangelical church in chile. *Journal of Labor Economics*, 43(3):000–000, 2025.

Gabrielle Beaudry, Rongqin Yu, Amanda E Perry, and Seena Fazel. Effectiveness of psychological interventions in prison to reduce recidivism: A systematic review and meta-analysis of randomised controlled trials. *The Lancet Psychiatry*, 8(9):759–773, 2021.

Yoshua Bengio, Aaron Courville, and Pascal Vincent. Representation learning: A review and new perspectives. *IEEE transactions on pattern analysis and machine intelligence*, 35(8):1798–1828, 2013.

Jessica Bouchard and Jennifer S Wong. Seeing the forest and the trees: Examining the impact of aggregate measures of recidivism on meta-analytic conclusions of intervention effects. *Criminology & Criminal Justice*, 24(1):226–248, 2024.

Yann Bramoullé, Habiba Djebbari, and Bernard Fortin. Identification of peer effects through social networks. *Journal of econometrics*, 150(1):41–55, 2009.

Yann Bramoullé, Habiba Djebbari, and Bernard Fortin. Peer effects in networks: A survey. *Annual Review of Economics*, 12(1):603–629, 2020.

Paul Brehm and Martin Saavedra. Vaccines and verdicts: How smallpox court decisions affect anti-vaccine discourse and mortality. *The Economic Journal*, 135(668):1229–1260, 2025.

Benjamin W Campbell, Skyler Cranmer, Nathan Doogan, and Keith Warren. Relationship between network clustering in a therapeutic community and reincarceration following discharge. *Journal of substance abuse treatment*, 97:14–20, 2019.

Joshua Cape, Minh Tang, and Carey E Priebe. Signal-plus-noise matrix models: eigenvalue deviations and fluctuations. *Biometrika*, 106(1):243–250, 2019.

Jae Ho Chang and Subhadeep Paul. Embedding network autoregression for time series analysis and causal peer effect inference. *arXiv preprint arXiv:2406.05944*, 2024.

Elynn Y Chen, Jianqing Fan, and Xuening Zhu. Community network auto-regression for high-dimensional time series. *arXiv preprint arXiv:2007.05521*, 2020.

Al P Christensen, H Golino, and A Tomaševic. Transforemotion: sentiment analysis for text, image and video using transformer models (version 0.1. 4)[r], 2024.

Ethan Cohen-Cole, Xiaodong Liu, and Yves Zenou. Multivariate choices and identification of social interactions. *Journal of Applied Econometrics*, 33(2):165–178, 2018.

George De Leon. The therapeutic community: Theory, model, and method. 2000.

Jacob Devlin, Ming-Wei Chang, Kenton Lee, and Kristina Toutanova. Bert: Pre-training of deep bidirectional transformers for language understanding. *Proceedings of the 2019*

conference of the North American chapter of the association for computational linguistics: human language technologies, volume 1 (long and short papers), pages 4171–4186, 2019.

Jennifer L Doleac. Encouraging desistance from crime. *Journal of Economic Literature*, 61(2):383–427, 2023.

Nathan J Doogan and Keith Warren. Semantic networks, schema change, and reincarceration outcomes of therapeutic community graduates. *Journal of substance abuse treatment*, 70:7–13, 2016.

Julia Dressel and Hany Farid. The accuracy, fairness, and limits of predicting recidivism. *Science advances*, 4(1):eaao5580, 2018.

Roberto Galbiati, Aurélie Ouss, and Arnaud Philippe. Jobs, news and reoffending after incarceration. *The Economic Journal*, 131(633):247–270, 2021.

Gloria Gennaro and Elliott Ash. Emotion and reason in political language. *The Economic Journal*, 132(643):1037–1059, 2022.

Michelle Girvan and Mark EJ Newman. Community structure in social and biological networks. *Proceedings of the national academy of sciences*, 99(12):7821–7826, 2002.

Paul Goldsmith-Pinkham and Guido W Imbens. Social networks and the identification of peer effects. *Journal of Business Economic Statistics*, 31(3):253–264, 2013.

Bryan S Graham. An econometric model of network formation with degree heterogeneity. *Econometrica*, 85(4):1033–1063, 2017.

Peter Hall and Christopher C Heyde. *Martingale limit theory and its application*. Academic press, 2014.

Alex Hayes and Keith Levin. Peer effects in the linear-in-means model may be inestimable even when identified. *arXiv preprint arXiv:2410.10772*, 2024.

Peter Hoff. Additive and multiplicative effects network models. *Statistical Science*, 2021.

Peter D Hoff, Adrian E Raftery, and Mark S Handcock. Latent space approaches to social network analysis. *Journal of the american Statistical association*, 97(460):1090–1098, 2002.

Zubin Jelveh, Bruce Kogut, and Suresh Naidu. Political language in economics. *The Economic Journal*, 134(662):2439–2469, 2024.

Ida Johnsson and Hyungsik Roger Moon. Estimation of peer effects in endogenous social networks: Control function approach. *Review of Economics and Statistics*, 103(2):328–345, 2021.

Eleni Kalamara, Arthur Turrell, Chris Redl, George Kapetanios, and Sujit Kapadia. Making text count: economic forecasting using newspaper text. *Journal of Applied Econometrics*, 37(5):896–919, 2022.

Harry H Kelejian and Ingmar R Prucha. A generalized spatial two-stage least squares procedure for estimating a spatial autoregressive model with autoregressive disturbances. *The journal of real estate finance and economics*, 17:99–121, 1998.

Oscar Kjell, Salvatore Giorgi, and H Andrew Schwartz. The text-package: An r-package for analyzing and visualizing human language using natural language processing and transformers. *Psychological methods*, 2023.

Logan M Lee. Halfway home? residential housing and reincarceration. *American Economic Journal: Applied Economics*, 15(3):117–149, 2023.

Mike Lewis, Yinhan Liu, Naman Goyal, Marjan Ghazvininejad, Abdelrahman Mohamed, Omer Levy, Ves Stoyanov, and Luke Zettlemoyer. Bart: Denoising sequence-to-sequence pre-training for natural language generation, translation, and comprehension. *arXiv preprint arXiv:1910.13461*, 2019.

Jinming Li, Gongjun Xu, and Ji Zhu. Statistical inference on latent space models for network data. *arXiv preprint arXiv:2312.06605*, 2023.

Tianxi Li, Elizaveta Levina, and Ji Zhu. Network cross-validation by edge sampling. *Biometrika*, 107(2):257–276, 2020.

Zhiyuan “Jerry” Lin, Jongbin Jung, Sharad Goel, and Jennifer Skeem. The limits of human predictions of recidivism. *Science advances*, 6(7):eaaz0652, 2020.

Quentin Lippmann. Gender and lawmaking in times of quotas. *Journal of Public Economics*, 207:104610, 2022.

Zhuang Ma, Zongming Ma, and Hongsong Yuan. Universal latent space model fitting for large networks with edge covariates. *Journal of Machine Learning Research*, 21(4):1–67, 2020.

Charles F Manski. Identification of endogenous social effects: The reflection problem. *The review of economic studies*, 60(3):531–542, 1993.

Edward McFowland III and Cosma Rohilla Shalizi. Estimating causal peer influence in homophilous social networks by inferring latent locations. *Journal of the American Statistical Association*, 118(541):707–718, 2023.

Hamed Meshkin, Joel Zirkle, Ghazal Arabidarrehdor, Anik Chaturbedi, Shilpa Chakravartula, John Mann, Bradlee Thrasher, and Zhihua Li. Harnessing large language models’

zero-shot and few-shot learning capabilities for regulatory research. *Briefings in Bioinformatics*, 25(5):bbae354, 2024.

Tomas Mikolov, Kai Chen, Greg Corrado, and Jeffrey Dean. Efficient estimation of word representations in vector space. *arXiv preprint arXiv:1301.3781*, 2013. URL <https://arxiv.org/abs/1301.3781>.

Shanjukta Nath, Keith Warren, and Subhadeep Paul. Identifying peer influence in therapeutic communities adjusting for latent homophily. *The Annals of Applied Statistics*, 19(1):529–565, 2025.

Mark Newman. *Networks*. Oxford university press, 2018.

Fernando B Perfas. *Therapeutic community: past, present, and moving forward*. Hexagram Publishing, 2014.

Carrie Pettus-Davis, Derek Brown, Chris Veeh, and Tanya Renn. The economic burden of incarceration in the united states. *Institute for justice research and development*, 2016.

Alec Radford, Karthik Narasimhan, Tim Salimans, and Ilya Sutskever. Improving language understanding by generative pre-training. 2018. URL <https://api.semanticscholar.org/CorpusID:49313245>.

Steve Rathje, Dan-Mircea Mirea, Ilia Sucholutsky, Raja Marjeh, Claire E Robertson, and Jay J Van Bavel. Gpt is an effective tool for multilingual psychological text analysis. *Proceedings of the National Academy of Sciences*, 121(34):e2308950121, 2024.

Patrick Rubin-Delanchy, Joshua Cape, Minh Tang, and Carey E Priebe. A statistical interpretation of spectral embedding: the generalised random dot product graph. *Journal of the Royal Statistical Society Series B: Statistical Methodology*, 84(4):1446–1473, 2022.

JoAnn Y Sacks, Karen McKendrick, and Zachary Hamilton. A randomized clinical trial of a therapeutic community treatment for female inmates: Outcomes at 6 and 12 months after prison release. *Journal of addictive diseases*, 31(3):258–269, 2012.

Kevin T Schnepel. Good jobs and recidivism. *The Economic Journal*, 128(608):447–469, 2018.

Robert Tibshirani. Regression shrinkage and selection via the lasso. *Journal of the Royal Statistical Society Series B: Statistical Methodology*, 58(1):267–288, 1996.

Cody Tuttle. Snapping back: Food stamp bans and criminal recidivism. *American Economic Journal: Economic Policy*, 11(2):301–327, 2019.

Ashish Vaswani, Noam Shazeer, Niki Parmar, Jakob Uszkoreit, Llion Jones, Aidan N Gomez, Łukasz Kaiser, and Illia Polosukhin. Attention is all you need. *Advances in neural information processing systems*, 30, 2017.

Zhiqiang Wang, Yiran Pang, and Yanbin Lin. Large language models are zero-shot text classifiers. *arXiv preprint arXiv:2312.01044*, 2023.

K Warren, C Harvey, G De Leon, and T Gregoire. I am my brother’s keeper: Affirmations and corrective reminders as predictors of reincarceration following graduation from a corrections-based therapeutic community. *Offender Substance Abuse Report*, 8(3):1–4, 2007.

Keith Warren, Benjamin Campbell, and Skyler Cranmer. Tightly bound: the relationship of network clustering coefficients and reincarceration at three therapeutic communities. *Journal of Studies on Alcohol and Drugs*, 81(5):673–680, 2020.

Fangzheng Xie and Yanxun Xu. Efficient estimation for random dot product graphs via a one-step procedure. *Journal of the American Statistical Association*, 118(541):651–664, 2023.

Crystal S Yang. Does public assistance reduce recidivism? *American Economic Review*, 107(5):551–555, 2017.

Wenpeng Yin, Jamaal Hay, and Dan Roth. Benchmarking zero-shot text classification: Datasets, evaluation and entailment approach. *arXiv preprint arXiv:1909.00161*, 2019.

Denis Yukhnenko, Leen Farouki, and Seena Fazel. Criminal recidivism rates globally: A 6-year systematic review update. *Journal of criminal justice*, 88:102115, 2023.

Tianyu Zhang and Noah Simon. Regression in tensor product spaces by the method of sieves. *Electronic Journal of Statistics*, 17(2):3660–3727, 2023. doi: 10.1214/23-EJS2188.

Xuening Zhu, Danyang Huang, Rui Pan, and Hansheng Wang. Multivariate spatial autoregressive model for large scale social networks. *Journal of Econometrics*, 215(2):591–606, 2020.

A Mathematical Appendix

Notations: For a matrix A we denote its spectral norm as $\|A\|$ and the Frobenius norm as $\|A\|_F$. We interchangeably use the notation A' and A^T to represent the transpose of a matrix A . We use the stochastic order notation $o_p(1)$ to mean that if $x_N = o_p(1)$, then $x_N \xrightarrow{p} 0$.

A.1 Proof of Lemma 1

Proof. We start from the moment condition:

$$\begin{aligned} & \mathbb{E}[(\mathbf{K}_i - \mathbb{E}[\mathbf{K}_i|\mathbf{U}_i])^T(\mathbf{Y}_i - \mathbb{E}[\mathbf{Y}_i|\mathbf{U}_i] - (\mathbf{Z}_i - \mathbb{E}[\mathbf{Z}_i|\mathbf{U}_i])\beta)] \\ &= \mathbb{E}[(\mathbf{K}_i - \mathbb{E}[\mathbf{K}_i|\mathbf{U}_i])^T((\mathbf{Z}_i - \mathbb{E}[\mathbf{Z}_i|\mathbf{U}_i])(\beta_0 - \beta) + (\mathbf{E}_i - \mathbb{E}[\mathbf{E}_i|\mathbf{U}_i]))] \\ &= \mathbb{E}[(\mathbf{K}_i - \mathbb{E}[\mathbf{K}_i|\mathbf{U}_i])^T(\mathbf{Z}_i - \mathbb{E}[\mathbf{Z}_i|\mathbf{U}_i])(\beta_0 - \beta)] + \mathbb{E}[(\mathbf{K}_i - \mathbb{E}[\mathbf{K}_i|\mathbf{U}_i])^T(\mathbf{E}_i - \mathbb{E}[\mathbf{E}_i|\mathbf{U}_i])] \end{aligned}$$

We can easily see that the conditional expectation of the second part, conditioning on \mathbf{U}_i is (adapting the arguments from [Johnsson and Moon \[2021\]](#))

$$\begin{aligned} \mathbb{E}[(\mathbf{K}_i - \mathbb{E}[\mathbf{K}_i|\mathbf{U}_i])^T(\mathbf{E}_i - \mathbb{E}[\mathbf{E}_i|\mathbf{U}_i])|\mathbf{U}_i] &= \mathbb{E}[\mathbf{K}_i^T \mathbf{E}_i|\mathbf{U}_i] - \mathbb{E}[\mathbf{K}_i|\mathbf{U}_i]^T \mathbb{E}[\mathbf{E}_i|\mathbf{U}_i] \\ &= \mathbb{E}[\mathbb{E}[\mathbf{K}_i^T \mathbf{E}_i|\mathbf{U}_i, \mathbf{X}, \mathbf{A}|\mathbf{U}_i]] - \mathbb{E}[\mathbf{K}_i|\mathbf{U}_i]^T \mathbb{E}[\mathbf{E}_i|\mathbf{U}_i] \\ &= \mathbb{E}[\mathbf{K}_i^T \mathbb{E}[\mathbf{E}_i|\mathbf{U}_i, \mathbf{X}, \mathbf{A}|\mathbf{U}_i]] - \mathbb{E}[\mathbf{K}_i|\mathbf{U}_i]^T \mathbb{E}[\mathbf{E}_i|\mathbf{U}_i] \\ &= \mathbb{E}[\mathbf{K}_i^T \mathbb{E}[\mathbf{E}_i|\mathbf{U}_i|\mathbf{U}_i]] - \mathbb{E}[\mathbf{K}_i|\mathbf{U}_i]^T \mathbb{E}[\mathbf{E}_i|\mathbf{U}_i] = 0. \end{aligned}$$

Note that in the above, in line 2, we have used the fact that \mathbf{K}_i is a function of \mathbf{A} and \mathbf{X} , and therefore, conditional on them, we can take \mathbf{K}_i outside the expectation. Further, in line 4, we have used the fact that under the assumptions on the model $\mathbb{E}[\mathbf{E}_i|\mathbf{U}_i, \mathbf{X}, \mathbf{A}] = \mathbb{E}[\mathbf{E}_i|\mathbf{U}_i]$. Therefore, by the law of iterated expectations,

$$\mathbb{E}[(\mathbf{K}_i - \mathbb{E}[\mathbf{K}_i|\mathbf{U}_i])^T(\mathbf{E}_i - \mathbb{E}[\mathbf{E}_i|\mathbf{U}_i])] = 0.$$

Therefore, the moment condition implies, $\beta = \beta_0$, as long as the $3p \times (m + 2p)$ matrix $\mathbb{E}[(\mathbf{K}_i - \mathbb{E}[\mathbf{K}_i|\mathbf{U}_i])^T((\mathbf{Z}_i - \mathbb{E}[\mathbf{Z}_i|\mathbf{U}_i])]$ is invertible. \square

A.2 Proof of Theorem 1

We derive the asymptotic distribution of the 2SLS estimator $\hat{\beta}_{v,IV}$ in three steps similar to the structure in [Johnsson and Moon \[2021\]](#).

We start from the IV-2SLS estimator described in [5](#). Substituting $\mathbf{Y}_N = \mathbf{Z}_N\beta_0 + \mathbf{E}_N$ in Equation [5](#), we have

$$\begin{aligned} \sqrt{N}(\hat{\beta}_{2SLS} - \beta_0) &= \left(\mathbf{Z}_N^T \mathbf{M}_{\hat{\Phi}_N} \mathbf{K}_N (\mathbf{K}_N^T \mathbf{M}_{\hat{\Phi}_N} \mathbf{K}_N)^{-1} \mathbf{K}_N^T \mathbf{M}_{\hat{\Phi}_N} \mathbf{Z}_N \right)^{-1} \\ &\quad \times \mathbf{Z}_N^T \mathbf{M}_{\hat{\Phi}_N} \mathbf{K}_N (\mathbf{K}_N^T \mathbf{M}_{\hat{\Phi}_N} \mathbf{K}_N)^{-1} \mathbf{K}_N^T \mathbf{M}_{\hat{\Phi}_N} \left(\tilde{\mathbf{E}}_N + \mathbf{h}^E(\mathbf{U}_N) - \hat{\Phi}_N \boldsymbol{\alpha}_{L_N}^E \right). \end{aligned}$$

This is because $\tilde{\mathbf{E}}_N = \mathbf{E}_N - h^E(\mathbf{U}_N)$, and $\mathbf{M}_{\hat{\Phi}_N} \hat{\Phi}_N = \mathbf{0}$. The next lemma is our first step in developing an asymptotic normality result.

Lemma 3. Assume the assumptions in section 3.7. Then, we have

1. $\frac{1}{N}(\mathbf{K}'_N \mathbf{P}_{\hat{\Phi}_N} \mathbf{Z}_N - \mathbf{K}'_N \mathbf{P}_{\Phi_N} \mathbf{Z}_N) = o_p(1)$.
2. $\frac{1}{N}(\mathbf{K}'_N \mathbf{P}_{\hat{\Phi}_N} \mathbf{K}_N - \mathbf{K}'_N \mathbf{P}_{\Phi_N} \mathbf{K}_N) = o_p(1)$.
3. $\frac{1}{\sqrt{N}}(\mathbf{K}'_N \mathbf{P}_{\hat{\Phi}_N} \tilde{\mathbf{E}}_N - \mathbf{K}'_N \mathbf{P}_{\Phi_N} \tilde{\mathbf{E}}_N) = o_p(1)$.
4. $\frac{1}{\sqrt{N}}\{\mathbf{K}'_N \mathbf{M}_{\hat{\Phi}_N}(\mathbf{h}^E(\mathbf{U}_N) - \hat{\Phi}_N \boldsymbol{\alpha}_{L_N}^E)\} = o_p(1)$.

Consequently,

$$\begin{aligned} \sqrt{N}(\hat{\beta}_{2SLS} - \beta^0) &= \left(\frac{1}{N} \mathbf{Z}_N^T \mathbf{M}_{\Phi_N} \mathbf{K}_N \left(\frac{1}{N} \mathbf{K}_N^T \mathbf{M}_{\Phi_N} \mathbf{K}_N \right)^{-1} \frac{1}{N} \mathbf{K}_N^T \mathbf{M}_{\Phi_N} \mathbf{Z}_N \right)^{-1} \\ &\quad \times \frac{1}{N} \mathbf{Z}_N^T \mathbf{M}_{\Phi_N} \mathbf{K}_N \left(\frac{1}{N} \mathbf{K}_N^T \mathbf{M}_{\Phi_N} \mathbf{K}_N \right)^{-1} \frac{1}{\sqrt{N}} \mathbf{K}_N^T \mathbf{M}_{\Phi_N} \tilde{\mathbf{E}}_N + o_p(1) \end{aligned}$$

The next lemma further shows that under our assumptions, the sieve estimators effectively approximate the various conditional mean functions. This is done in the next lemma.

Lemma 4. Under the assumptions in section 3.7, we have the following results

1. $\frac{1}{N} \mathbf{K}'_N \mathbf{P}_{\Phi_N} \mathbf{Z}_N = \frac{1}{N} \sum_{i \leq N} [\mathbf{k}_i - \mathbf{h}^K(\mathbf{u}_i)][\mathbf{z}_i - \mathbf{h}^Z(\mathbf{u}_i)]' + o_p(1)$.
2. $\frac{1}{N} \mathbf{K}'_N \mathbf{P}_{\Phi_N} \mathbf{K}_N = \frac{1}{N} \sum_{i \leq N} [\mathbf{k}_i - \mathbf{h}^K(\mathbf{u}_i)][\mathbf{k}_i - \mathbf{h}^K(\mathbf{u}_i)]' + o_p(1)$.
3. $\frac{1}{\sqrt{N}} \mathbf{K}'_N \mathbf{P}_{\Phi_N} \tilde{\mathbf{E}}_N = \frac{1}{N} \sum_{i \leq N} [\mathbf{k}_i - \mathbf{h}^K(\mathbf{u}_i)] \tilde{\mathbf{e}}_i' + o_p(1)$.

As a consequence of these results, $\sqrt{N}(\hat{\beta}_{2SLS} - \beta^0)$ can be written as

$$\left(\frac{1}{N} \tilde{\mathbf{Z}}'_N \tilde{\mathbf{K}}_N \left(\tilde{\mathbf{K}}'_N \tilde{\mathbf{K}}_N \right)^{-1} \tilde{\mathbf{K}}'_N \tilde{\mathbf{Z}}_N \right)^{-1} \times \frac{1}{\sqrt{N}} \tilde{\mathbf{Z}}'_N \tilde{\mathbf{K}}_N \left(\tilde{\mathbf{K}}'_N \tilde{\mathbf{K}}_N \right)^{-1} \tilde{\mathbf{K}}'_N \tilde{\mathbf{E}}_N + o_p(1) \quad (8)$$

Now it remains to be shown that the first term in (8) is asymptotically normal. For this, we show that the vectorized estimator $\sqrt{N}(\hat{\beta}_{v,2SLS} - \beta_v^0) \in \mathbb{R}^{m(m+2p)}$ is asymptotically normal. First, by vectorizing (8), we note that,

$$\begin{aligned} \sqrt{N}(\hat{\beta}_{v,2SLS} - \beta_v^0) &= \frac{1}{N} \left[\mathbf{I}_m \otimes \left\{ \tilde{\mathbf{Z}}'_N \tilde{\mathbf{K}}_N \left(\tilde{\mathbf{K}}'_N \tilde{\mathbf{K}}_N \right)^{-1} \tilde{\mathbf{K}}'_N \tilde{\mathbf{Z}}_N \right\}^{-1} \tilde{\mathbf{Z}}'_N \tilde{\mathbf{K}}_N \left(\tilde{\mathbf{K}}'_N \tilde{\mathbf{K}}_N \right)^{-1} \right] \\ &\quad \times \frac{1}{\sqrt{N}} \text{vec}(\tilde{\mathbf{K}}'_N \tilde{\mathbf{E}}_N) + o_p(1). \end{aligned} \quad (9)$$

Let $\mathbf{Q} \in \mathbb{R}^{3p \times m}$ be an arbitrary matrix with $\|\mathbf{Q}\|_F^2 = 1$ and $\mathbf{q} := \text{vec}(\mathbf{Q})$. Writing the i -th row of $\tilde{\mathbf{E}}_N$ by $\tilde{\mathbf{e}}_i$ and the i -th row of $\tilde{\mathbf{K}}_N$ by $\tilde{\mathbf{k}}_i$,

$$\text{vec}(\tilde{\mathbf{K}}_N' \tilde{\mathbf{E}}_N)' \mathbf{q} = \text{tr}(\tilde{\mathbf{E}}_N' \tilde{\mathbf{K}}_N \mathbf{Q}) = \sum_{i \leq N} \tilde{\mathbf{k}}_i' \mathbf{Q} \tilde{\mathbf{e}}_i.$$

Now, let $\mathcal{F}_{Ni} := \sigma(\mathbf{X}_N, \mathbf{A}, \mathbf{u}_s, \mathbf{e}_s; s \leq i)$ be a filtration. Then, $T_{Ni} := \frac{1}{\sqrt{N}} \tilde{\mathbf{k}}_i' \mathbf{Q} \tilde{\mathbf{e}}_i$ is a martingale difference adapted to \mathcal{F}_{Ni} . For simplicity, let $\boldsymbol{\iota}_i^E := \mathbf{Q} \tilde{\mathbf{e}}_i$, which are i.i.d from $(0_{3p}, \mathbf{Q} \Sigma_{\tilde{\mathbf{E}}} \mathbf{Q}')$. We check the sufficient conditions for Corollary 3.1 of [Hall and Heyde \[2014\]](#) to apply the Martingale central limit theorem.

(i). For any $\epsilon > 0$, we have

$$\sum_i \mathbb{E}[T_{Ni}^2 1_{\{|T_{Ni}| > \epsilon\}} | \mathcal{F}_{N,i-1}] = o_p(1).$$

Proof. We have

$$\begin{aligned} \sum_i \mathbb{E}[T_{Ni}^2 1_{\{|T_{Ni}| > \epsilon\}} | \mathcal{F}_{N,i-1}] &\leq \frac{1}{\epsilon^2} \sum_i \mathbb{E}[T_{Ni}^4 | \mathcal{F}_{N,i-1}] \\ &= \frac{1}{N^2 \epsilon^2} \sum_i \mathbb{E}[(\boldsymbol{\iota}_i^E' \tilde{\mathbf{k}}_i \tilde{\mathbf{k}}_i' \boldsymbol{\iota}_i^E)^2 | \mathcal{F}_{N,i-1}]. \end{aligned}$$

By [Chen et al. \[2020\]](#), equation 45 in Lemma A.8],

$$\begin{aligned} \mathbb{E}[(\boldsymbol{\iota}_i^E' \tilde{\mathbf{k}}_i \tilde{\mathbf{k}}_i' \boldsymbol{\iota}_i^E)^2 | \mathcal{F}_{N,i-1}] &= \mathbb{V}(\boldsymbol{\iota}_i^E' \tilde{\mathbf{k}}_i \tilde{\mathbf{k}}_i' \boldsymbol{\iota}_i^E | \mathcal{F}_{N,i-1}) + \text{tr}(\tilde{\mathbf{k}}_i \tilde{\mathbf{k}}_i' \mathbf{Q} \Sigma_{\tilde{\mathbf{E}}} \mathbf{Q}')^2 \\ &\leq c \text{tr}[(\tilde{\mathbf{k}}_i \tilde{\mathbf{k}}_i')^2] + \text{tr}(\tilde{\mathbf{k}}_i \tilde{\mathbf{k}}_i' \mathbf{Q} \Sigma_{\tilde{\mathbf{E}}} \mathbf{Q}')^2 \\ &\leq \text{tr}[(\tilde{\mathbf{k}}_i \tilde{\mathbf{k}}_i')^2] \{c + 3p \text{tr}(\mathbf{Q} \Sigma_{\tilde{\mathbf{E}}} \mathbf{Q}')^2\}, \end{aligned}$$

so it suffices to verify $\frac{1}{N^2} \sum_i \text{tr}[(\tilde{\mathbf{k}}_i \tilde{\mathbf{k}}_i')^2] = o(1)$. Note that

$$\frac{1}{N^2} \sum_i (\tilde{\mathbf{k}}_i' \tilde{\mathbf{k}}_i)^2 = \frac{1}{N^2} \sum_i \left(\sum_{j \leq 3p} \tilde{k}_{ij}^2 \right)^2 \leq \frac{3p}{N^2} \sum_{i,j} \tilde{k}_{ij}^4 = o_p(1)$$

which can be shown similarly as Lemma 5. For this, we show that

$$\frac{1}{N^2} \sum_{i \leq N, j \leq p} (\mathbf{g}_i' \mathbf{G} \mathbf{X}_j)^4 = o_p(1)$$

for example. As $\frac{1}{N^2} \sum_j \|\mathbf{X}_j\|^4 = \frac{1}{N^2} \sum_j (\sum_{i \leq N} X_{ij}^2)^2 = O_p(1)$, it remains to show that $\sum_i \|\mathbf{g}_i' \mathbf{G}\|^4 = o_p(1)$. Observe that

$$\sum_i \|\mathbf{g}_i' \mathbf{G}\|^4 \leq N \|\mathbf{G}^2\|_{2,\infty}^4 \leq N \|\mathbf{G}\|_{2,\infty}^4 \leq \frac{N \|\mathbf{A}\|_{2,\infty}^4}{\delta_{\min}^4} = o_p(1)$$

as $\|\mathbf{G}\|_{2,\infty}^2 \leq \frac{\|\mathbf{A}\|_{2,\infty}^2}{\delta_{\min}^2}$. □

(ii).

$$\sum_i \mathbb{E}[T_{Ni}^2 | \mathcal{F}_{N,i-1}] = \mathbf{q}'(\Sigma_{\tilde{E}} \otimes \Sigma_{\tilde{K}})\mathbf{q} + o_p(1).$$

Proof. By Lemma 5, we have

$$\frac{1}{N} \sum_i \mathbb{E}(\boldsymbol{\iota}_i^{E'} \tilde{\mathbf{k}}_i \tilde{\mathbf{k}}_i' \boldsymbol{\iota}_i^E | \mathcal{F}_{N,i-1}) = \text{tr} \left[\frac{1}{N} \sum_i \tilde{\mathbf{k}}_i \tilde{\mathbf{k}}_i' \mathbb{E}(\boldsymbol{\iota}_1^E \boldsymbol{\iota}_1^{E'}) \right] = \text{tr}(\Sigma_{\tilde{K}} \mathbf{Q} \Sigma_{\tilde{E}} \mathbf{Q}') + o_p(1).$$

□

This shows that $\frac{1}{\sqrt{N}} \text{vec}(\tilde{\mathbf{K}}_N' \tilde{\mathbf{E}}_N)$ has the limiting distribution $\mathcal{N}(0, \Sigma_{\tilde{E}} \otimes \Sigma_{\tilde{K}})$. Lemma 5 implies that

$$\begin{aligned} \frac{1}{N} \mathbf{I}_m \otimes \left[\left\{ \tilde{\mathbf{Z}}_N' \tilde{\mathbf{K}}_N \left(\tilde{\mathbf{K}}_N' \tilde{\mathbf{K}}_N \right)^{-1} \tilde{\mathbf{K}}_N' \tilde{\mathbf{Z}}_N \right\}^{-1} \tilde{\mathbf{Z}}_N' \tilde{\mathbf{K}}_N \left(\tilde{\mathbf{K}}_N' \tilde{\mathbf{K}}_N \right)^{-1} \right] \\ = \mathbf{I}_m \otimes \left\{ \left(\Sigma_{\tilde{Z}\tilde{K}} \Sigma_{\tilde{K}}^{-1} \Sigma_{\tilde{K}\tilde{Z}} \right)^{-1} \Sigma_{\tilde{Z}\tilde{K}} \Sigma_{\tilde{K}}^{-1} \right\} + o_p(1), \end{aligned}$$

so the conclusion of Theorem 1 follows by applying Slutsky's theorem to (9). For the asymptotic covariance form, we can use the relationship

$$(\mathbf{I} \otimes \mathbf{B})(\mathbf{V}_1 \otimes \mathbf{V}_2)(\mathbf{I} \otimes \mathbf{B})' = \mathbf{V}_1 \otimes (\mathbf{B} \mathbf{V}_2 \mathbf{B}')$$

for $\mathbf{B}, \mathbf{V}_1, \mathbf{V}_2$ with appropriate dimensions.

A.3 Proof of additional lemmas

A.3.1 Proof of Lemma 3

This part of the proof follows similar logic as in [Johnsson and Moon \[2021\]](#); however, since our terms are matrix-valued instead of vector-valued, our bounds involve the matrix spectral and Frobenius norms, as well as the matrix trace. We first prove the four results claimed in the lemma.

Proof. 1. We start with the following expansion for part 1 of the lemma.

$$\begin{aligned}
& \frac{1}{N} (\mathbf{K}'_N \mathbf{P}_{\hat{\Phi}_N} \mathbf{Z}_N - \mathbf{K}'_N \mathbf{P}_{\Phi_N} \mathbf{Z}_N) \\
&= \mathbf{K}'_N \left\{ \frac{\hat{\Phi}_N}{N} \left(\frac{\hat{\Phi}'_N \hat{\Phi}_N}{N} \right)^{-1} \frac{\hat{\Phi}'_N}{N} - \frac{\Phi_N}{N} \left(\frac{\Phi'_N \Phi_N}{N} \right)^{-1} \frac{\Phi'_N}{N} \right\} \mathbf{Z}_N \\
&= \mathbf{K}'_N \left\{ \frac{\hat{\Phi}_N - \Phi_N}{N} \left(\frac{\hat{\Phi}'_N \hat{\Phi}_N}{N} \right)^{-1} \frac{\hat{\Phi}'_N}{N} + \frac{\Phi_N}{N} \left(\left(\frac{\hat{\Phi}'_N \hat{\Phi}_N}{N} \right)^{-1} - \left(\frac{\Phi'_N \Phi_N}{N} \right)^{-1} \right) \frac{\Phi'_N}{N} \right. \\
&\quad \left. + \frac{\Phi_N}{N} \left(\frac{\hat{\Phi}'_N \hat{\Phi}_N}{N} \right)^{-1} \frac{\hat{\Phi}'_N - \Phi'_N}{N} \right\} \mathbf{Z}_N \\
&= \mathbf{K}'_N \left\{ \frac{\hat{\Phi}_N - \Phi_N}{N} \left(\frac{\hat{\Phi}'_N \hat{\Phi}_N}{N} \right)^{-1} \frac{\hat{\Phi}_N - \Phi_N}{N} + \frac{\hat{\Phi}'_N - \Phi'_N}{N} \left(\frac{\hat{\Phi}'_N \hat{\Phi}_N}{N} \right)^{-1} \frac{\Phi'_N}{N} \right. \\
&\quad \left. + \frac{\Phi_N}{N} \left(\left(\frac{\hat{\Phi}'_N \hat{\Phi}_N}{N} \right)^{-1} - \left(\frac{\Phi'_N \Phi_N}{N} \right)^{-1} \right) \frac{\Phi'_N}{N} \right. \\
&\quad \left. + \frac{\Phi_N}{N} \left(\frac{\hat{\Phi}'_N \hat{\Phi}_N}{N} \right)^{-1} \frac{\hat{\Phi}'_N - \Phi'_N}{N} \right\} \mathbf{Z}_N \\
&= I_1 + I_2 + I_3 + I_4, \text{ say.}
\end{aligned}$$

We show that all these terms $\|I_1\|, \|I_2\|, \|I_3\|, \|I_4\| = o_p(1)$ which collectively imply

$$\left\| \frac{1}{N} (\mathbf{K}'_N \mathbf{P}_{\hat{\Phi}_N} \mathbf{Z}_N - \mathbf{K}'_N \mathbf{P}_{\Phi_N} \mathbf{Z}_N) \right\| = o_p(1).$$

As we assume that m, p are fixed, the spectral-norm being $o_p(1)$, is sufficient for all entries to be $o_p(1)$. First note that,

$$\begin{aligned}
\|I_1\| &\leq \left\| \frac{\mathbf{K}_N}{\sqrt{N}} \right\|_F \left\| \frac{\hat{\Phi}_N - \Phi_N}{\sqrt{N}} \right\|_F \left\| \left(\frac{\hat{\Phi}'_N \hat{\Phi}_N}{N} \right)^{-1} \right\| \left\| \frac{\mathbf{Z}_N}{\sqrt{N}} \right\|_F \\
&= O_p(1) \underbrace{O_{hp} \left(\sum_{k \leq L_N} \zeta_1(k)^2 \frac{\log^{2c} N}{N} \right)}_{\text{Lemma 2}} \underbrace{O_p(1)}_{\text{Lemma 7}} O(1) = o_p(1)
\end{aligned}$$

under Assumption 3 using the results of Lemmas 2 and 7. Next,

$$\begin{aligned}
\|I_2\| &\leq \left\| \frac{\mathbf{K}_N}{\sqrt{N}} \right\|_F \left\| \frac{\hat{\Phi}_N - \Phi_N}{\sqrt{N}} \right\|_F \left\| \left(\frac{\hat{\Phi}'_N \hat{\Phi}_N}{N} \right)^{-1} \right\| \left\| \frac{\Phi_N}{\sqrt{N}} \right\|_F \left\| \frac{\mathbf{Z}_N}{\sqrt{N}} \right\|_F \\
&\leq O_p(1) O_{hp} \left(\sqrt{\zeta_0(L_N)^2 \sum_{k \leq L_N} \zeta_1(k)^2 \frac{\log^{2c} N}{N}} \right) = o_p(1)
\end{aligned}$$

by $\|\Phi_N\|_F^2 = \sum_{i \leq N} \|\phi^{L_N}(\mathbf{u}_i)\|^2 \leq N\zeta_0(L_N)^2$. $\|I_4\| = o_p(1)$ follows in a similar way. Finally noting that,

$$\begin{aligned} I_3 &= \frac{\mathbf{K}'_N \Phi_N}{N} \left(\frac{\hat{\Phi}'_N \hat{\Phi}_N}{N} \right)^{-1} \left\{ \left(\frac{\Phi'_N \Phi_N}{N} \right) - \left(\frac{\hat{\Phi}'_N \hat{\Phi}_N}{N} \right) \right\} \left(\frac{\Phi'_N \Phi_N}{N} \right)^{-1} \frac{\Phi'_N \mathbf{Z}_N}{N} \\ &= \frac{\mathbf{K}'_N \Phi_N}{N} \left(\frac{\hat{\Phi}'_N \hat{\Phi}_N}{N} \right)^{-1} \left(\frac{\Phi'_N (\Phi_N - \hat{\Phi}_N)}{N} \right) \left(\frac{\Phi'_N \Phi_N}{N} \right)^{-1} \frac{\Phi'_N \mathbf{Z}_N}{N} \\ &\quad + \frac{\mathbf{K}'_N \Phi_N}{N} \left(\frac{\hat{\Phi}'_N \hat{\Phi}_N}{N} \right)^{-1} \left(\frac{(\Phi_N - \hat{\Phi}_N)' \hat{\Phi}_N}{N} \right) \left(\frac{\Phi'_N \Phi_N}{N} \right)^{-1} \frac{\Phi'_N \mathbf{Z}_N}{N} \end{aligned}$$

and we get $\|I_3\| = o_p(1)$.

2. This can be shown in the same way as 1.

3. Using the similar expansion as 1, we have

$$\begin{aligned} &\frac{1}{\sqrt{N}} (\mathbf{K}'_N \mathbf{P}_{\hat{\Phi}_N} \tilde{\mathbf{E}}_N - \mathbf{K}'_N \mathbf{P}_{\Phi_N} \tilde{\mathbf{E}}_N) \\ &= \mathbf{K}'_N \left\{ \frac{\hat{\Phi}_N - \Phi_N}{N} \left(\frac{\hat{\Phi}'_N \hat{\Phi}_N}{N} \right)^{-1} \frac{\hat{\Phi}_N - \Phi_N}{N} + \frac{\hat{\Phi}_N - \Phi_N}{N} \left(\frac{\hat{\Phi}'_N \hat{\Phi}_N}{N} \right)^{-1} \frac{\Phi_N}{N} \right. \\ &\quad + \frac{\Phi_N}{N} \left(\left(\frac{\hat{\Phi}'_N \hat{\Phi}_N}{N} \right)^{-1} - \left(\frac{\Phi'_N \Phi_N}{N} \right)^{-1} \right) \frac{\Phi'_N}{N} \\ &\quad \left. + \frac{\Phi_N}{N} \left(\frac{\hat{\Phi}'_N \hat{\Phi}_N}{N} \right)^{-1} \frac{\hat{\Phi}_N - \Phi_N}{N} \right\} \tilde{\mathbf{E}}_N \\ &= J_1 + J_2 + J_3 + J_4, \text{ say.} \end{aligned}$$

First,

$$\begin{aligned} \|J_1\| &\leq \left\| \frac{\mathbf{K}_N}{\sqrt{N}} \right\|_F \left\| \frac{\hat{\Phi}_N - \Phi_N}{\sqrt{N}} \right\|_F \left\| \left(\frac{\hat{\Phi}'_N \hat{\Phi}_N}{N} \right)^{-1} \right\| \left\| \frac{(\hat{\Phi}_N - \Phi_N)' \tilde{\mathbf{E}}_N}{\sqrt{N}} \right\|_F \\ &= O_p(1) O_{hp} \left(\sqrt{\sum_{k \leq L_N} \frac{\zeta_1(k)^2 \log^{2c} N}{N}} \right) O_p(1) \left\| \frac{(\hat{\Phi}_N - \Phi_N)' \tilde{\mathbf{E}}_N}{\sqrt{N}} \right\|_F. \end{aligned}$$

We have

$$\begin{aligned} &\mathbb{E} \left[\left\| \frac{(\hat{\Phi}_N - \Phi_N)' \tilde{\mathbf{E}}_N}{\sqrt{N}} \right\|_F^2 \mid \mathbf{X}, \mathbf{A}, \mathbf{U} \right] \\ &= \frac{1}{N} \text{tr}[(\hat{\Phi}_N - \Phi_N)(\hat{\Phi}_N - \Phi_N)' \mathbb{E}(\tilde{\mathbf{E}}_N \tilde{\mathbf{E}}_N' \mid \mathbf{X}, \mathbf{A}, \mathbf{U})] = \frac{\|\hat{\Phi}_N - \Phi_N\|_F^2}{N} \text{tr}(\Sigma_{\tilde{\mathbf{E}}}) \end{aligned}$$

where

$$\Sigma_{\tilde{\mathbf{E}}} := \mathbb{E}(\tilde{\mathbf{e}}_1 \tilde{\mathbf{e}}_1' \mid \mathbf{U}) = \text{Var}(\tilde{\mathbf{e}}_1 \mid \mathbf{U}) = O_p(m)$$

which in turn verifies $\|J_1\| = o_p(1)$. We omit the rest of the proof as it works in a similar way.

4. Note that

$$\begin{aligned} \frac{1}{\sqrt{N}} \mathbf{K}'_N \mathbf{M}_{\hat{\Phi}_N} (\mathbf{h}^E(\mathbf{U}_N) - \hat{\Phi}_N \boldsymbol{\alpha}_{L_N}^E) &= \frac{1}{\sqrt{N}} \mathbf{K}'_N \mathbf{M}_{\hat{\Phi}_N} \mathbf{h}^E(\mathbf{U}_N) \\ &= \frac{1}{\sqrt{N}} \mathbf{K}'_N (\mathbf{M}_{\hat{\Phi}_N} - \mathbf{M}_{\Phi_N}) \mathbf{h}^E(\mathbf{U}_N) + \frac{1}{\sqrt{N}} \mathbf{K}'_N \mathbf{M}_{\Phi_N} (\mathbf{h}^E(\mathbf{U}_N) - \Phi_N \boldsymbol{\alpha}_{L_N}^E) \\ &= I'_1 + I'_2, \text{ say.} \end{aligned}$$

$\|I'_1\| = o_p(1)$ follows in the similar way as 1. We finish the proof by observing that

$$\begin{aligned} \|I'_2\| &\leq \frac{\|\mathbf{K}_N\|_F}{\sqrt{N}} \|\mathbf{h}^E(\mathbf{U}_N) - \Phi_N \boldsymbol{\alpha}_{L_N}^E\|_F \\ &= \frac{\|\mathbf{K}_N\|_F}{\sqrt{N}} \sqrt{\sum_{j \leq m} \|\mathbf{h}_j^E(\mathbf{U}_N) - \Phi_N \boldsymbol{\alpha}_{L_N}^j\|^2} \\ &\leq O_p(1) \sup_{i \leq N, j \leq m} \sqrt{mN \{ \mathbf{h}_j^E(\mathbf{u}_i) - \boldsymbol{\phi}^{L_N}(\mathbf{u}_i)' \boldsymbol{\alpha}_{L_N}^j \}^2} = O_p(L_N^{-\kappa} \sqrt{N}) = o_p(1) \end{aligned}$$

by the Assumption 2-(iii). □

A.3.2 Proof of Lemma 4

Proof. We only need to show that

1. $\frac{1}{N} \sum_{i \leq N} [\hat{\mathbf{h}}^K(\mathbf{u}_i) - \mathbf{h}^K(\mathbf{u}_i)][\hat{\mathbf{h}}^Z(\mathbf{u}_i) - \mathbf{h}^Z(\mathbf{u}_i)]' = o_p(1)$
2. $\frac{1}{N} \sum_{i \leq N} [\hat{\mathbf{h}}^K(\mathbf{u}_i) - \mathbf{h}^K(\mathbf{u}_i)][\hat{\mathbf{h}}^K(\mathbf{u}_i) - \mathbf{h}^K(\mathbf{u}_i)]' = o_p(1)$
3. $\frac{1}{\sqrt{N}} \sum_{i \leq N} [\hat{\mathbf{h}}^K(\mathbf{u}_i) - \mathbf{h}^K(\mathbf{u}_i)] \tilde{\mathbf{e}}_i' = o_p(1).$

As 3 follows from 2, it suffices to address 1 and 2, and these follow by Lemma 9. □

A.4 Additional Technical Lemmas

First, we realize that

$$\mathbf{Y}_v = (\mathbf{D}' \otimes \mathbf{G}) \mathbf{Y}_v + (\mathbf{B}'_1 \otimes \mathbf{I}) \mathbf{X}_v + (\mathbf{B}'_2 \otimes \mathbf{G}) \mathbf{X}_v + \mathbf{E}_v$$

which has a solution of the form

$$\begin{aligned} \begin{bmatrix} \mathbf{Y}_1 \\ \vdots \\ \mathbf{Y}_m \end{bmatrix} &= \{\mathbf{I}_{Nm} - (\mathbf{D}' \otimes \mathbf{G})\}^{-1} \{(\mathbf{B}'_1 \otimes \mathbf{I}_N) + (\mathbf{B}'_2 \otimes \mathbf{G})\} \mathbf{X}_v + \mathbf{E}_v \\ &= \sum_{l=0}^{\infty} (\mathbf{D}' \otimes \mathbf{G})^l \{(\mathbf{B}'_1 \otimes \mathbf{I}_N) + (\mathbf{B}'_2 \otimes \mathbf{G})\} \mathbf{X}_v + \mathbf{E}_v \\ &= \sum_{l=0}^{\infty} \{(\mathbf{D}'^l)' \otimes \mathbf{G}^l\} \{(\mathbf{B}'_1 \otimes \mathbf{I}_N) + (\mathbf{B}'_2 \otimes \mathbf{G})\} \mathbf{X}_v + \mathbf{E}_v \end{aligned}$$

provided that $\rho(\mathbf{D}' \otimes \mathbf{G}) < 1$, i.e., $\rho(\mathbf{D}) < 1, \rho(\mathbf{G}) < 1$.

Lemma 5. *Assume that*

$$\max_{i_1, \dots, i_4 \leq N} \mathbb{E} \left(\frac{\|\mathbf{a}_{i_1}\|^2 \|\mathbf{a}_{i_2}\|^2 \|\mathbf{a}_{i_3}\| \|\mathbf{a}_{i_4}\| \|\mathbf{A}\|_{2,\infty}^2}{\delta_{i_1}^2 \delta_{i_2}^2 \delta_{\min}^4} \right) = o(1/N^2).$$

Write $\Sigma_{\tilde{K}\tilde{Z}} := \lim_{N \rightarrow \infty} \frac{1}{N} \mathbb{E}(\tilde{\mathbf{K}}' \tilde{\mathbf{Z}})$, $\Sigma_{\tilde{Z}\tilde{K}} := \lim_{N \rightarrow \infty} \frac{1}{N} \mathbb{E}(\tilde{\mathbf{Z}}' \tilde{\mathbf{K}})$, and $\Sigma_{\tilde{K}} := \lim_{N \rightarrow \infty} \frac{1}{N} \mathbb{E}(\tilde{\mathbf{K}}' \tilde{\mathbf{K}})$. Then, $\frac{1}{N} \tilde{\mathbf{K}}' \tilde{\mathbf{Z}}_N = \Sigma_{\tilde{K}\tilde{Z}} + o_p(1)$, $\frac{1}{N} \tilde{\mathbf{Z}}' \tilde{\mathbf{K}}_N = \Sigma_{\tilde{Z}\tilde{K}} + o_p(1)$, and $\frac{1}{N} \tilde{\mathbf{K}}' \tilde{\mathbf{K}}_N = \Sigma_{\tilde{K}} + o_p(1)$.

Proof. We only show

$$\begin{aligned} \frac{1}{N} \tilde{\mathbf{K}}' \tilde{\mathbf{Z}} &= \frac{1}{N} \begin{bmatrix} \mathbf{X}'(\tilde{\mathbf{G}}\tilde{\mathbf{Y}}) & \mathbf{X}'\mathbf{X} & \mathbf{X}'(\tilde{\mathbf{G}}\mathbf{X}) \\ (\tilde{\mathbf{G}}\mathbf{X})'(\tilde{\mathbf{G}}\tilde{\mathbf{Y}}) & (\tilde{\mathbf{G}}\mathbf{X})'\mathbf{X} & (\tilde{\mathbf{G}}\mathbf{X})'(\tilde{\mathbf{G}}\mathbf{X}) \\ (\tilde{\mathbf{G}}^2\mathbf{X})'(\tilde{\mathbf{G}}\tilde{\mathbf{Y}}) & (\tilde{\mathbf{G}}^2\mathbf{X})'\mathbf{X} & (\tilde{\mathbf{G}}^2\mathbf{X})'(\tilde{\mathbf{G}}\mathbf{X}) \end{bmatrix} \\ &= \begin{bmatrix} \Sigma_{X,(\tilde{\mathbf{G}}\tilde{\mathbf{Y}})} & \Sigma_X & \Sigma_{X,(\tilde{\mathbf{G}}\mathbf{X})} \\ \Sigma_{(\tilde{\mathbf{G}}\mathbf{X}),(\tilde{\mathbf{G}}\tilde{\mathbf{Y}})} & \Sigma_{(\tilde{\mathbf{G}}\mathbf{X}),X} & \Sigma_{(\tilde{\mathbf{G}}\mathbf{X})} \\ \Sigma_{(\tilde{\mathbf{G}}^2\mathbf{X}),(\tilde{\mathbf{G}}\tilde{\mathbf{Y}})} & \Sigma_{(\tilde{\mathbf{G}}^2\mathbf{X}),X} & \Sigma_{(\tilde{\mathbf{G}}^2\mathbf{X}),(\tilde{\mathbf{G}}\mathbf{X})} \end{bmatrix} + o_p(1) \end{aligned}$$

where $(\tilde{\mathbf{G}}\tilde{\mathbf{Y}}) := \mathbf{G}\tilde{\mathbf{Y}} - \mathbb{E}(\mathbf{G}\tilde{\mathbf{Y}}|\mathbf{U})$ (and the rest terms are defined analogously) as the convergence of $\frac{1}{N} \tilde{\mathbf{Z}}' \tilde{\mathbf{K}}$, $\frac{1}{N} \tilde{\mathbf{K}}' \tilde{\mathbf{K}}$ can be proved in the same way. The block entries are defined as $\Sigma_{X,(\tilde{\mathbf{G}}\tilde{\mathbf{Y}})} := \frac{1}{N} \mathbb{E}[\mathbf{X}'(\tilde{\mathbf{G}}\tilde{\mathbf{Y}})]$, $\Sigma_X := \mathbb{E}(\mathbf{x}_1 \mathbf{x}_1')$, and the rest are defined analogously. We only show that $\frac{1}{N} (\tilde{\mathbf{G}}^2\mathbf{X})'(\tilde{\mathbf{G}}\tilde{\mathbf{Y}}) - \Sigma_{(\tilde{\mathbf{G}}^2\mathbf{X}),(\tilde{\mathbf{G}}\tilde{\mathbf{Y}})} = o_p(1)$ as the rest can be shown in the same way. i.e.,

$$\left| \frac{1}{N} (\tilde{\mathbf{G}}^2\mathbf{X}_j)'(\tilde{\mathbf{G}}\tilde{\mathbf{Y}}_i) - \sigma_{ji,(\tilde{\mathbf{G}}^2\mathbf{X}),(\tilde{\mathbf{G}}\tilde{\mathbf{Y}})} \right| = o_p(1)$$

for all $i \leq m$ and $j \leq p$. We only need to show that $\sigma_{ji,(\tilde{\mathbf{G}}^2\mathbf{X}),(\tilde{\mathbf{G}}\tilde{\mathbf{Y}})} = \lim_{N \rightarrow \infty} \frac{1}{N} \mathbb{E}[(\tilde{\mathbf{G}}^2\mathbf{X}_j)'(\tilde{\mathbf{G}}\tilde{\mathbf{Y}}_i)]$ exists and $\mathbb{V} \left[\frac{1}{N} (\tilde{\mathbf{G}}^2\mathbf{X}_j)'(\tilde{\mathbf{G}}\tilde{\mathbf{Y}}_i) \right] = o(1)$. Observe that $(\tilde{\mathbf{G}}^2\mathbf{X}) = \mathbf{G}^2\mathbf{X}$ and

$$\frac{1}{N} \mathbb{E} \left[(\tilde{\mathbf{G}}^2\mathbf{X}_j)'(\tilde{\mathbf{G}}\tilde{\mathbf{Y}}_i) \right] = \frac{1}{N} \sum_{k \leq N} \mathbb{E}[(\mathbf{g}'_k \mathbf{G}\mathbf{X}_j)(\mathbf{g}'_k \tilde{\mathbf{Y}}_i)]$$

as $(\mathbf{x}_i, \mathbf{u}_i, \mathbf{e}_i)$ are i.i.d. and X_{ij} is uncorrelated with \mathbf{u}_i . Second, it suffices to show that

$$\begin{aligned} \frac{1}{N^2} \mathbb{E} \left[(\mathbf{G}^2\mathbf{X}_j)'(\tilde{\mathbf{G}}\tilde{\mathbf{Y}}_i)(\tilde{\mathbf{G}}\tilde{\mathbf{Y}}_i)' \mathbf{G}^2\mathbf{X}_j \right] \\ = \frac{1}{N^2} \sum_{k,h \leq N} \mathbb{E} \left[(\mathbf{g}'_k \mathbf{G}\mathbf{X}_j)(\mathbf{g}'_h \mathbf{G}\mathbf{X}_j)(\mathbf{g}'_k \tilde{\mathbf{Y}}_i)(\mathbf{g}'_h \tilde{\mathbf{Y}}_i) \right] = o(1). \end{aligned}$$

Using the block selector $\mathbf{L}_i := \mathbf{e}_i' \otimes \mathbf{I}_N$, by $\mathbf{L}_i \mathbf{Y}_v = \mathbf{Y}_i$ we get

$$\begin{aligned}
\mathbf{g}'_k \mathbf{Y}_i &= \sum_{l=0}^{\infty} \mathbf{g}'_k \{(\mathbf{D}^l \mathbf{e}_i)' \otimes \mathbf{G}^l\} \{(\mathbf{B}'_1 \otimes \mathbf{I}_N) + (\mathbf{B}'_2 \otimes \mathbf{G})\} \mathbf{X}_v + \mathbf{E}_v \\
&= \sum_{l=0}^{\infty} \{(\mathbf{B}_1 \mathbf{D}^l \mathbf{e}_i)' \otimes (\mathbf{g}'_k \mathbf{G}^l) + (\mathbf{B}_2 \mathbf{D}^l \mathbf{e}_i)' \otimes (\mathbf{g}'_k \mathbf{G}^{l+1})\} \mathbf{X}_v \\
&\quad + \sum_{l=0}^{\infty} \{(\mathbf{D}^l \mathbf{e}_i)' \otimes (\mathbf{g}'_k \mathbf{G}^l)\} \mathbf{E}_v \\
&= \sum_{l=0}^{\infty} \sum_{o=1}^p \sum_{s=1}^N \left[(\mathbf{e}'_o \mathbf{B}_1 \mathbf{D}^l \mathbf{e}_i) (\mathbf{e}'_k \mathbf{G}^{l+1} \mathbf{e}_s) + (\mathbf{e}'_o \mathbf{B}_2 \mathbf{D}^l \mathbf{e}_i) (\mathbf{e}'_k \mathbf{G}^{l+2} \mathbf{e}_s) \right] X_{so} \\
&\quad + \sum_{l=0}^{\infty} \sum_{o=1}^p \sum_{s=1}^N (\mathbf{e}'_o \mathbf{D}^l \mathbf{e}_i) (\mathbf{e}'_k \mathbf{G}^{l+1} \mathbf{e}_s) E_{so} \\
&= \sum_{o=1}^p \sum_{s=1}^N \underbrace{\sum_{l=0}^{\infty} (\mathbf{B}_1 \mathbf{D}^l \mathbf{e}_i \mathbf{e}'_k \mathbf{G}^{l+1} + \mathbf{B}_2 \mathbf{D}^l \mathbf{e}_i \mathbf{e}'_k \mathbf{G}^{l+2})}_{=: (\mathcal{B}_{ik})_{os}} X_{so} \\
&\quad + \sum_{o=1}^p \sum_{s=1}^N \underbrace{\sum_{l=0}^{\infty} (\mathbf{D}^l \mathbf{e}_i \mathbf{e}'_k \mathbf{G}^{l+1})}_{=: (\mathcal{C}_{ik})_{os}} E_{so} = \sum_{o=1}^p \sum_{s=1}^N \{(\mathcal{B}_{ik})_{os} X_{so} + (\mathcal{C}_{ik})_{os} E_{so}\}
\end{aligned}$$

where the penultimate line follows by $(\mathbf{b}' \otimes \mathbf{a}') \text{vec}(\mathbf{X}) = \mathbf{a}' \mathbf{X} \mathbf{b} = \sum_{s,o} a_s b_o X_{so}$. So,

$$\mathbb{E}(\mathbf{g}'_k \mathbf{Y}_i | \mathbf{U}) = \sum_{o=1}^p \sum_{s=1}^N \mathbb{E}\{(\mathcal{B}_{ik})_{os} X_{so} + (\mathcal{C}_{ik})_{os} E_{so} | \mathbf{U}\} = \sum_{o=1}^p \sum_{s=1}^N \mathbb{E}\{(\mathcal{C}_{ik})_{os} E_{so} | \mathbf{U}\}$$

hence

$$\begin{aligned}
\frac{1}{N} \sum_{k \leq N} \mathbb{E}[(\mathbf{g}'_k \mathbf{G} \mathbf{X}_j)(\mathbf{g}'_k \tilde{\mathbf{Y}}_i)] &= \frac{1}{N} \sum_{k,o,s} \mathbb{E}[(\mathbf{g}'_k \mathbf{G} \mathbf{X}_j) \{(\mathcal{B}_{ik})_{os} X_{so} + (\mathcal{C}_{ik})_{os} E_{so} - \mathbb{E}((\mathcal{C}_{ik})_{os} E_{so} | \mathbf{U})\}] \\
&= \frac{1}{N} \sum_{k,o,s} \mathbb{E}[(\mathcal{B}_{ik})_{os} X_{so} \mathbf{X}'_j \mathbf{G}' \mathbf{g}_k] = \frac{1}{N} \sum_{k,o,s} \mathbb{E}(X_{so} \mathbf{X}'_j) \mathbb{E}[(\mathcal{B}_{ik})_{os} \mathbf{G}' \mathbf{g}_k] \\
&= \frac{1}{N} \sum_{k,o,s} \sigma_{oj,X} \mathbf{e}'_s \mathbb{E}[(\mathcal{B}_{ik})_{os} \mathbf{G}' \mathbf{g}_k] = \frac{1}{N} \sum_{k,o,s} \sigma_{oj,X} \mathbb{E}[(\mathcal{B}_{ik})_{os} \mathbf{G}'_s \mathbf{g}_k]
\end{aligned}$$

as \mathbf{X} and \mathbf{U} are uncorrelated. We have $\sum_{s,k} (\mathcal{B}_{ik})_{os} (\mathbf{G}' \mathbf{G}')_{sk} = \sum_k (\mathcal{B}_{ik} \mathbf{G}' \mathbf{G}')_{ok} = (\mathbf{1} \otimes \mathbf{e}_o)' \text{vec}(\mathcal{B}_{ik} \mathbf{G}' \mathbf{G}')$ and

$$\begin{aligned}
\mathcal{B}_{ik}(\mathbf{G}')^2 &= \sum_{l=0}^{\infty} (\mathbf{B}_1 \mathbf{D}^l \mathbf{e}_i \mathbf{e}'_k \mathbf{G}^{l+1} + \mathbf{B}_2 \mathbf{D}^l \mathbf{e}_i \mathbf{e}'_k \mathbf{G}^{l+2})(\mathbf{G}')^2 \\
&= \sum_{l=0}^{\infty} \mathbf{B}_1 (\mathbf{D}^l \mathbf{e}_i \mathbf{e}'_k \mathbf{G}^l) \mathbf{G} (\mathbf{G}')^2 + \sum_{l=0}^{\infty} \mathbf{B}_2 (\mathbf{D}^l \mathbf{e}_i \mathbf{e}'_k \mathbf{G}^l) \mathbf{G}^2 (\mathbf{G}')^2,
\end{aligned}$$

$$\begin{aligned}
\text{vec}(\mathcal{B}_{ik} \mathbf{G}' \mathbf{G}') &= \{((\mathbf{G}^2 \mathbf{G}') \otimes \mathbf{B}_1) + ((\mathbf{G}^2 \mathbf{G}' \mathbf{G}') \otimes \mathbf{B}_2)\} \sum_l ((\mathbf{G}') \otimes \mathbf{D})^l \text{vec}(\mathbf{e}_i \mathbf{e}'_k) \\
&= \{((\mathbf{G}^2 \mathbf{G}') \otimes \mathbf{B}_1) + ((\mathbf{G}^2 \mathbf{G}' \mathbf{G}') \otimes \mathbf{B}_2)\} (\mathbf{I}_{Nm} - (\mathbf{G}') \otimes \mathbf{D})^{-1} (\mathbf{e}_k \otimes \mathbf{e}_i).
\end{aligned}$$

As $\rho(\mathbf{G}), \rho(\mathbf{D}) < 1$, and by the dominated convergence theorem, $\sigma_{ji, (G^2 X), (G^2 Y)}$ exists.

Next, writing

$$\begin{aligned}\eta_{os,k} &:= (\mathcal{C}_{ik})_{os} E_{so} - \mathbb{E}((\mathcal{C}_{ik})_{os} E_{so} | \mathbf{U}) \\ &= \sum_{l=0}^{\infty} \{(\mathbf{D}^l \mathbf{e}_i \mathbf{e}'_k \mathbf{G}^{l+1})_{os} E_{so} - \mathbb{E}((\mathbf{D}^l \mathbf{e}_i \mathbf{e}'_k \mathbf{G}^{l+1})_{os} E_{so} | \mathbf{U})\},\end{aligned}$$

we have

$$\begin{aligned}&\frac{1}{N^2} \sum_{k,h \leq N} \mathbb{E} \left[(\mathbf{g}'_k \mathbf{G} \mathbf{X}_j) (\mathbf{g}'_h \mathbf{G} \mathbf{X}_j) (\mathbf{g}'_k \tilde{\mathbf{Y}}_i) (\mathbf{g}'_h \tilde{\mathbf{Y}}_i) \right] \\ &= \frac{1}{N^2} \sum_{k,h,s_1,s_2,o_1,o_2} \mathbb{E} [(\mathbf{g}'_k \mathbf{G} \mathbf{X}_j) (\mathbf{g}'_h \mathbf{G} \mathbf{X}_j) \{(\mathcal{B}_{ik})_{o_1 s_1} X_{s_1 o_1} + \eta_{o_1 s_1, k}\} \{(\mathcal{B}_{ih})_{o_2 s_2} X_{s_2 o_2} + \eta_{o_2 s_2, h}\}].\end{aligned}$$

Note that

$$\begin{aligned}(\mathcal{B}_{ik})_{os} &= \sum_{l_1=0}^{\infty} (\mathbf{b}'_{1,o} (\mathbf{D}^{l_1})_i \mathbf{g}'_k \mathbf{G}^{l_1} + \mathbf{b}'_{2,o} (\mathbf{D}^{l_1})_i \mathbf{g}'_k \mathbf{G}^{l_1+1})_s \\ &\leq (\|\mathbf{b}_{1,o}\| + \|\mathbf{b}_{2,o}\|) \sum_{l_1=0}^{\infty} \mathbf{g}'_k (\mathbf{G}^{l_1-1} + \mathbf{G}^{l_1}) \mathbf{G}_s \leq 2C \|\mathbf{g}_k\| \|\mathbf{G}_s\|\end{aligned}$$

for some constant $C > 0$ and

$$\|\mathbf{g}_k\|^2 = \frac{\|\mathbf{a}_k\|^2}{\delta_k^2}, \quad \|\mathbf{G}_s\|^2 = \sum_{j \leq N} \frac{a_{sj}^2}{\delta_j^2} \leq \frac{\|\mathbf{a}_s\|^2}{\delta_{\min}^2} \text{ so } \|\mathbf{g}_k\| \|\mathbf{G}_s\| \leq \frac{\|\mathbf{a}_k\| \|\mathbf{a}_s\|}{\delta_k \delta_{\min}}.$$

Then,

$$\begin{aligned}&\frac{1}{N^2} \sum_{k,h,s_1,s_2,o_1,o_2} \mathbb{E} [(\mathcal{B}_{ik})_{o_1 s_1} (\mathcal{B}_{ih})_{o_2 s_2} X_{s_1 o_1} X_{s_2 o_2} (\mathbf{g}'_k \mathbf{G} \mathbf{X}_j \mathbf{X}'_j \mathbf{G}' \mathbf{g}_h)] \\ &\lesssim \frac{1}{N^2} \sum_{k,h,s_1,s_2,o_1,o_2} \mathbb{E} (\|\mathbf{g}_k\|^2 \|\mathbf{g}_h\|^2 \|\mathbf{G}_{s_1}\| \|\mathbf{G}_{s_2}\|) \mathbb{E} (X_{s_1 o_1} X_{s_2 o_2} \|\mathbf{g}'_k \mathbf{G}\| \|\mathbf{g}'_h \mathbf{G}\| \|\mathbf{X}_j\|^2) \\ &\leq \max_{k,h,s_1,s_2} \mathbb{E} \left(\frac{\|\mathbf{a}_k\|^2 \|\mathbf{a}_h\|^2 \|\mathbf{a}_{s_1}\| \|\mathbf{a}_{s_2}\| \|\mathbf{G}\|_{2,\infty}^2}{\delta_k^2 \delta_h^2 \delta_{\min}^2} \right) \sum_{s_1,s_2,o_1,o_2} \mathbb{E} (X_{s_1 o_1} X_{s_2 o_2} \|\mathbf{X}_j\|^2) \\ &\leq \max_{k,h,s_1,s_2} \mathbb{E} \left(\frac{\|\mathbf{a}_k\|^2 \|\mathbf{a}_h\|^2 \|\mathbf{a}_{s_1}\| \|\mathbf{a}_{s_2}\| \|\mathbf{A}\|_{2,\infty}^2}{\delta_k^2 \delta_h^2 \delta_{\min}^4} \right) \sum_{s_1,s_2,o_1,o_2} \mathbb{E} (X_{s_1 o_1} X_{s_2 o_2} \|\mathbf{X}_j\|^2)\end{aligned}$$

which is $o(1)$ by the fact that

$$\begin{aligned}\sum_{1 \leq s_1, s_2, s_3 \leq N} \mathbb{E} (X_{s_1 o_1} X_{s_2 o_2} X_{s_3 j}^2) &\leq N \{ \mathbb{E} (X_{1 o_1} X_{1 o_2} X_{1 j}^2) + N \mathbb{E} (X_{1 o_1} X_{1 o_2}) \mathbb{E} (X_{1 j}^2) \} \\ &= O(N^2).\end{aligned}$$

Next, noting that $\mathbb{E}[(\mathcal{C}_{ik})_{os} E_{so} | \mathbf{U}] = (\mathcal{C}_{ik})_{os} \mathbb{E}[E_{so} | \mathbf{U}]$ and

$$\sum_{l=0}^{\infty} \sum_{k,s,o} (\mathbf{D}^l \mathbf{e}_i \mathbf{e}'_k \mathbf{G}^{l+1})_{os} \tilde{E}_{so} \leq \sum_l \sum_{k,s,o} C \mathbf{g}'_k \mathbf{G}^{l-1} \mathbf{G}_s \tilde{E}_{so},$$

we have

$$\begin{aligned} \frac{1}{N^2} \sum_{k,h,s_1,s_2,o_1,o_2} \mathbb{E}(\eta_{o_1s_1,k} \eta_{o_2s_2,h}) &= \frac{1}{N^2} \sum_{k,h,s_1,s_2,o_1,o_2} \mathbb{E}[(\mathcal{C}_{ik})_{o_1s_1} (\mathcal{C}_{ih})_{o_2s_2} \tilde{E}_{s_1o_1} \tilde{E}_{s_2o_2}] \\ &= \frac{1}{N^2} \sum_{k,h,s_1,s_2,o_1,o_2} \mathbb{E}(\tilde{E}_{s_1o_1} \tilde{E}_{s_2o_2}) \mathbb{E}[(\mathcal{C}_{ik})_{o_1s_1} (\mathcal{C}_{ih})_{o_2s_1}] = o(1) \end{aligned}$$

by similar arguments. This completes the proof. \square

Lemma 6. *Let Assumption 3 hold. Under the conditions on RDPG model in Rubin-Delanchy et al. [2022] and sparsity parameter $\rho_N = \omega(\frac{\log^4 N}{N})$, we have*

$$\frac{1}{N} \|\hat{\Phi}_N - \Phi_N\|_F^2 = O_{hp} \left(\frac{\log^{2c} N}{N} \sum_{k \leq L_N} \zeta_1(k)^2 \right)$$

and under the conditions on the sparse LSM model with sparsity parameter $\omega_N = \omega(N^{-1/2})$ in Li et al. [2023], we have

$$\frac{1}{N} \|\hat{\Phi}_N - \Phi_N\|_F^2 = O_{hp} \left(\frac{1}{N\omega_N} \sum_{k \leq L_N} \zeta_1(k)^2 \right).$$

Proof.

$$\frac{1}{N} \|\hat{\Phi}_N - \Phi_N\|_F^2 = \frac{1}{N} \sum_{i \leq N, k \leq L_N} |\phi_k(\hat{\mathbf{u}}_i) - \phi_k(\mathbf{H}' \mathbf{u}_i)|^2 \leq \frac{1}{N} \sum_{i \leq N, k \leq L_N} \zeta_1(k)^2 \|\hat{\mathbf{u}}_i - \mathbf{H}' \mathbf{u}_i\|^2$$

By the results on Adjacency Spectral Embedding in RDPG model in Rubin-Delanchy et al. [2022], the last term is less than

$$\|\hat{\mathbf{U}} - \mathbf{U}\mathbf{H}\|_{2,\infty}^2 \sum_{k \leq L_N} \zeta_1(k)^2 = O_{hp} \left(\frac{\log^{2c} N}{N} \sum_{k \leq L_N} \zeta_1(k)^2 \right)$$

if \mathbf{A} follows the RDPG. If we instead assume that \mathbf{A} is generated from LSM with sparsity factor ω_n , the last term is bounded by

$$\frac{1}{N} \|\hat{\mathbf{U}} - \mathbf{U}\|_F^2 \sum_{k \leq L_N} \zeta_1(k)^2 = O_p \left(\frac{1}{N\omega_n} \sum_{k \leq L_N} \zeta_1(k)^2 \right)$$

by the result of the concentration of the MLE in LSM Li et al. [2023]. \square

Clearly, Lemma 6 provides a result on the concentration of the sieve design matrix when the true latent positions \mathbf{U} are replaced with their estimated counterparts $\hat{\mathbf{U}}$. Both the RDPG and the LSM models can accommodate sparse networks through the sparsity parameters ρ_N and ω_N respectively. However, our result with the RDPG model has a better concentration of the $\hat{\Phi}_N$ to Φ_N , for whenever ω_N is smaller than $\frac{1}{\log^{2c} N}$, i.e., if the network is even slightly sparse. However, we emphasize that our results for both models accommodate sparse networks with density requirement for RDPG being $\frac{\log^4 N}{N}$ and LSM being $\frac{N^{1/2}}{N}$.

Lemma 7. *Given Assumptions 2-(ii), (iii), and 3,*

$$\operatorname{plim}_{N \rightarrow \infty} \lambda_{\min} \left(\frac{\Phi'_N \Phi_N}{N} \right) = \operatorname{plim}_{N \rightarrow \infty} \lambda_{\min} \left(\frac{\hat{\Phi}'_N \hat{\Phi}_N}{N} \right) = \lim_{N \rightarrow \infty} \lambda_{\min} (\mathbb{E}[\phi^{L_N}(\mathbf{u}_1) \phi^{L_N}(\mathbf{u}_1)']) .$$

Proof. We first show

$$\left| \lambda_{\min} \left(\frac{\Phi'_N \Phi_N}{N} \right) - \lambda_{\min} (\mathbb{E}[\phi^{L_N}(\mathbf{u}_1) \phi^{L_N}(\mathbf{u}_1)']) \right| = o_p(1).$$

Temporarily write $\mathbf{W}^{(i)} := \phi^{L_N}(\mathbf{u}_i) \phi^{L_N}(\mathbf{u}_i)'$. By Lemma 5 of [Johnsson and Moon \[2021\]](#), we have

$$\begin{aligned} \left| \lambda_{\min} \left(\frac{\Phi'_N \Phi_N}{N} \right) - \lambda_{\min} (\mathbb{E}[\mathbf{W}^{(1)}]) \right| &\leq \left\| \frac{\Phi'_N \Phi_N}{N} - \mathbb{E}(\mathbf{W}^{(1)}) \right\|_F \\ &= \left\| \frac{1}{N} \sum_{i=1}^N \{\mathbf{W}^{(i)} - \mathbb{E}(\mathbf{W}^{(i)})\} \right\|_F . \end{aligned}$$

Then for $\tilde{\mathbf{W}}^{(i)} := \mathbf{W}^{(i)} - \mathbb{E}(\mathbf{W}^{(i)}) = (\tilde{w}_{kl}^{(i)})_{k,l \leq L_N}$, by assumption, we have

$$\begin{aligned} \mathbb{E} \left\| \frac{1}{N} \sum_{i=1}^N \tilde{\mathbf{W}}^{(i)} \right\|_F^2 &= \mathbb{E} \sum_{1 \leq k, l \leq L_N} \left(\frac{1}{N} \sum_{i=1}^N \tilde{w}_{kl}^{(i)} \right)^2 = \sum_{1 \leq k, l \leq L_N} \frac{N}{N^2} \mathbb{E}(\tilde{w}_{kl}^{(1)2}) \\ &\leq \frac{1}{N} \sum_{1 \leq k, l \leq L_N} \mathbb{E}(w_{kl}^{(1)2}) = \frac{1}{N} \sum_{1 \leq k, l \leq L_N} \mathbb{E}[\phi_k(\mathbf{u}_1)^2 \phi_l(\mathbf{u}_1)^2] \\ &\leq \frac{1}{N} \left[\mathbb{E} \sum_{k \leq L_N} \phi_k(\mathbf{u}_1)^2 \right]^2 \leq \frac{1}{N} \left(\mathbb{E} \sup_{\mathbf{u} \in \mathcal{U}} \|\phi^{L_N}(\mathbf{u})\|^2 \right)^2 \leq \frac{\zeta_0(L_N)^4}{N} = o(1). \end{aligned}$$

Next,

$$\begin{aligned} \left| \lambda_{\min} \left(\frac{\hat{\Phi}'_N \hat{\Phi}_N}{N} \right) - \lambda_{\min} \left(\frac{\Phi'_N \Phi_N}{N} \right) \right| &\leq \left\| \frac{\hat{\Phi}'_N \hat{\Phi}_N}{N} - \frac{\Phi'_N \Phi_N}{N} \right\|_F \\ &\leq \left\| \frac{\hat{\Phi}_N - \Phi_N}{\sqrt{N}} \right\|_F^2 + \left\| \frac{\Phi'_N (\hat{\Phi}_N - \Phi_N)}{N} \right\|_F + \left\| \frac{(\hat{\Phi}_N - \Phi_N)' \Phi_N}{N} \right\|_F . \end{aligned}$$

Since $\|\Phi_N\|_F^2 = \sum_{i \leq N} \|\phi^{L_N}(\mathbf{u}_i)\|^2 \leq N \zeta_0(L_N)^2$,

$$\left\| \frac{(\hat{\Phi}_N - \Phi_N)' \Phi_N}{N} \right\|_F = O_{hp} \left(\sqrt{\zeta_0(L_N)^2 \sum_{k \leq L_N} \zeta_1(k)^2 \frac{\log^{2c} N}{N}} \right)$$

and by the assumptions, we have the conclusion. \square

In the following lemma, we write

$$\mathbf{Q}_{L_N} := \mathbb{E}[\phi^{L_N}(\mathbf{u}_1) \phi^{L_N}(\mathbf{u}_1)'].$$

Lemma 8. Under Assumption 2 in section 3.7, we have $\lambda_{\min}(\frac{1}{N}\Phi'_N\Phi_N) = \lambda_{\min}(\mathbf{Q}_{L_N}) + o_p(1)$.

Proof. Denote the j -th column of Φ_N by $\phi_j(\mathbf{U})$. Let $\hat{\mathbf{Q}}_{L_N} := \frac{1}{N}\Phi'_N\Phi_N$. Let $q_{ij} := \mathbb{E}[\phi_i(\mathbf{u}_1)' \phi_j(\mathbf{u}_1)]$. Then, for $z_{ij}(\mathbf{u}_k) := \phi_i(\mathbf{u}_k)\phi_j(\mathbf{u}_k) - q_{ij}$ which has zero mean,

$$\begin{aligned}\mathbb{E}\|\hat{\mathbf{Q}}_{L_N} - \mathbf{Q}_{L_N}\|_F^2 &= \sum_{1 \leq i, j \leq L_N} \mathbb{E} \left[\left(\frac{1}{N} \phi_i(\mathbf{U})' \phi_j(\mathbf{U}) - q_{ij} \right)^2 \right] \\ &= \sum_{1 \leq i, j \leq L_N} \mathbb{E} \left[\left(\frac{1}{N} \sum_{k \leq N} z_{ij}(\mathbf{u}_k) \right)^2 \right] = \frac{1}{N} \sum_{1 \leq i, j \leq L_N} \mathbb{E} [z_{ij}(\mathbf{u}_1)^2] \\ &\leq \frac{1}{N} \sum_{1 \leq i, j \leq L_N} \mathbb{E} [\phi_i(\mathbf{u}_1)^2 \phi_j(\mathbf{u}_1)^2] = \frac{1}{N} \mathbb{E} [\|\phi^{L_N}(\mathbf{u}_1)\|^4] \\ &\leq \frac{\zeta_0(L_N)^2}{N} \text{tr}(\mathbf{Q}_{L_N}) = O \left(\frac{\zeta_0(L_N)^2 L_N}{N} \right).\end{aligned}$$

So, the conclusion follows as $\|\hat{\mathbf{Q}}_{L_N} - \mathbf{Q}_{L_N}\|_F = o_p(1)$. \square

Lemma 9. Let $\hat{\alpha}_j^f := (\Phi'_N\Phi_N)^{-1}\Phi'_N\mathbf{h}_j^f(\mathbf{U}_N)$ for some $j \in \mathcal{I}(f)$ and $\hat{\mathbf{h}}_j^f := \hat{\mathbf{h}}_j^f(\mathbf{U}_N) = \Phi_N\hat{\alpha}_j^f$. Then, Under assumption on sieve approximation in section 3.7,

$$\|\hat{\alpha}_j^f - \alpha^j\| = O_p(L_N^{-\kappa}), \quad \frac{1}{N}\|\mathbf{h}_j^f(\mathbf{u}) - \hat{\mathbf{h}}_j^f(\mathbf{u})\|^2 = O_p(L_N^{-2\kappa}).$$

Proof. Let $B_N := \{\lambda_{\min}(\frac{1}{N}\Phi'_N\Phi_N) \geq 1/2\}$. Then, $B_N = \{1/\lambda_{\min}(\frac{1}{N}\Phi'_N\Phi_N) \leq 2\}$ implies

$$\begin{aligned}\|\hat{\alpha}_j^f - \alpha^j\| &= \left\| \left(\frac{1}{N}\Phi'_N\Phi_N \right)^{-1} \frac{1}{N}\Phi'_N\{\mathbf{h}_j^f(\mathbf{U}) - \Phi_N\alpha^j\} \right\| \leq 2 \left\| \frac{1}{N}\Phi'_N\{\mathbf{h}_j^f(\mathbf{U}) - \Phi_N\alpha^j\} \right\| \\ &\leq \frac{2\sqrt{2}}{\sqrt{N}} \|\mathbf{h}_j^f(\mathbf{U}) - \Phi_N\alpha^j\| \lesssim \|\mathbf{h}_j^f(\mathbf{U}) - \Phi_N\alpha^j\|_{\infty} = O(L_N^{-\kappa}).\end{aligned}$$

As $\Pr(B_N) \rightarrow 1$,

$$\|\hat{\alpha}_j^f - \alpha^j\| = O_p(L_N^{-\kappa}).$$

Next,

$$\begin{aligned}\frac{1}{N}\|\mathbf{h}_j^f(\mathbf{U}) - \hat{\mathbf{h}}_j^f(\mathbf{U})\|^2 &\leq \frac{1}{N}\|\mathbf{h}_j^f(\mathbf{U}) - \Phi_N\alpha^j\|^2 + \frac{1}{N}\|\Phi_N(\alpha^j - \hat{\alpha}_j^f)\|^2 \\ &= O(L_N^{-2\kappa}) + \frac{1}{N}\|\Phi'_N\Phi_N\|O_p(L_N^{-2\kappa}) = O_p(L_N^{-2\kappa}).\end{aligned}$$

\square

B Additional Tables and Figures

Table B1: Summary Statistics

Variable	N	Mean	SD	Min	p25	p50	p75	p95	Max
A. Female Unit									
Recidivism									
0	769	78%							
1	213	22%							
White	982								
Non White	204	21%							
White	778	79%							
LSI.R	982	25	7.2	0	21	25	30	35	57
Age	982	31	8.3	18	24	29	37	46	60
education	982								
less than HS	539	55%							
GED	109	11%							
HS	232	24%							
HS but < College Grad.	74	8%							
College Degree	28	3%							
B. Male Unit									
Recidivism									
0	1229	75%							
1	420	25%							
White	1649								
Non White	689	42%							
White	960	58%							
LSI.R	1649	26	10	0	22	25	29	35	354
Age	1649	29	8.8	18	21	26	35	46	60
education	1649								
less than HS	1018	62%							
GED	213	13%							
HS	293	18%							
HS but < College Grad.	94	6%							
College Degree	31	2%							

Notes: This table provides the summary statistics for the primary outcome “recidivism” and the pre-entry covariates.

Table B2: Peer Effects in Text Class Probabilities (Female) IV 2SLS without Adjustment

	Personal Growth ALR	Community Support ALR	Rule Violations ALR	Vi-
a. Sender Profiles				
Peer Personal Growth ALR	1.061 (0.239)	-0.091 (0.244)	0.189 (0.167)	
Peer Community Support ALR	-0.058 (0.301)	1.072 (0.307)	-0.165 (0.211)	
Peer Rule Violations ALR	-0.023 (0.336)	-0.257 (0.343)	1.375 (0.235)	
b. Receiver Profiles				
Peer Personal Growth ALR	1.060 (0.221)	0.227 (0.233)	-0.179 (0.150)	
Peer Community Support ALR	0.144 (0.284)	0.850 (0.300)	0.345 (0.193)	
Peer Rule Violations ALR	0.712 (0.265)	0.278 (0.279)	1.642 (0.180)	

Notes: This table deploys the IV 2SLS for multivariate outcomes but does not adjust for the endogeneity driven by endogeneity in network formation.

Table B3: Peer Effects in Text Class Probabilities (Male) IV 2SLS without Adjustment

	Personal Growth ALR	Community Support ALR	Rule Violations ALR
a. Sender Profiles			
Peer Personal Growth ALR	0.800 (0.332)	-0.266 (0.335)	-0.001 (0.218)
Peer Community Support ALR	0.222 (0.347)	1.224 (0.351)	0.014 (0.228)
Peer Rule Violations ALR	-0.146 (0.303)	-0.244 (0.306)	1.119 (0.199)
b. Receiver Profiles			
Peer Personal Growth ALR	1.258 (0.254)	0.309 (0.274)	0.013 (0.167)
Peer Community Support ALR	-0.212 (0.264)	0.706 (0.284)	-0.043 (0.173)
Peer Rule Violations ALR	0.138 (0.224)	0.012 (0.241)	1.063 (0.147)

Notes: This table deploys the IV 2SLS for multivariate outcomes but does not adjust for the endogeneity in network formation.

Figure B1: Overview of Methods Pipeline and Results

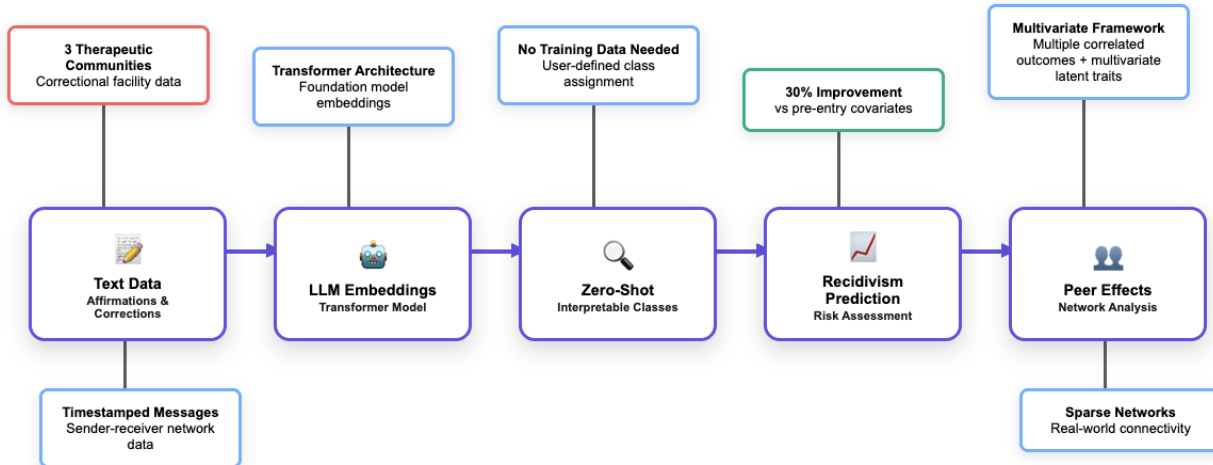


Figure B2: Entry, Exit Dates, Length of Stay and Time to Recidivism

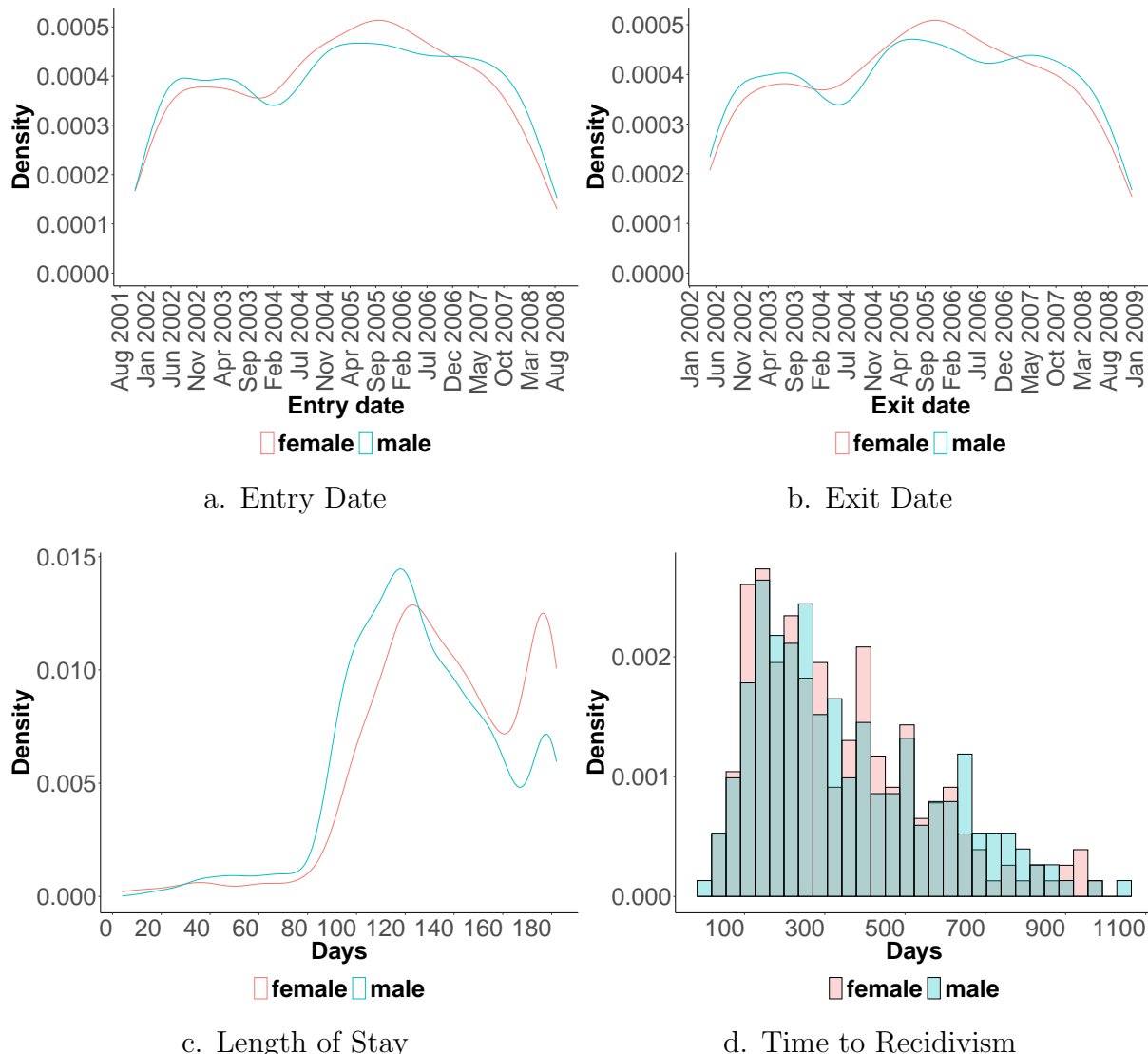


Figure B3: Exchanges of Affirmations and Corrections (Count)

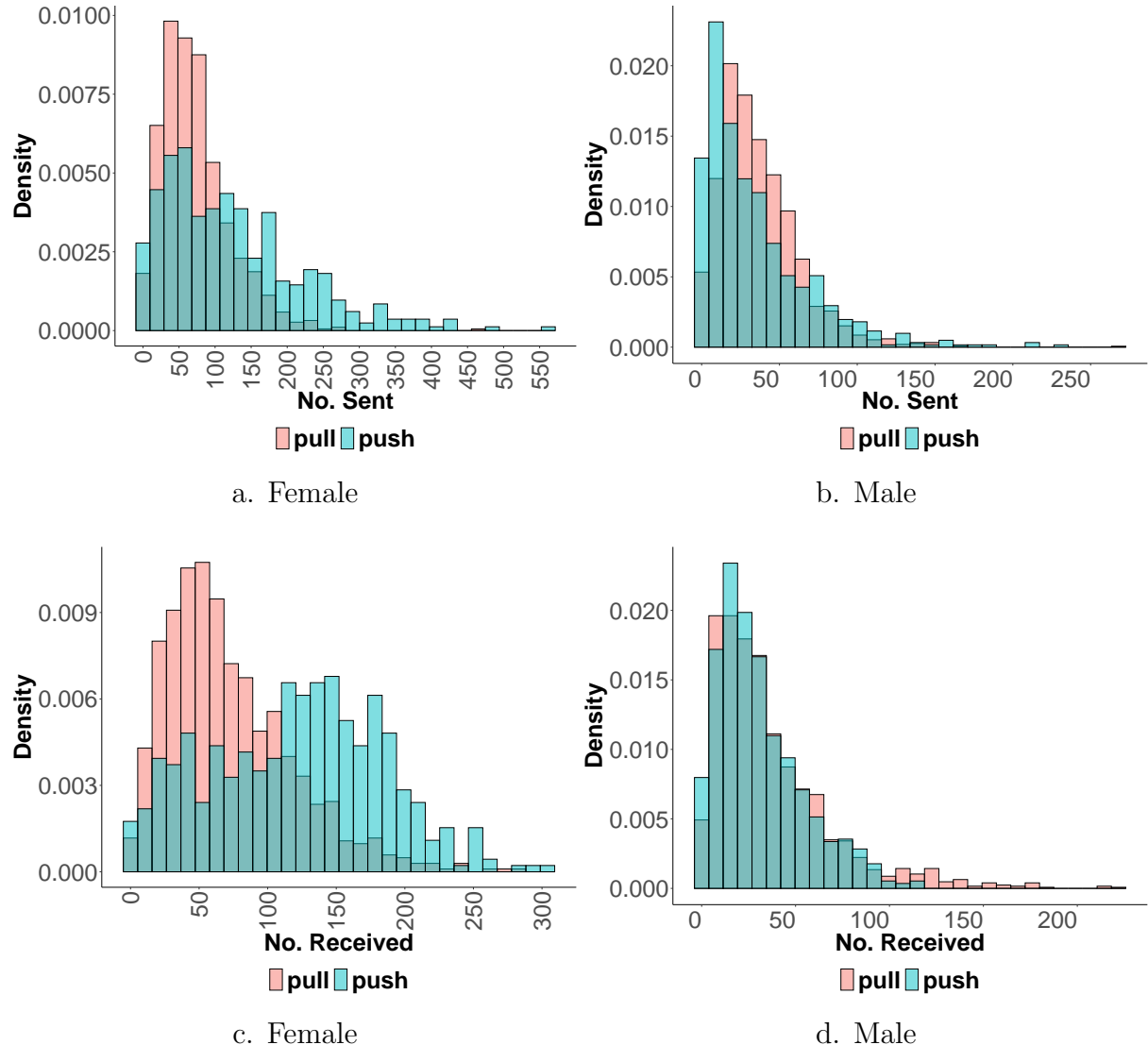
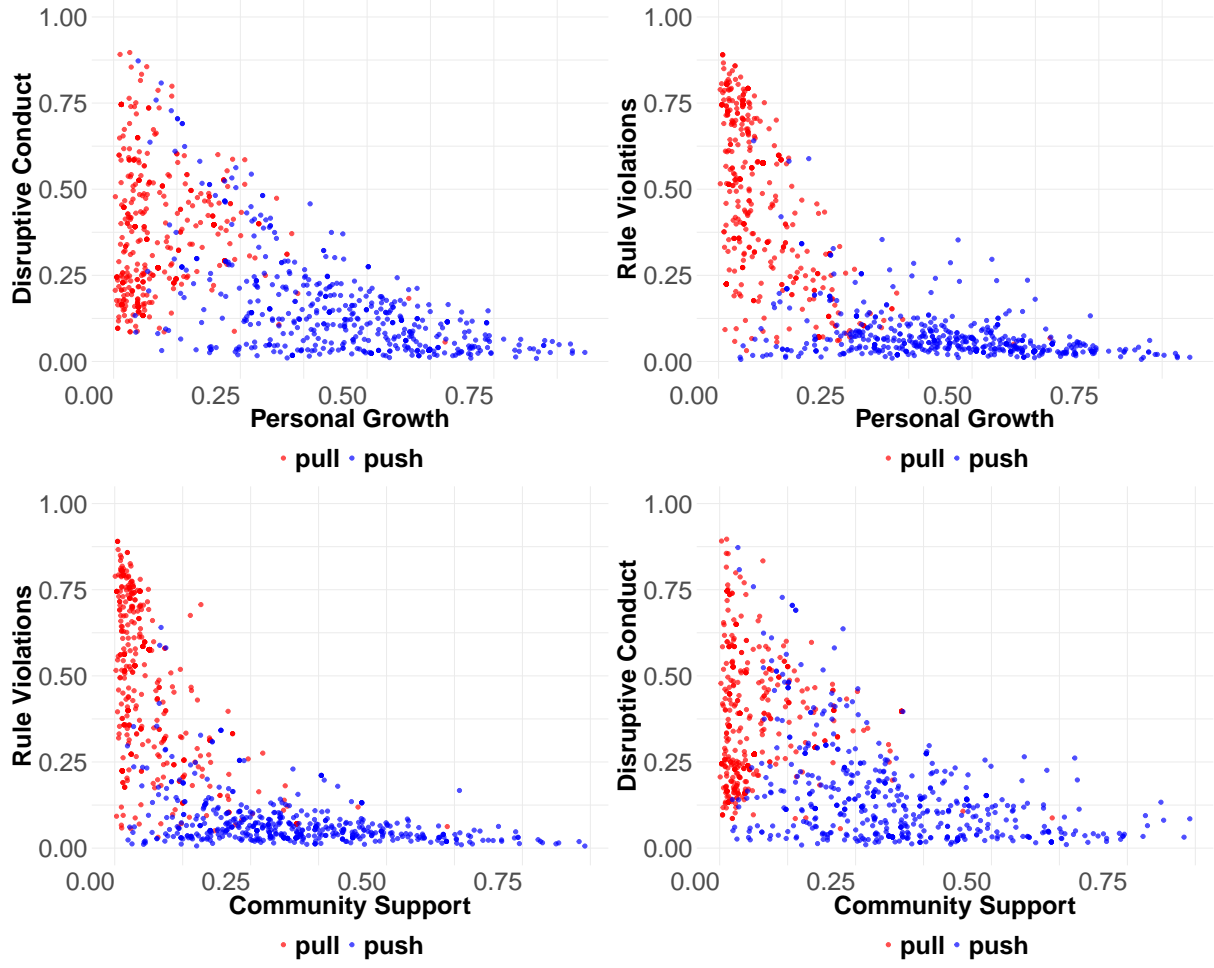
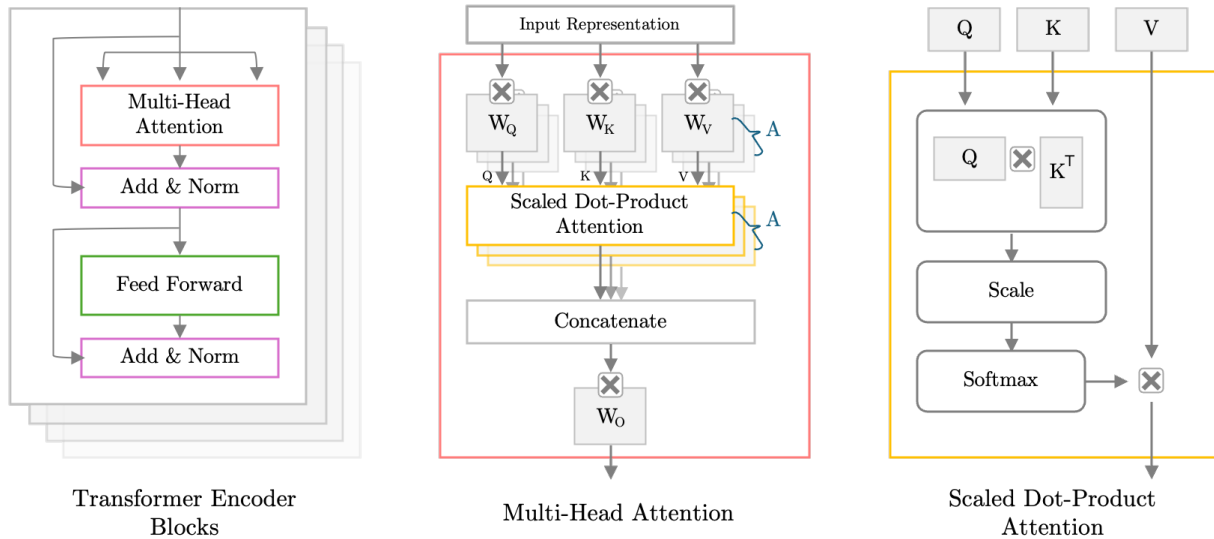


Figure B4: Class Probabilities and Message Type in Male Units



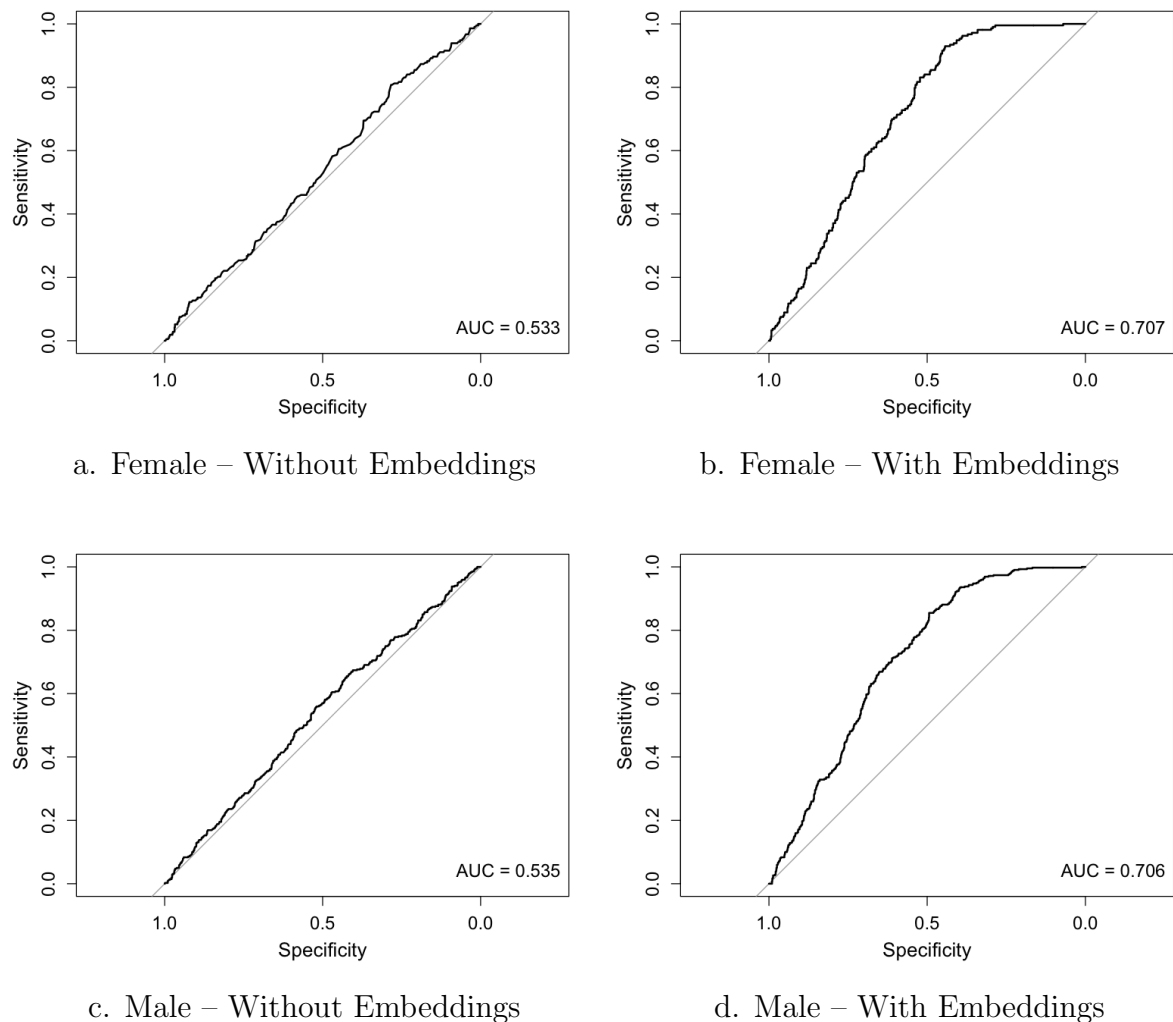
Notes: Random sample of 1000 text messages was drawn from the male units for this analysis, with 50% sampling by message type.

Figure B5: BERT Architecture



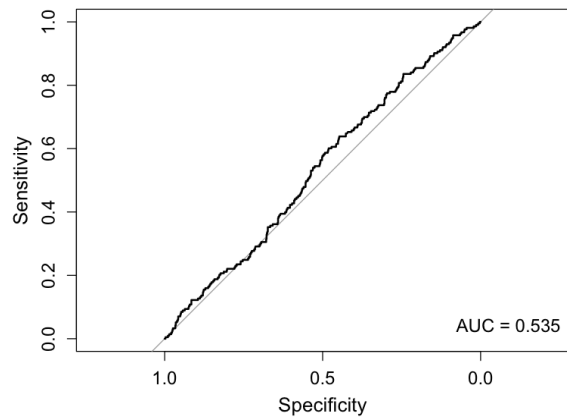
Notes: The architecture has been reproduced from the framework in [Vaswani et al. \[2017\]](#).

Figure B6: Predict Recidivism with and without text embeddings Aggregated by Receiver

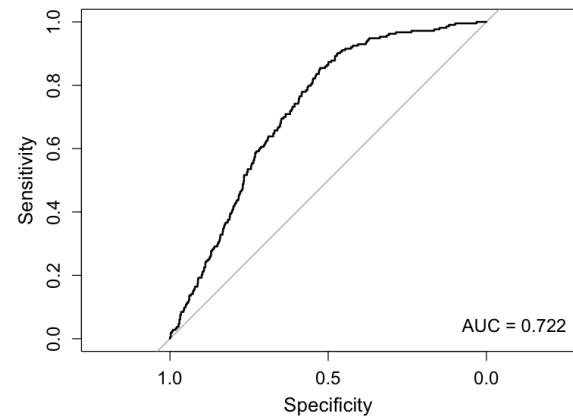


Notes: Five-fold cross-fitting is used to estimate the out-of-sample AUC for all models.

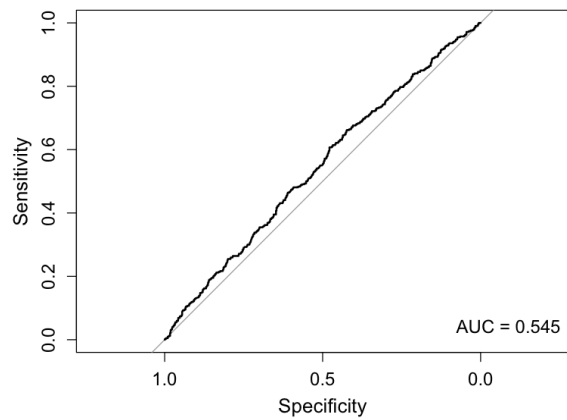
Figure B7: Predict Recidivism with and without class probabilities Aggregated by Receiver



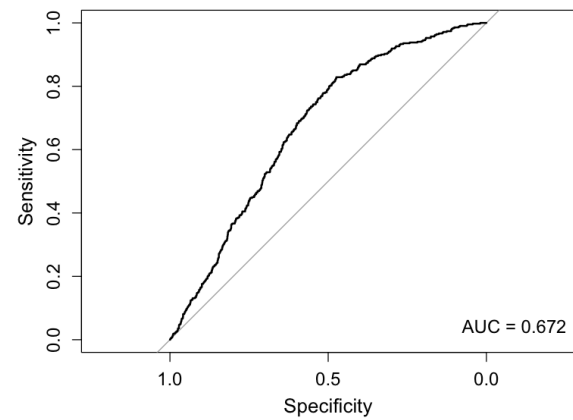
a. Female – Without Class Prob.



b. Female – With Class Prob.



c. Male – Without Class Prob.



d. Male – With Class Prob.

Notes: Five-fold cross-fitting is used to estimate the out-of-sample AUC for all models. The class probabilities are obtained using Zero-Shot classification, and we use the additive log ratios for this analysis, with disruptive behavior as the baseline category.